Calibration, imaging and mm peculiarities

Rosita Paladino
INAF Istituto di Radioastronomia
Italian Node of ALMA Regional Center

rosita.paladino@inaf.it

Calibration, imaging and mm peculiarities

Rosita Paladino
INAF Istituto di Radioastronomia
Italian Node of ALMA Regional Center

rosita.paladino@inaf.it

Radio telescopes
ERA sections 3.4, 3.5

Receivers
ERA sections 3.6.2, 3.6.4, 3.6.5

mm peculiarities
ALMA Technical handbook - https://almascience.eso.org/documents-and-tools/latest/alma-technical-handbook

Calibration
Imaging
Synthesis imaging in radioastronomy – Taylor, Carilli, Perley ASP conference series vol 180, 1999

NRAO synthesis school SIW2018 lectures

Radio telescopes

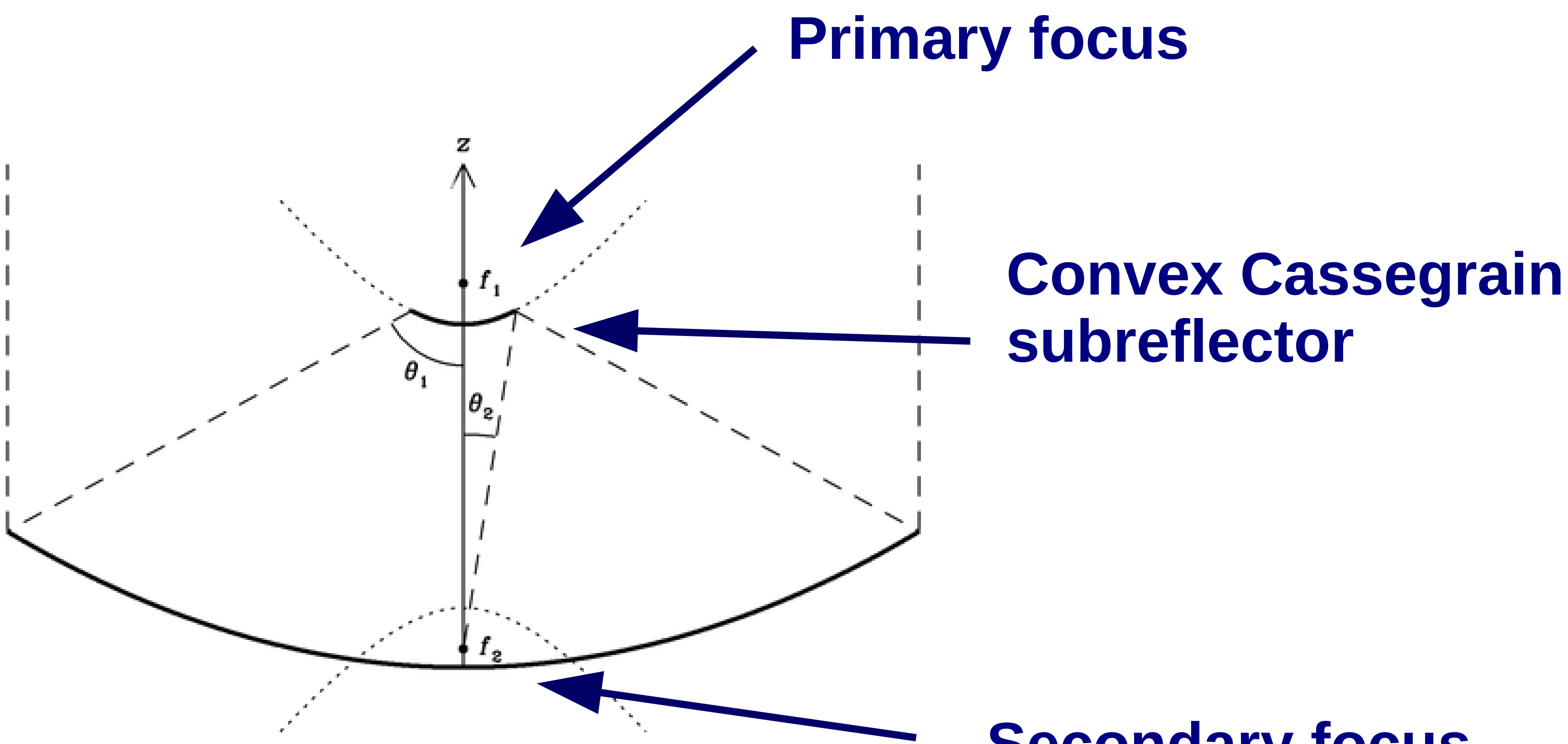

Both ALMA and VLA antennas have a Cassegrain optical configuration.

All (or most of the) receivers are in the Secondary focus

Radio telescopes

VLA

1.4 GHz - 40GHz

subreflector

secondary focus

Radio telescopes

ALMA 90 GHz – 900 GHz

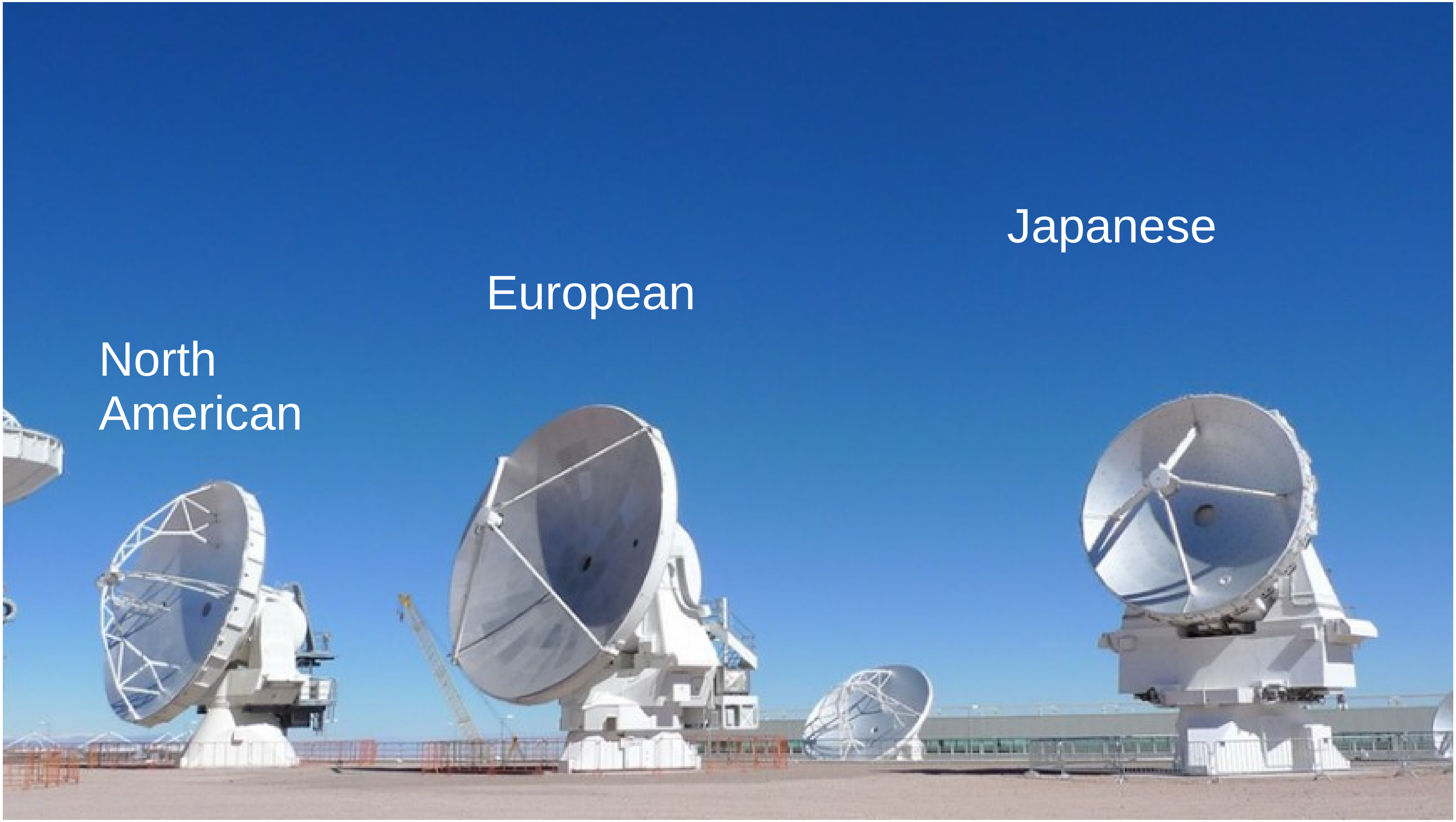

Radio telescopes

VLA feed horns
1.4 GHz - 40GHz

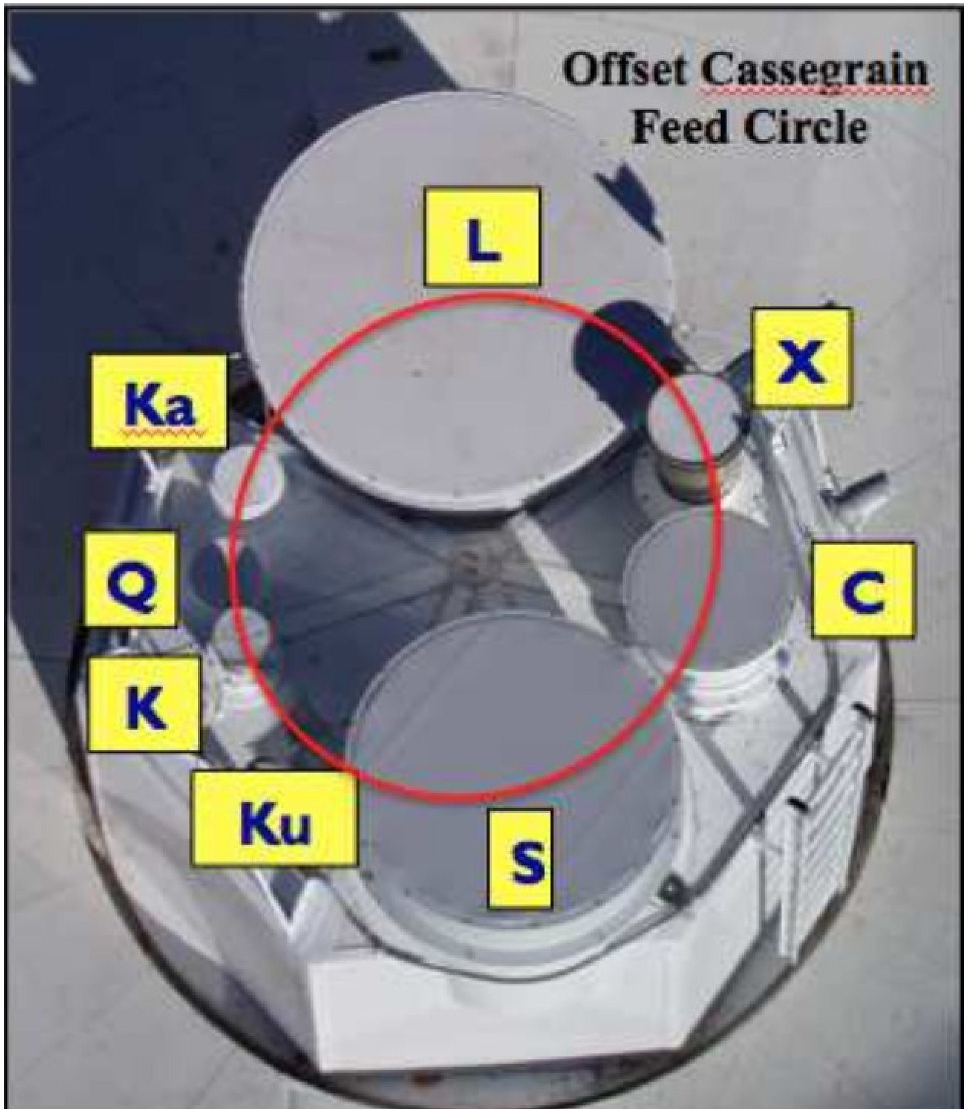

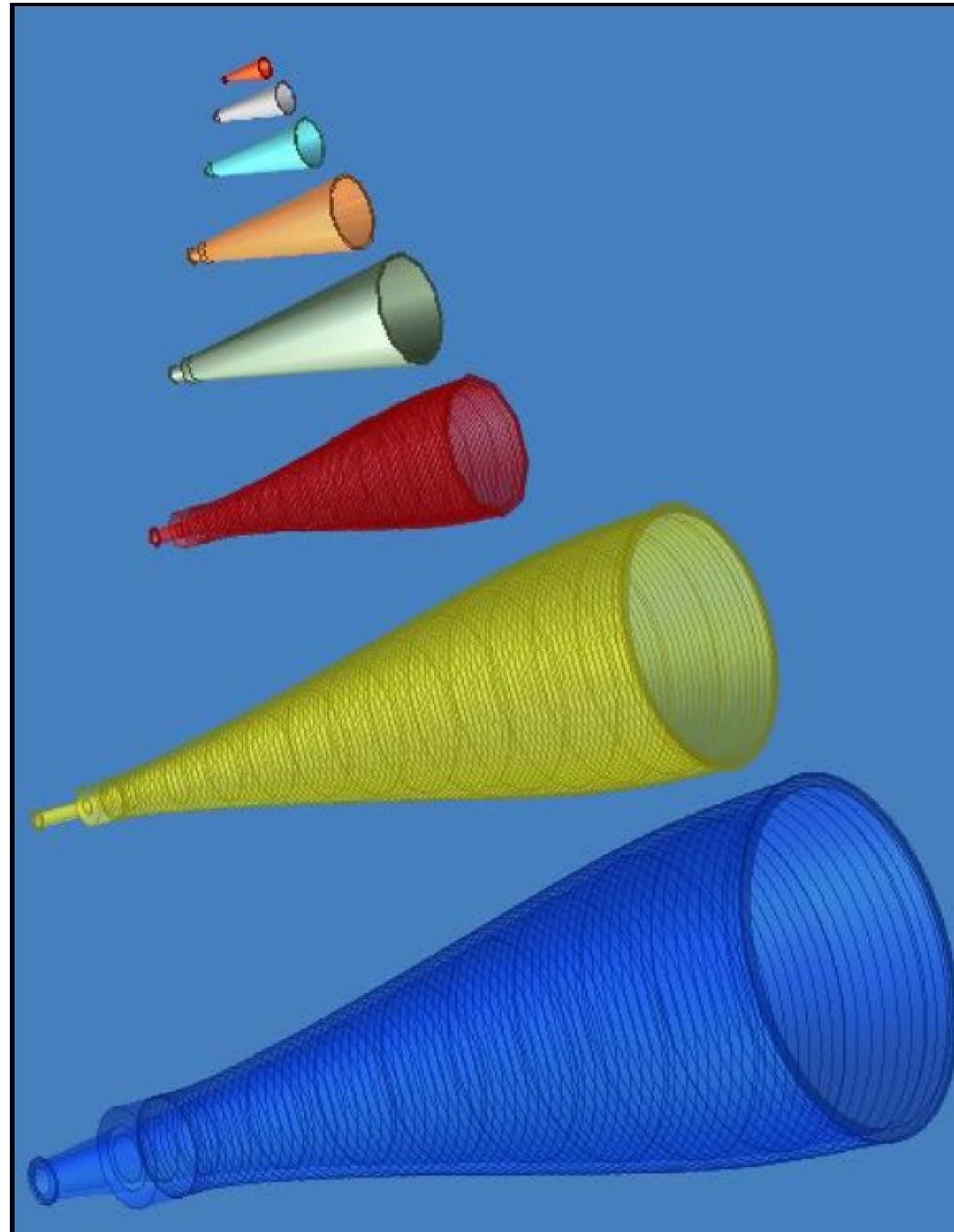

Radio telescopes

ALMA cryostat front view
<1 m in diameter

90 GHz – 900 GHz

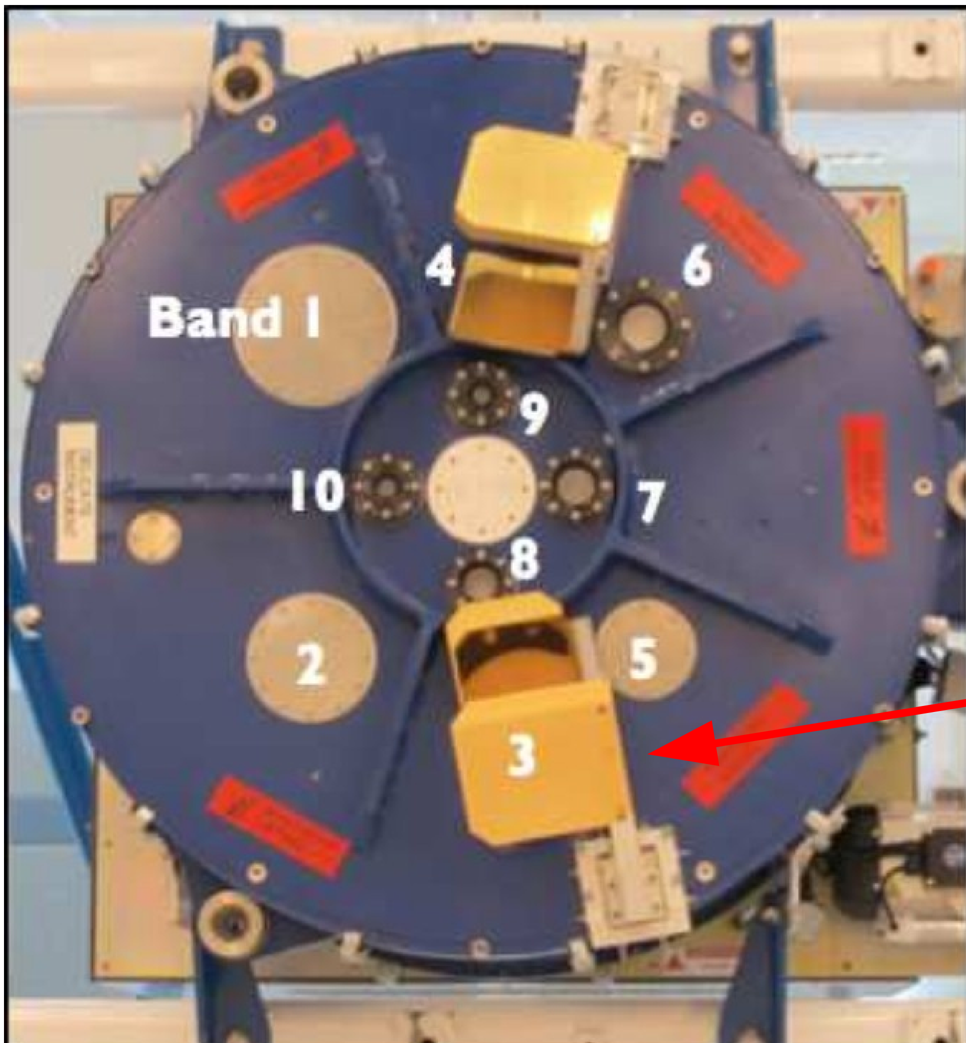

ALMA 90 GHz cartridge

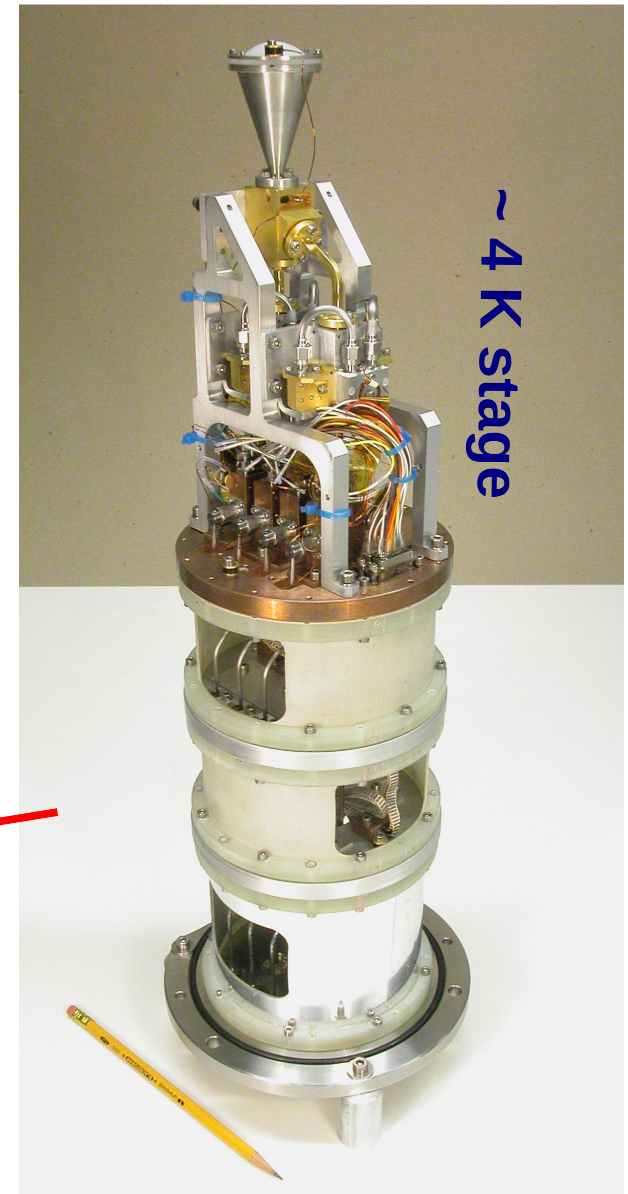

~50 cm

Antenna temperature

Radioastronomers find it convenient to refer to the power of various signals from a radio telescope in terms of the equivalent temperature of a matched termination on the receiver.

Rayleigh-Jeans approximation

$$P = kT \Delta\nu$$

P is the noise power in a bandwidth $\Delta\nu$ delivered to a matched load by a resistor at temperature T

We call **antenna temperature** the component of the power resulting from a cosmic source

$$T_A = \frac{P_A}{k \Delta\nu}$$

$$P_A = \frac{S_A A \Delta\nu}{2}$$

A cosmic source with $\mathbf{S_A = 1\ Jy = 10^{-26}\ W\ m^{-2}\ Hz^{-1}}$
observed with a 10 m antenna $A_e \sim 55\ m^2$
results in a $\mathbf{T_A \sim 0.02\ K}$

System temperatures

We call **system noise temperature** the output of a radio telescope.
The total noise temperature associated with a matched resistor that would produce the noise power level in the antenna receiving system.

$$T_s \sim T_A + T_{atm}(1 - e^{-\tau}) + T_{rx} + \ldots$$

At lower frequencies T_{rx} is dominant

At higher frequencies (mm/submm) the noise associated with the atmosphere T_{atm} is dominant, and acts like a blackbody emitter, attenuating the astronomical signal

T_A is typically very small compared to T_{sys}
How do we measure it???

Receivers

Radiometers

A radiometer measures the time-averaged power of the input noise in a well defined radio frequency range

$$\left[\nu_{RF} - \frac{\Delta\nu}{2} \Leftrightarrow \nu_{RF} + \frac{\Delta\nu}{2}\right]$$

$\Delta\nu$ is the receiver bandwidth

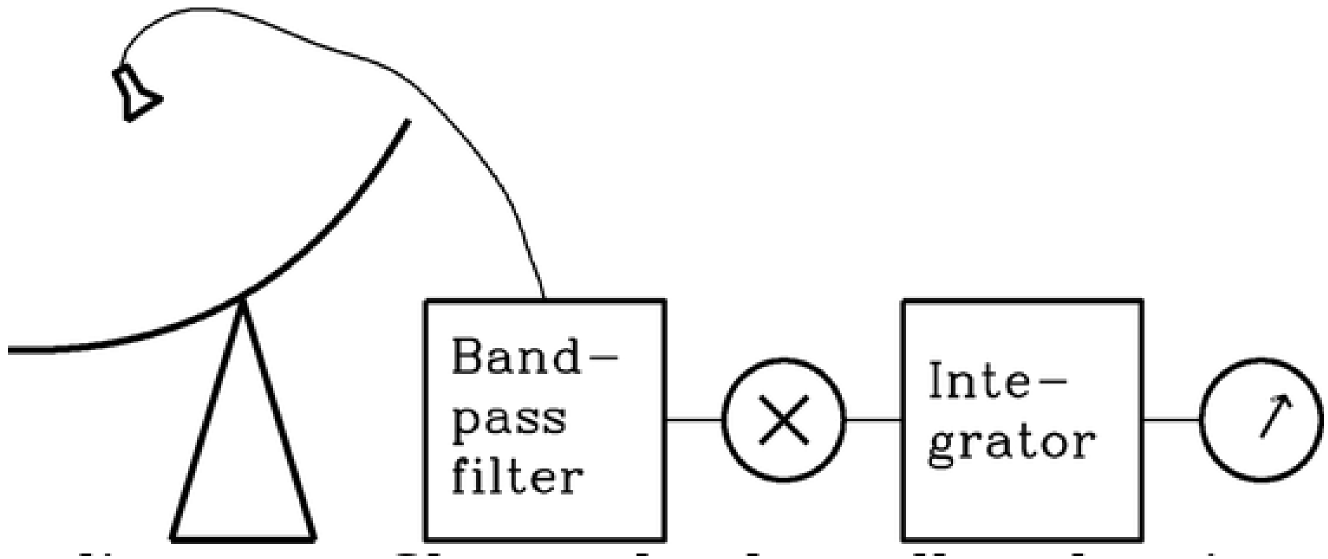

Receivers

Superheterodyne Receeiers

Nearly all practical receivers are superheterodyne.
The RF amplifier is followed by a mixer that multiplies the RF signal by a sine wave of frequency ν_{LO}
generated by a local oscillator (LO)

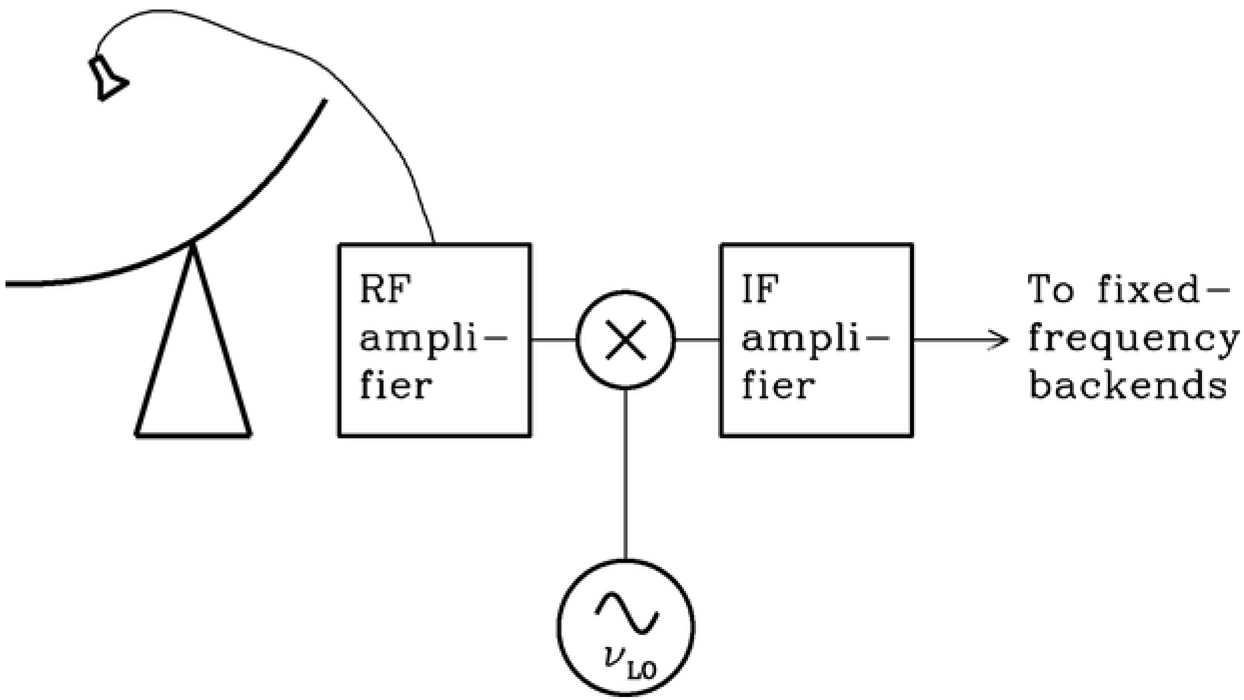

Radiometers

The noise voltage after the filter is a sine wave whose amplitude envelope varies randomly. A square-law detector output a voltage proportional to the square input voltage

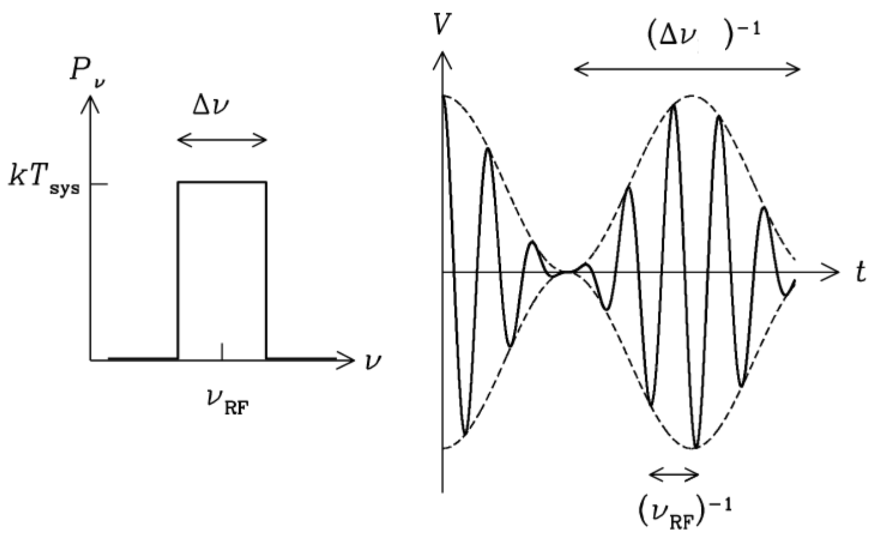

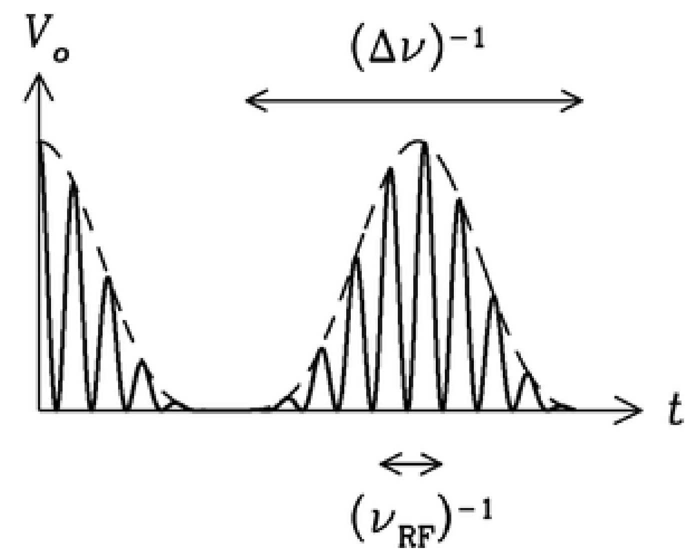

A sinusoid with frequency ν_{RF} whose envelope fluctuates on timescales $(\Delta\nu)^{-1} > (\nu_{RF})^{-1}$

Square of the input voltage.
Positive and proportional
to the square of the input power

Radiometers

The rapidly varying component and its envelope vary on timescales much shorter than the timescales of the signal power variations. **The unwanted rapid variation can be suppressed by taking the arithmetic mean of the detected envelope over some timescale**

$$\tau >> (\Delta\nu)^{-1}$$

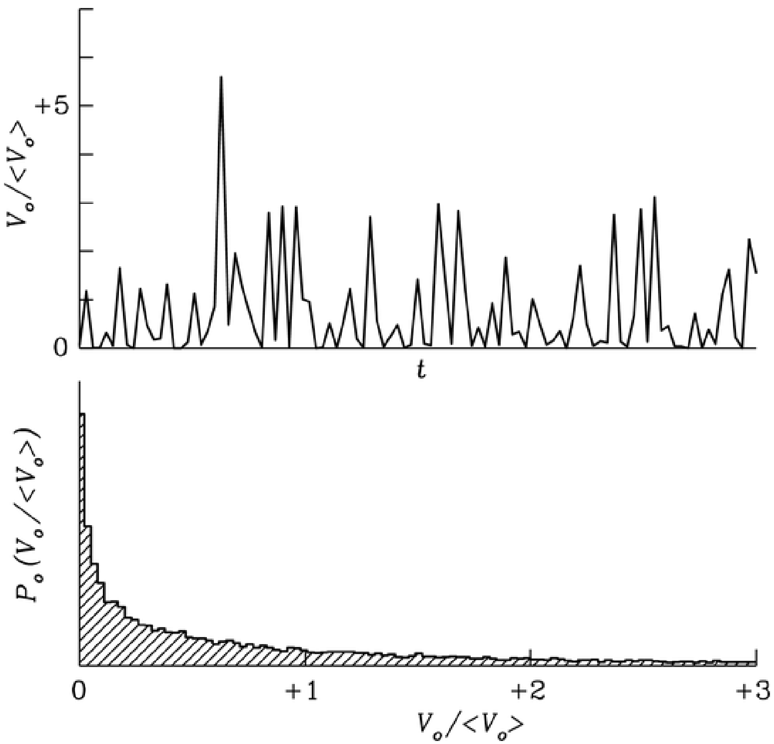

Output voltage from the square law detector when the input is **Gaussian noise power** T_S

with rms error $\sigma_T \approx \sqrt{2}\, T_S$

Output voltage histogram

Radiometers

Taking **N** independent samples of the noise power the rms error is reduced by a factor $N^{-1/2}$

$$N = (2\,\Delta\nu\,\tau)$$

Nyquist-Shannon theorem (ERA A.3)

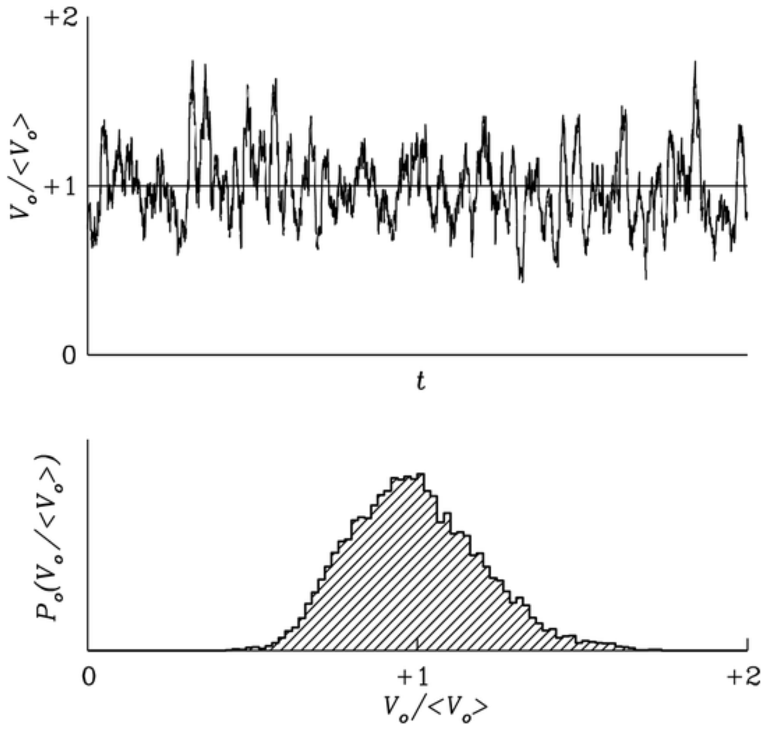

Output voltage from the square law detector when the input is **Gaussian noise power**

with N = 50

Output voltage histogram

Radiometers

The mean remains the same but the rms falls by a factor of 2

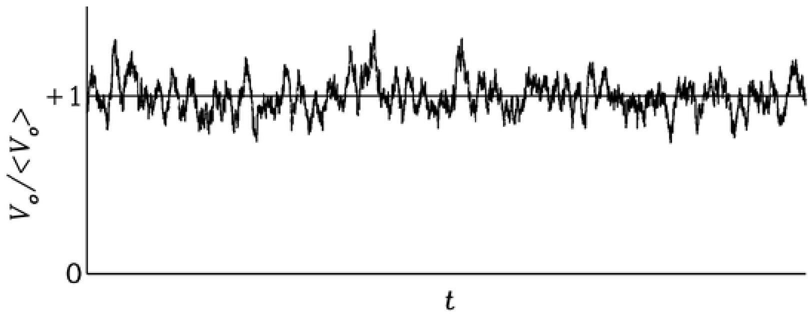

Output voltage from the square law detector when the input is **Gaussian noise power**

with N = 200

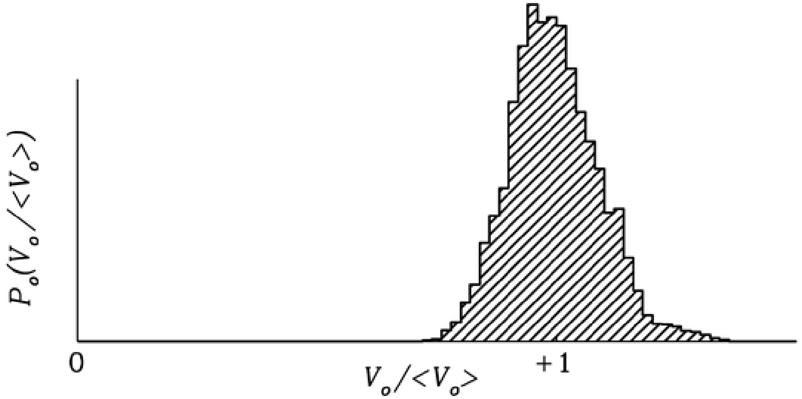

Output voltage histogram

Ideal radiometer equation

The rms uncertainty in each independent sample of the noise power T_{sys} is $\sqrt{2}\,T_{sys}$

(ERA Appendix B.6)

In the time interval τ the number of samples is $N=2\,\Delta\nu\,\tau$

The **rms receiver output fluctuation** is

$$\sigma_T \approx \sqrt{\frac{2}{N}}\,T_{sys} \approx \frac{T_{sys}}{\sqrt{\Delta\nu\,\tau}}$$

$\Delta\nu\,\tau$ can be quite large in practise (**not unusual 10^8**)

The weakest detectable signals have to be larger than this rms not than the total system noise.
So they can be as low as $10^{-4}\,T_{sys}$

Point source sensitivity

In the limit where temperature ΔT contributed by a point source is much smaller than T_{sys},

$$\Delta T = \frac{\eta A S}{2k}$$

the point source rms for a single antenna noise is:

$$\sigma_T = \frac{2 k T_{sys}}{\eta A \sqrt{\Delta \nu \tau}}$$

For an interferometer of N antennas, the point source rms noise is :

$$\sigma = \frac{2k}{\eta} \frac{T_{\mathrm{sys}}}{\sqrt{\Delta t \Delta \nu} \sqrt{N_{\mathrm{ant}}(N_{\mathrm{ant}} - 1)} A}$$

N_{ant}=2

$$\sigma = \frac{\sigma_T}{\sqrt{2}}$$

High sensitivity means low value of σ

Spectrometers

A spectrometer divides the passband into N adiacent narrow frequency ranges, and simultaneously measures the power in all N channels.

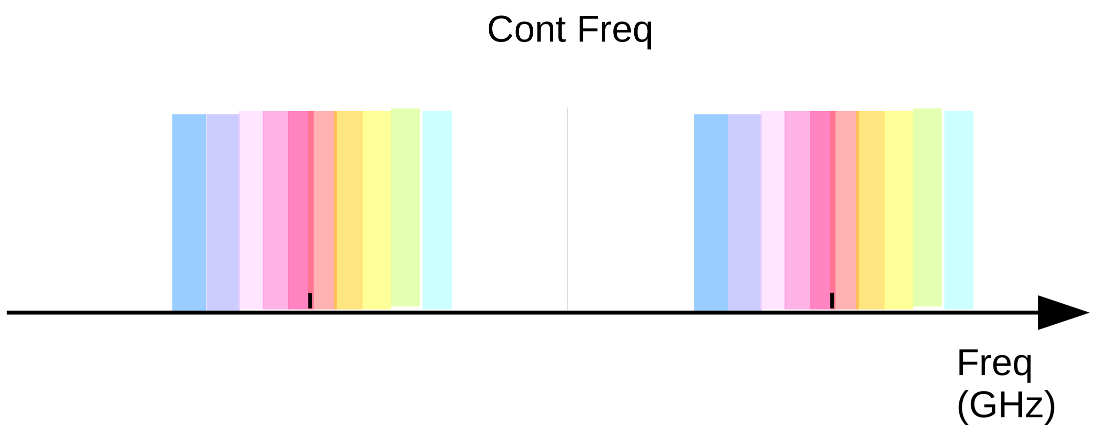

Modern interferometers use large band receivers.
Data are taken in multichannel mode regardless if they are meant for continuum or line observations.

The maximum number of channels in dual polarization mode is
8192 for the VLA
3840 for ALMA

Continuum images

- **Multi-Frequency synthesis (MFS)**

- Wide bandwidths allow higher sensitivity to continuum emission

$$\sigma = \frac{2k}{\eta}\frac{T_{\rm sys}}{\sqrt{\Delta t \Delta \nu}\sqrt{N_{\rm ant}(N_{\rm ant}-1)A}}$$

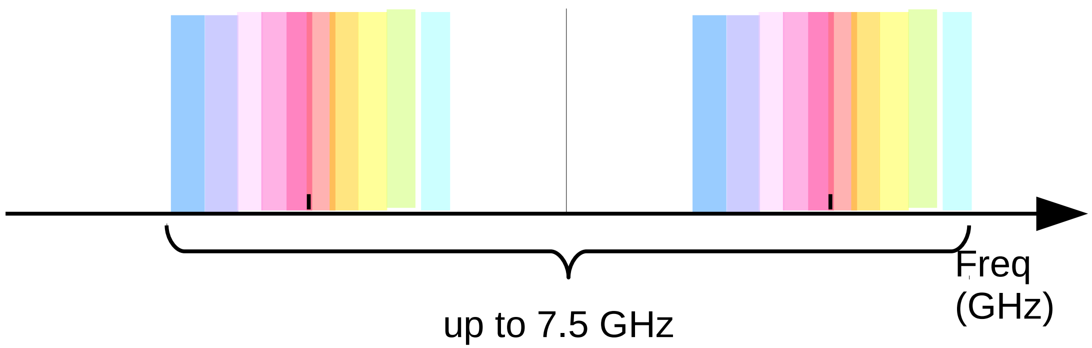

MFS
combines all channels

the result is a single image

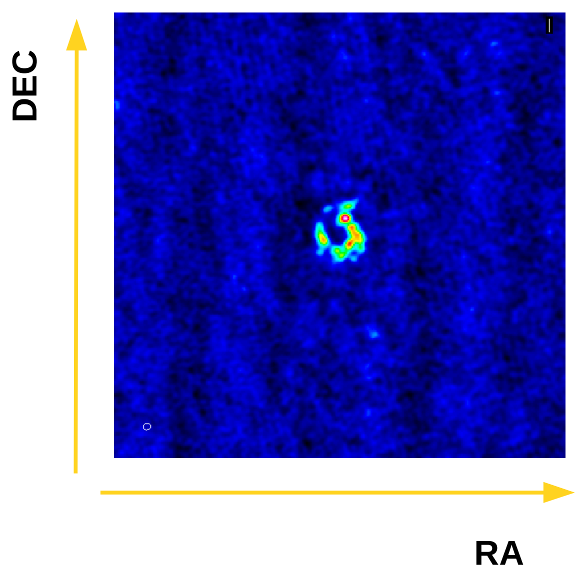

Continuum images

- **Multi-Frequency synthesis (MFS)**

- Wide bandwidths allow higher sensitivity to continuum emission but also **uv coverage is improved**

$$\sigma = \frac{2k}{\eta} \frac{T_{\rm sys}}{\sqrt{\Delta t \Delta \nu} \sqrt{N_{\rm ant}(N_{\rm ant}-1)} A}$$

- Distance in the uv-plane is proportional to b/λ so observing a large range in wavelengths changes points in the uv-plane into lines.

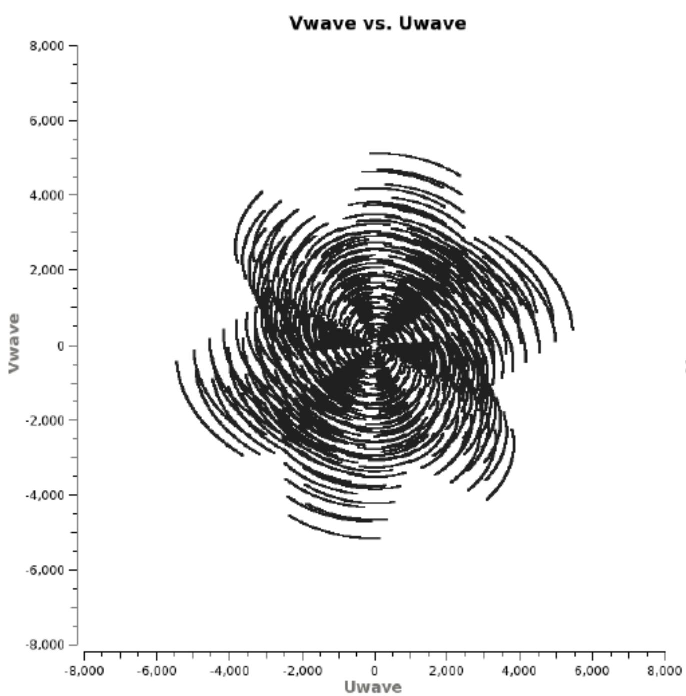

1.5 GHz

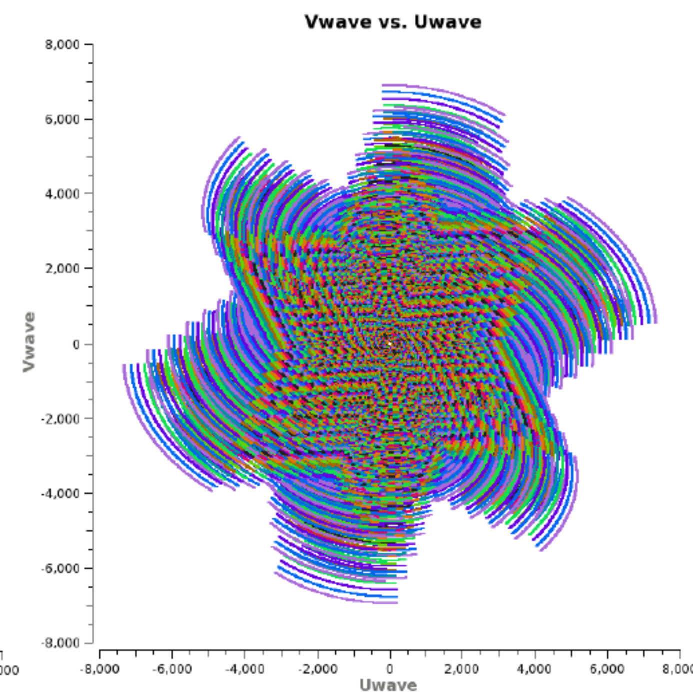

1 – 2 GHz

Spectral line observations

$$\sigma = \frac{2k}{\eta} \frac{T_{\rm sys}}{\sqrt{\Delta t \Delta \nu}\sqrt{N_{\rm ant}(N_{\rm ant}-1)A}}$$

- The imaging process is the same as for a continuum map **but** making an image for each channel (a cube with axes RA, DEC and velocity/frequency)

- The rms is larger than for continuum

- While imaging it is possible to average channels if the full spectral resolution is not needed

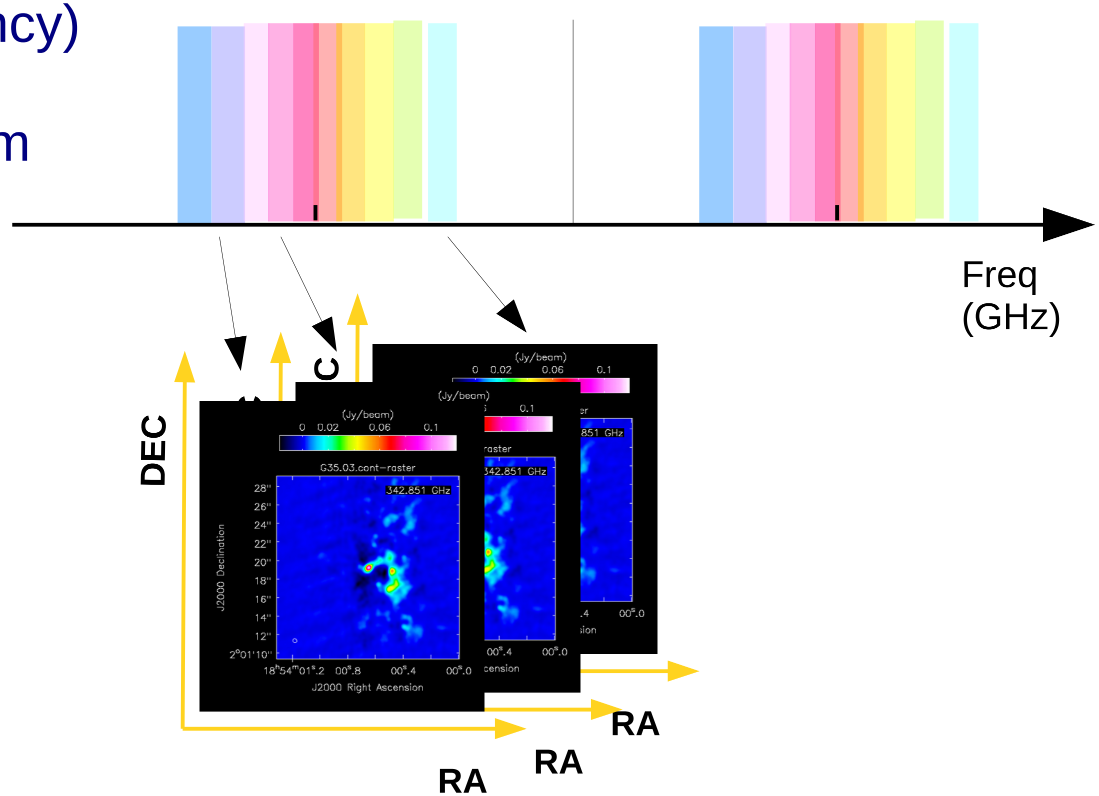

Spectral line observations

Spectral line images
are 3-dimensional.

One image from each channel

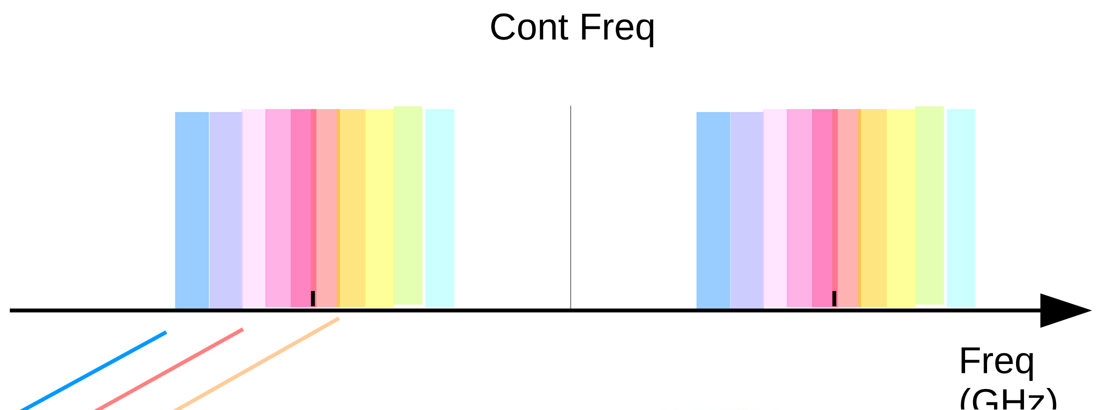

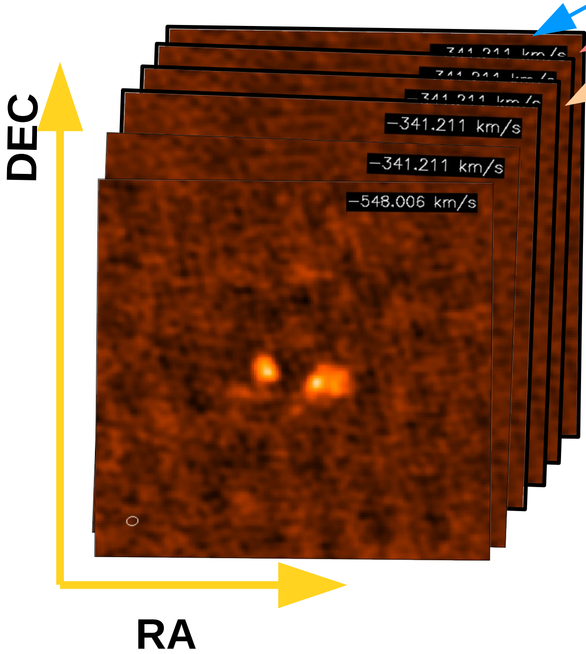

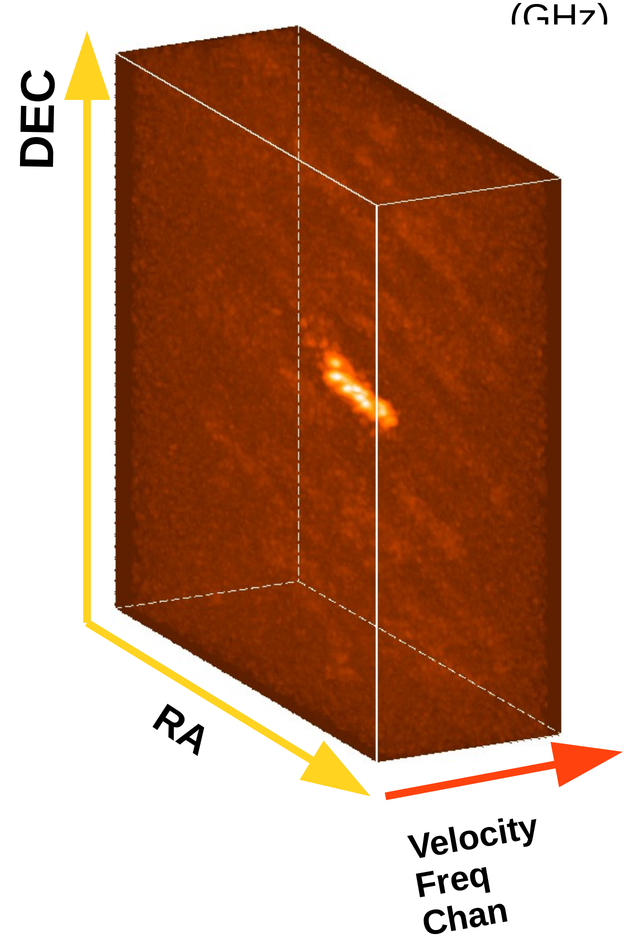

Spectral lines

1-D slice along velocity axis

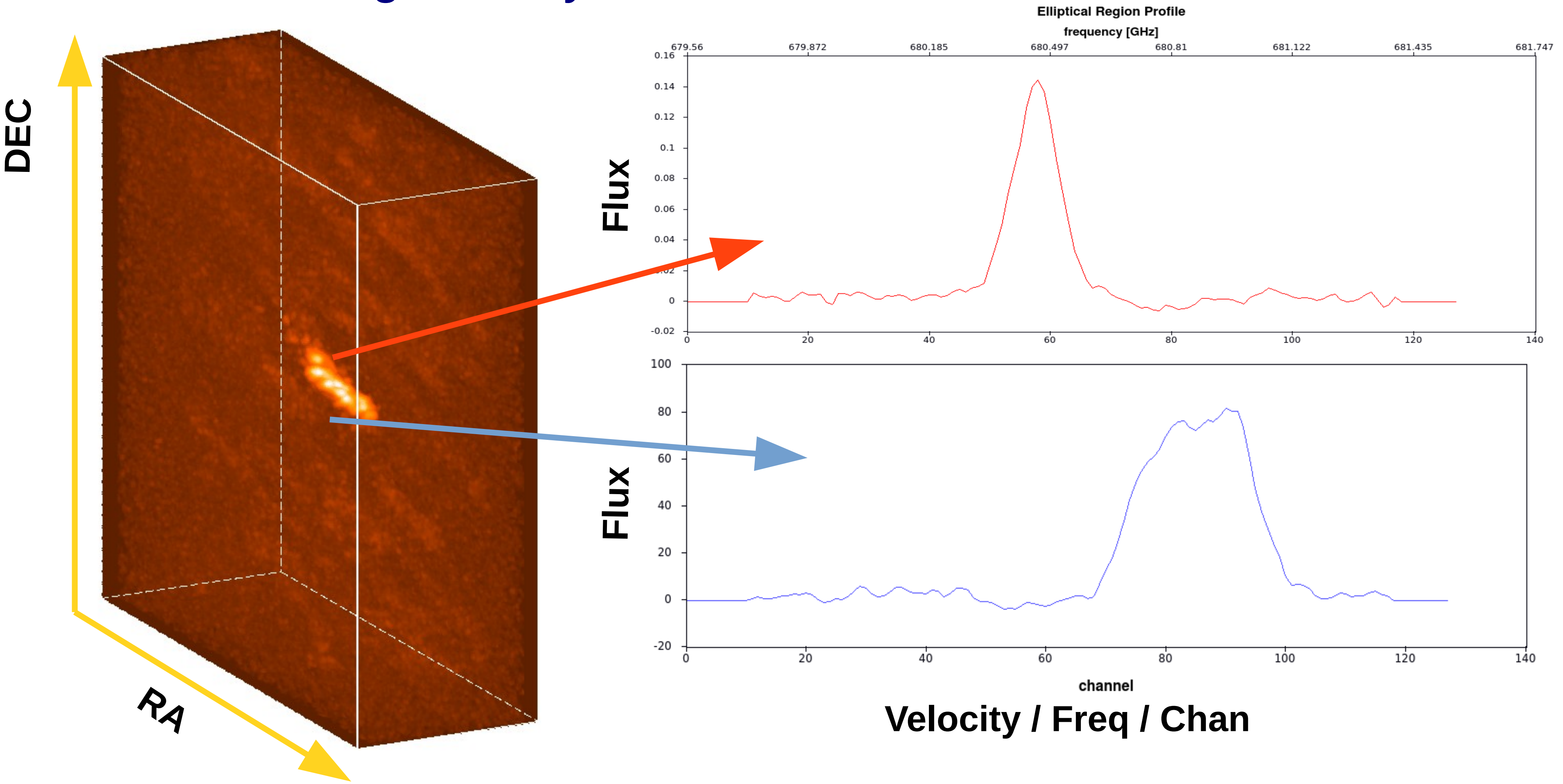

From each pixel one spectrum

Peculiarities @ mm

With increasing frequency:

- **No external human interferences in the data**

- **No ionospheric effect**

- Tropospheric effects: absorption and delay of signal
  - → stronger weather dependency
  - → T_{sys} dominated by atmospheric noise

- Time variability of quasars increases
  - → which flux calibrators?

Solved now

Peculiarities @ mm

Tropospheric opacity depends on altitude

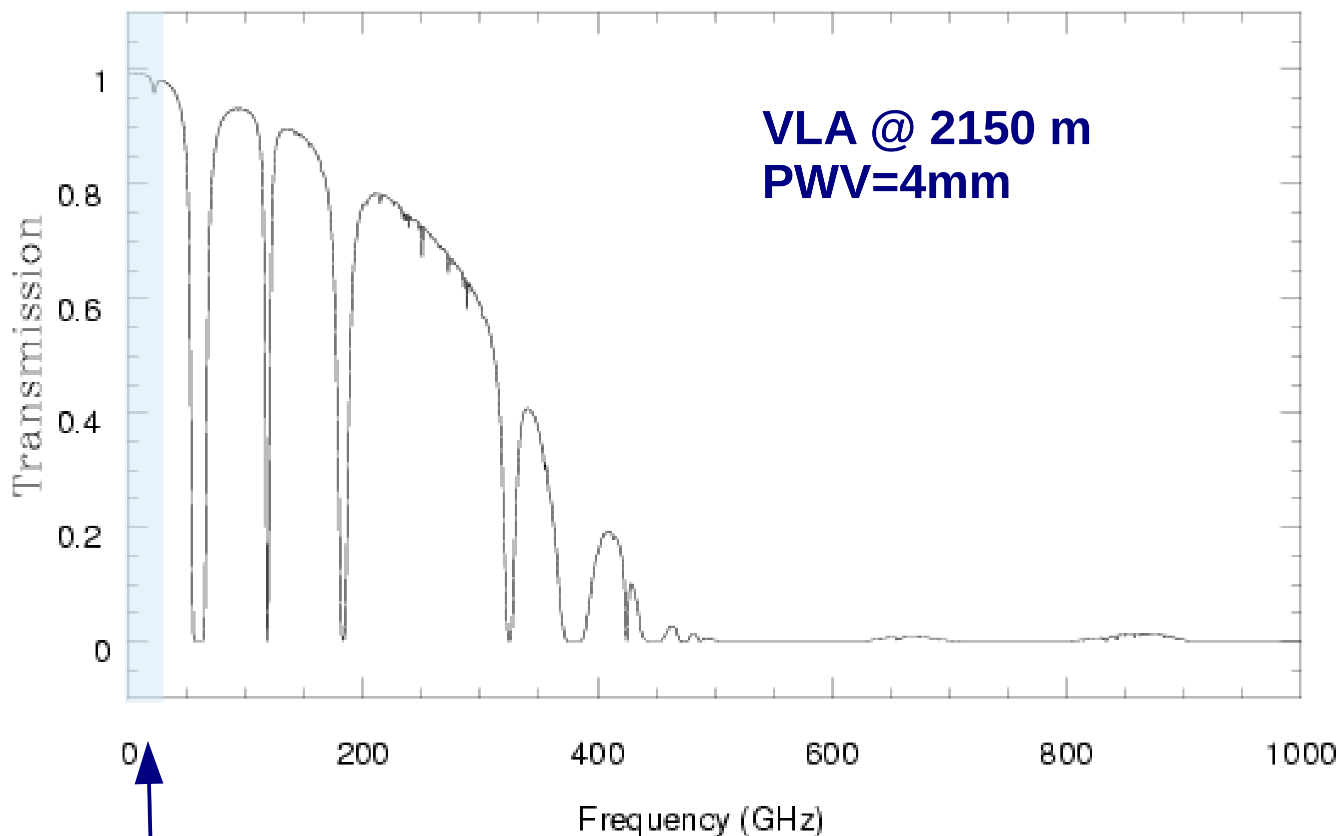

Atmospheric transmission not a problem @ $\lambda >$ cm

VLA bands

Peculiarities @ mm

Tropospheric opacity depends on altitude

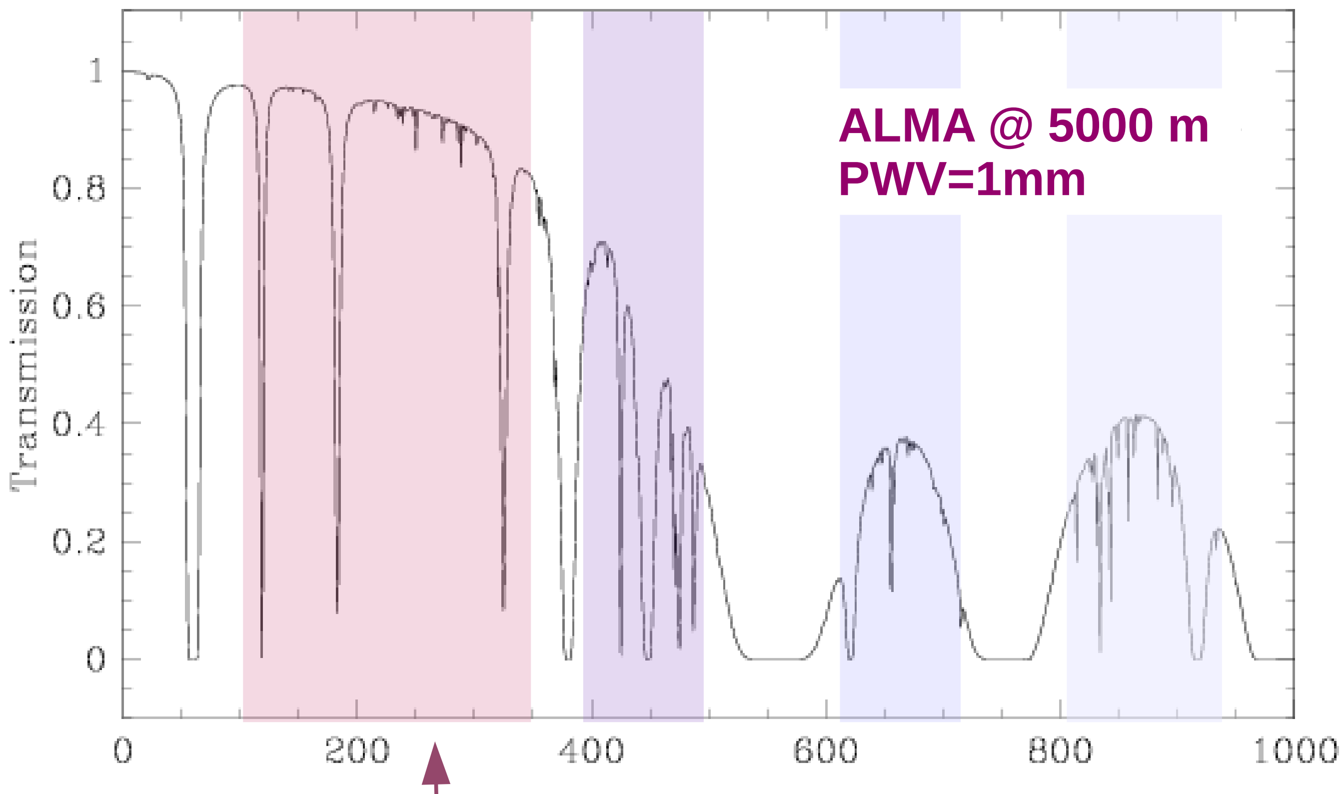

ALMA bands

Difference due to the scale height of water vapor

Peculiarities @ mm

PWV= Precipitable Water Vapour

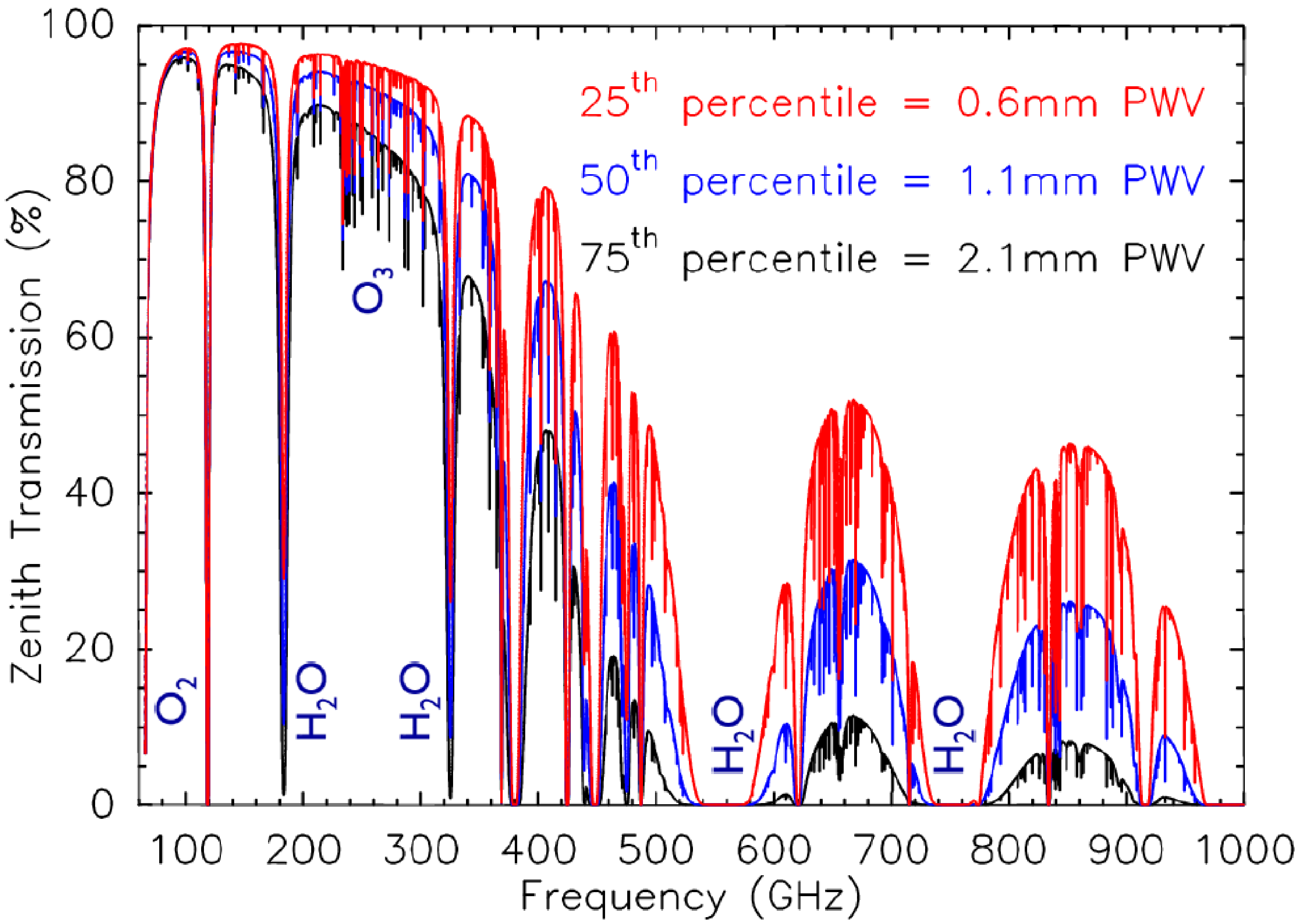

Peculiarities @ mm

e.g. to observe a 1 Jy source with a 10 m radiotelescope
we have to measure T_A ~ 0.02 K against T_{sys} ~ 100 K

$$T_{sys} \sim T_{atm} (1 - e^{-\tau}) + T_{rx}$$

At lower frequencies T_{rx} is dominant

At higher frequencies (mm/submm)
the noise associated with the atmosphere T_{atm} is dominant, and acts like a blackbody emitter, attenuating the astronomical signal

Peculiarities @ mm

System noise temperature

ALMA front end are equipped with an Amplitude Calibration Device (ACD)

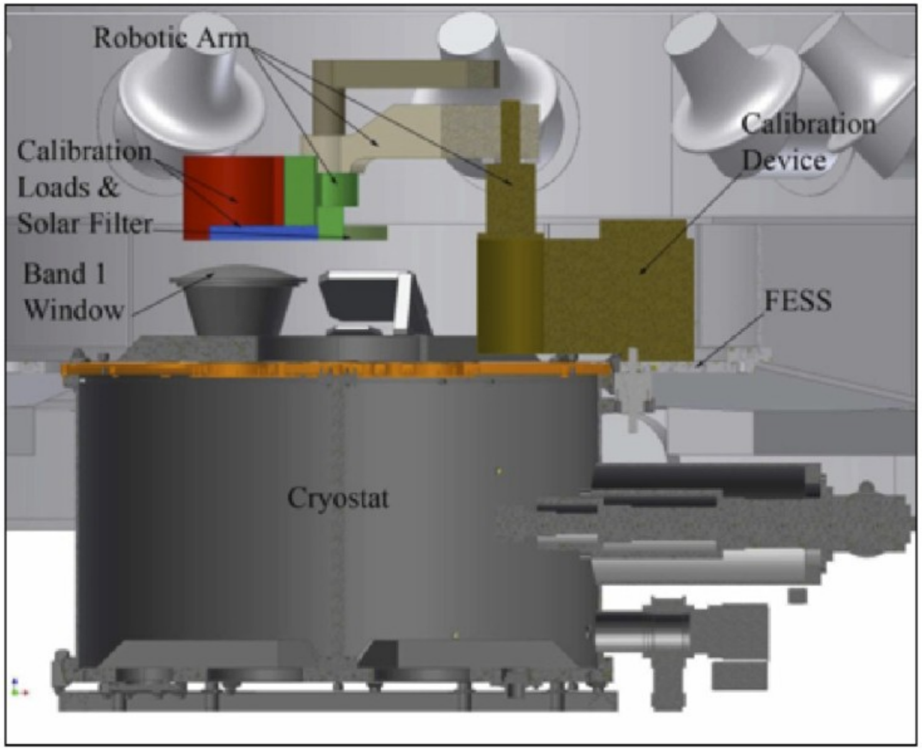

→ To measure T_{sys} and T_{rx} stored in tables

Every scan could have a Tsys measurement, but <400 GHz relatively constant ~10min.
Tsys spectra are applied off-line to the correlated data.

Assuming correlated data in units of % correlation multiplication by Tsys will change the unit to Kelvin

Peculiarities @ mm

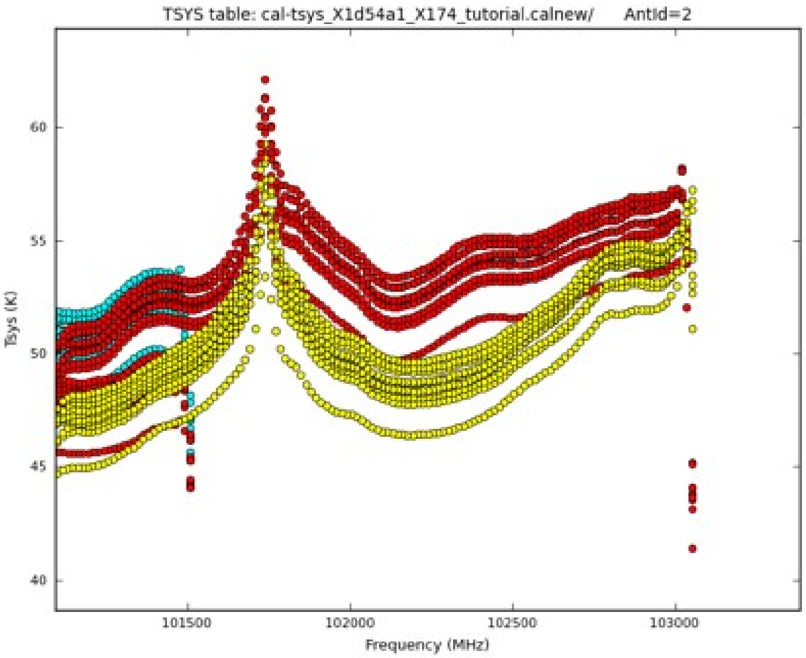

Tsys calibration

Spectral Tsys
band 3 (~100 GHz)

Before

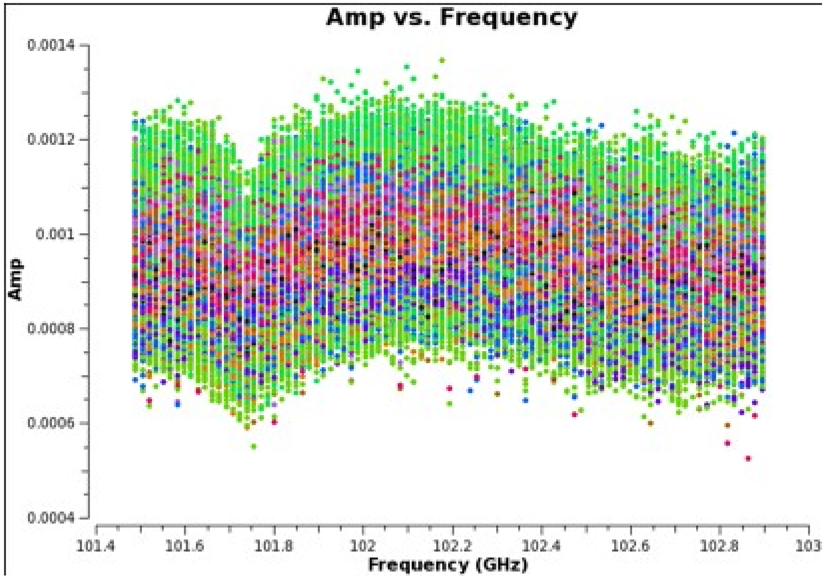

Peculiarities @ mm

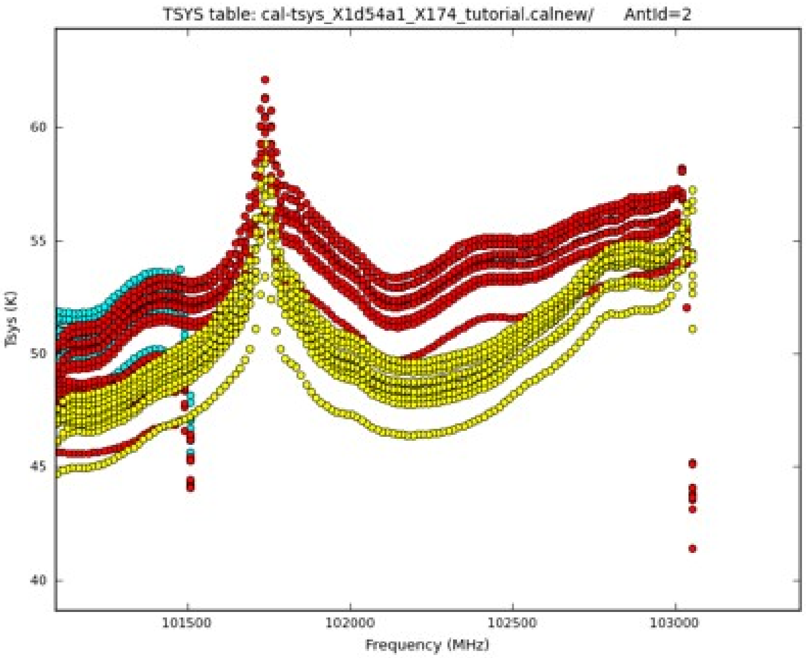

Tsys calibration

Spectral Tsys
band 3 (~100 GHz)

Before

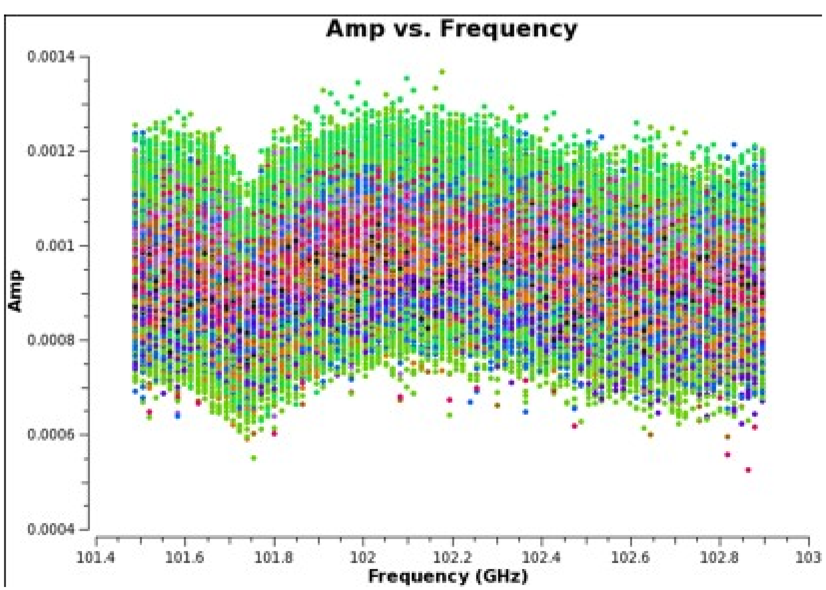

After

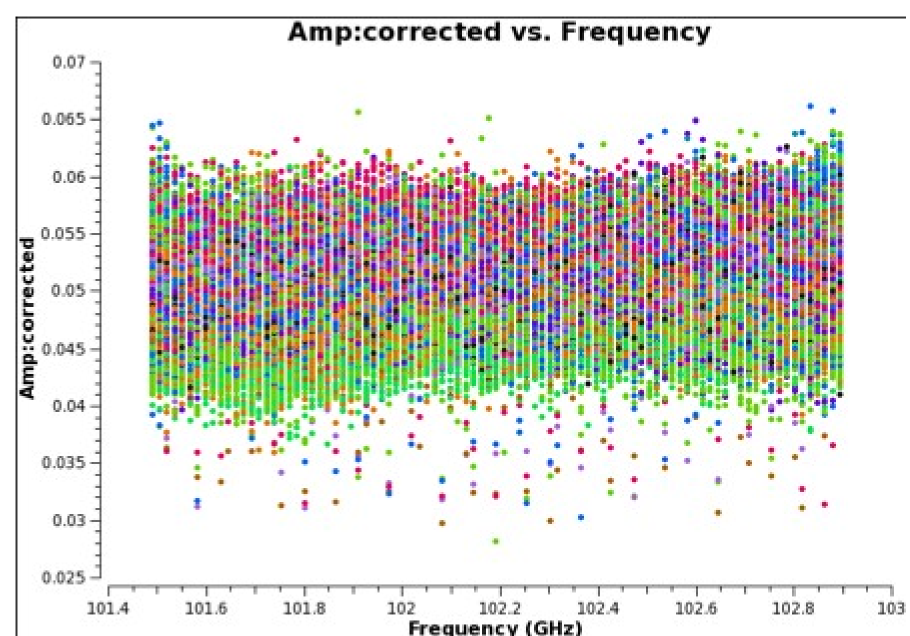

Peculiarities @ mm

Mean effect of atmosphere on Phase

Variations in precipitable water vapor (PWV) cause phase fluctuations, worse at higher frequencies, resulting in:

- Phase shift due to refractive index $n \neq 1$
- Low coherence (loss of sensitivity)

Patches of air with different pwv
(and hence index of refraction)
affect the incoming wave front differently.

Antenna 1, 2, 3 see slightly different disturbances

Sky above antenna 4 varies independently

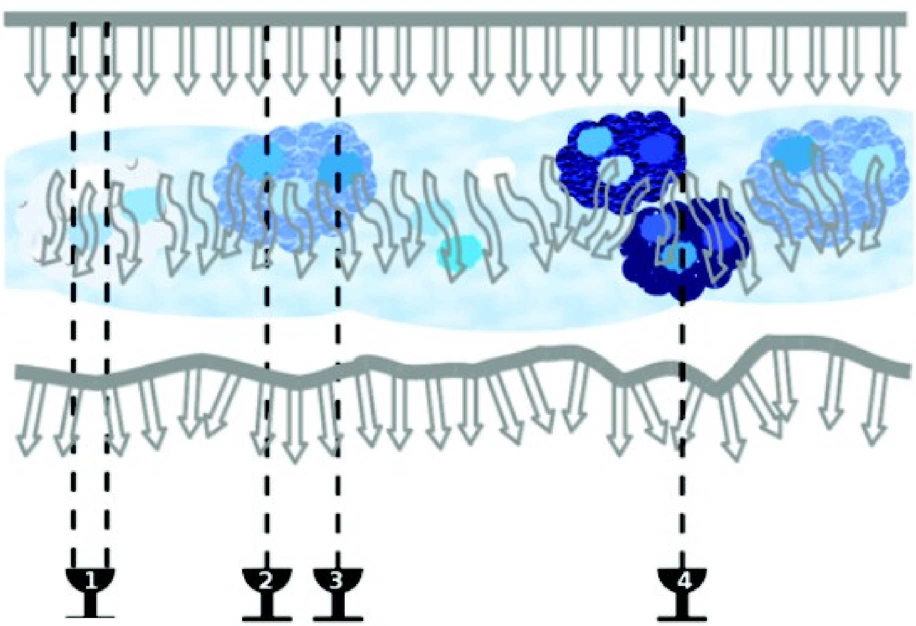

The phase change experienced by an e.m. wave can be related to pwv

$$\varphi_e \approx \frac{12.6\pi}{\lambda} \cdot pwv$$

Hogg, Guiraud, & Decker, 1981

Peculiarities @ mm

Mean effect of atmosphere on Phase

Variations in precipitable water vapor (PWV) cause phase fluctuations, worse at higher frequencies, resulting in:

- Phase shift due to refractive index n ≠
- Low coherence (loss of sensitivity)

Patches of air with different pwv
(and hence index of refraction)
affect the incoming wave front differently.

Antenna 1, 2, 3 see slightly different disturbances

Sky above antenna 4 varies independently

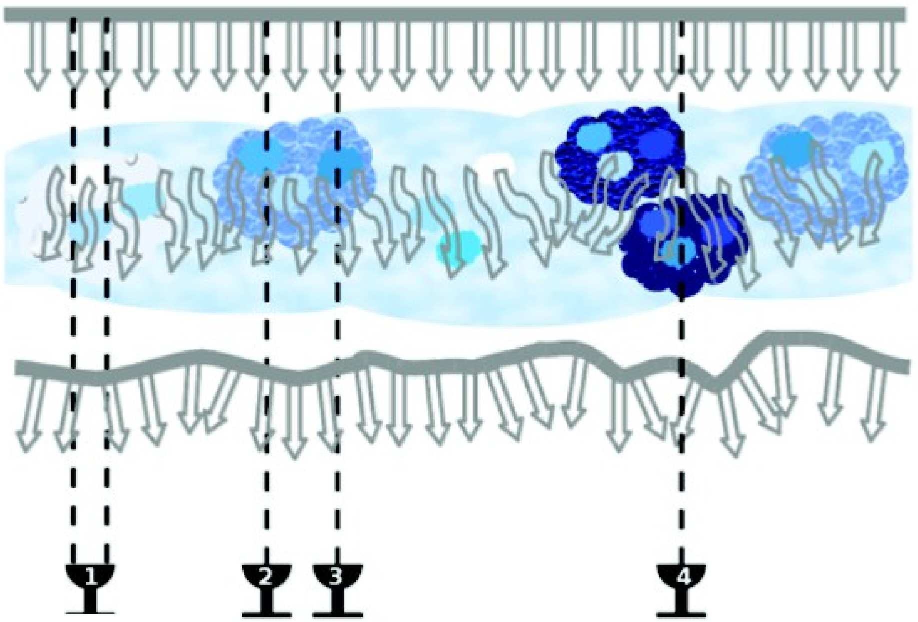

The phase change experienced by an e.m. wave can be related to pwv

$$\varphi_e \approx \frac{12.6\pi}{\lambda} \cdot pwv$$

Hogg, Guiraud, & Decker, 1981

Peculiarities @ mm

Atmospheric phase fluctuations

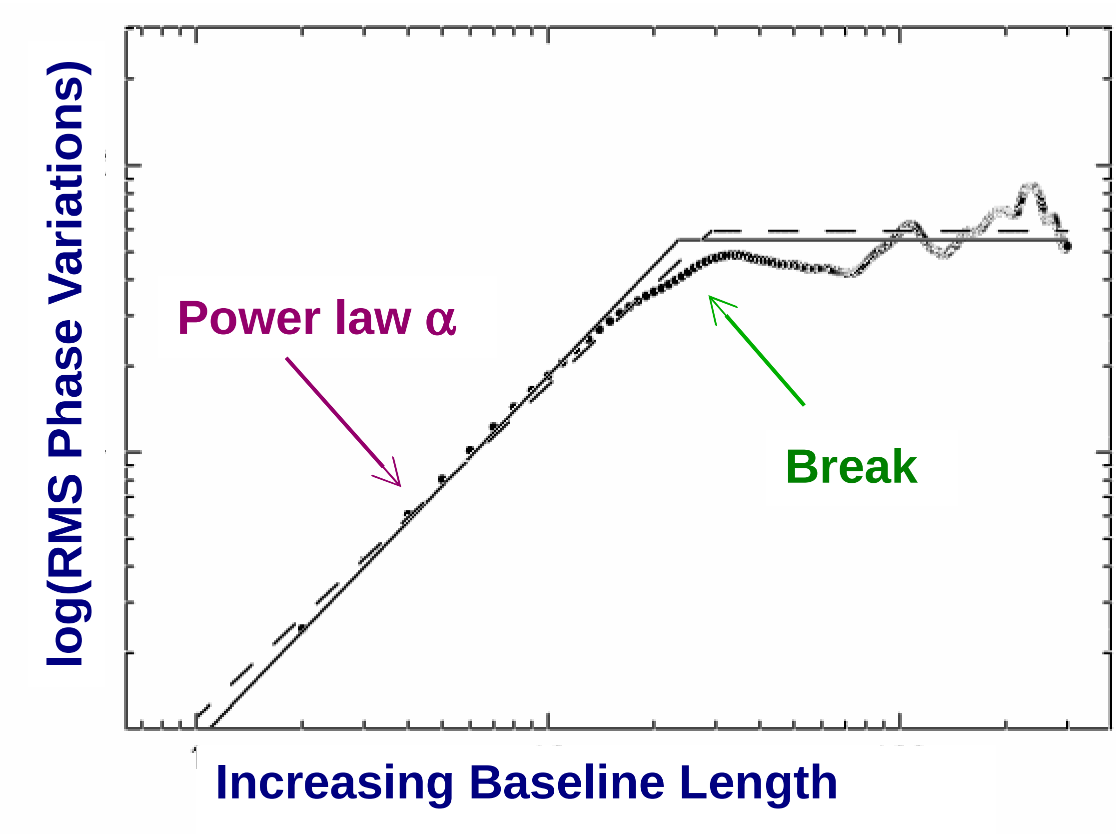

Phase noise

Kolmogorov turbulence theory

$$\varphi_{rms} = \frac{K\, b^{\alpha}}{\lambda}$$

b=baseline length (km)
α = 1/3 to 5/6 (thin or thick atmosphere)
λ = wavelength (mm)
K constant (~100 for ALMA)

The break is typically @ baseline lengths few hundred meters to few km (scale of the turbulent layers)

Break and maximum are weather and wavelength dependent

Peculiarities @ mm

Atmospheric phase fluctuations → decorrelation

We lose integrated flux because visibility vectors partly cancel out

$$\langle V \rangle = V_o \langle e^{i\varphi} \rangle = V_o e^{-(\varphi_{rms}^2)/2}$$

φ_{rms} = 1 radian → <V> = 0.60 V_0

In summary
Fluctuations in the line-of-sight pwv of an antenna
cause phase variations of the order of ~30 deg / sec at 90 GHz,
and scales linearly with frequency....

$$\varphi_e \approx \frac{12.6\pi}{\lambda} \cdot pwv$$

and the phase noise is worse at longer baselines...

$$\varphi_{rms} = \frac{K\, b^{\alpha}}{\lambda}$$

Peculiarities @ mm

WVR correction

Each ALMA 12 m antenna has a water **vapour radiometer**

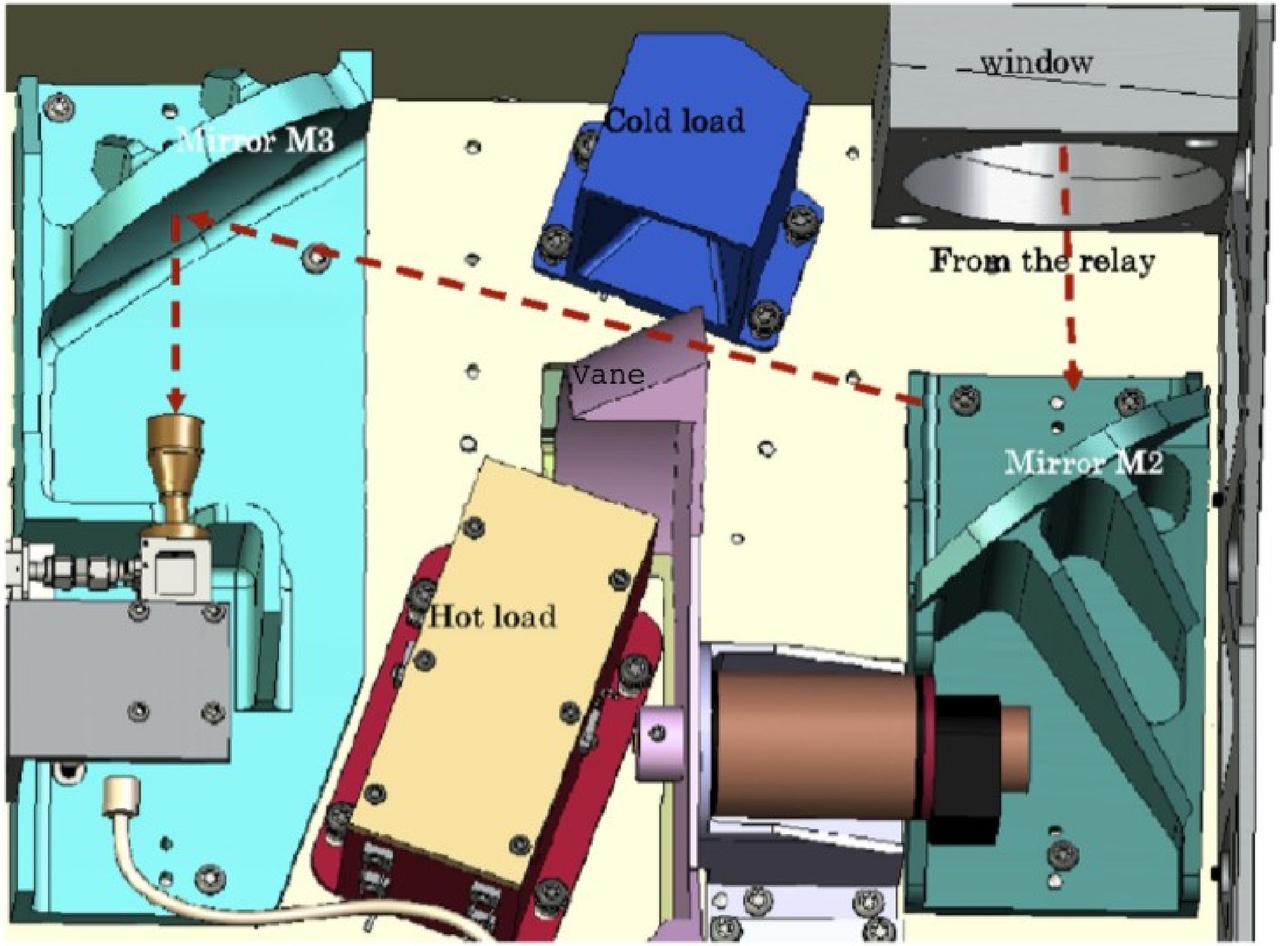

Peculiarities @ mm

WVR correction

Each ALMA 12 m antenna has a water **vapour radiometer**

Four “channels” flanking the peak of the 183 GHz water line

Data taken every second

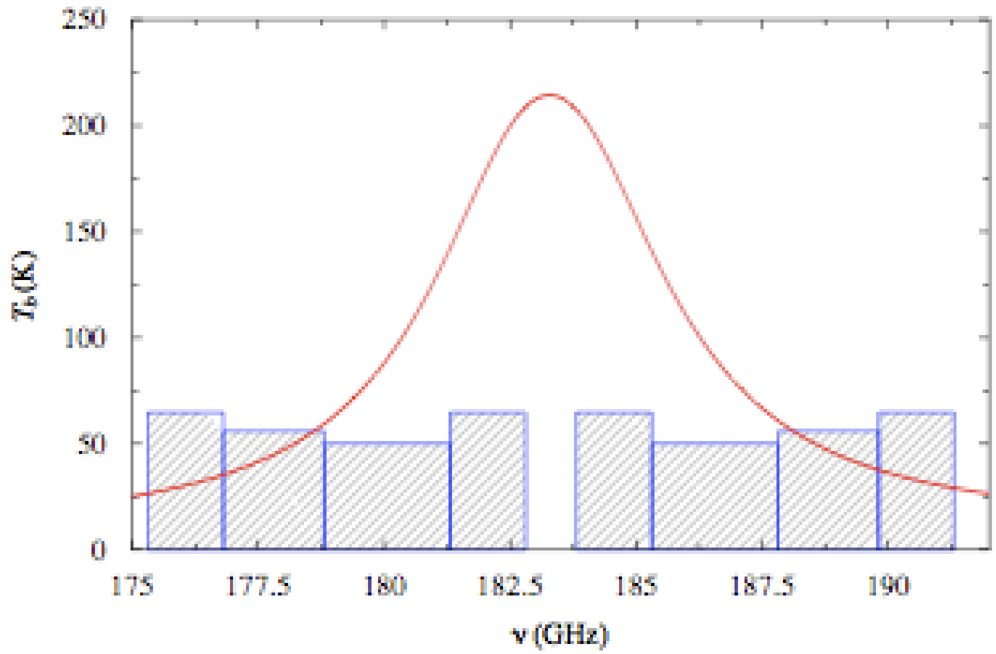

Peculiarities @ mm

WVR correction

Each ALMA 12 m antenna has a water **vapour radiometer**

Four “channels” flanking the peak of the 183 GHz water line

Data taken every second

Convert 183 GHZ brightness to PWV (wvrgcal):
model PWV, temperature and pressure
compare to the observed “spectrum”
compute the correction:

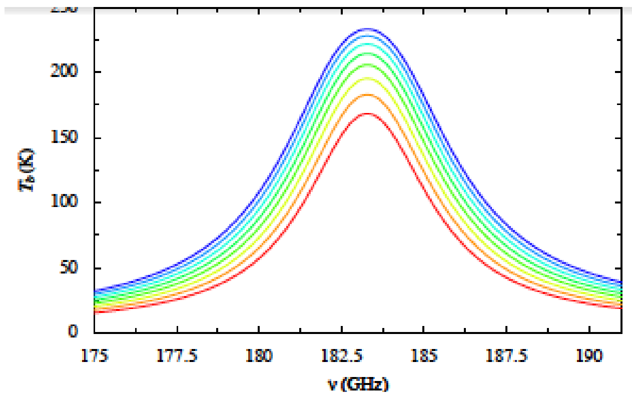

PWV from 0.6 to 1.3 mm

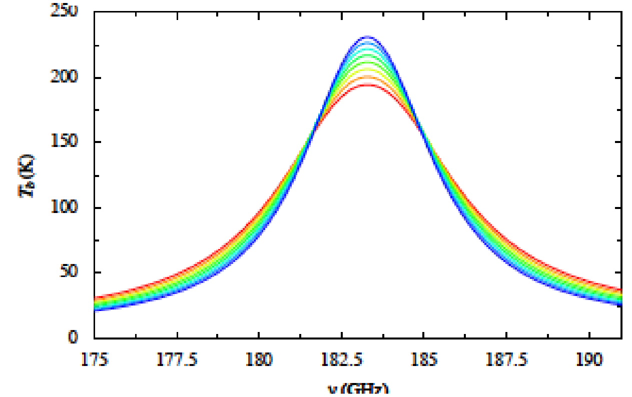

Temperature 230-300 K

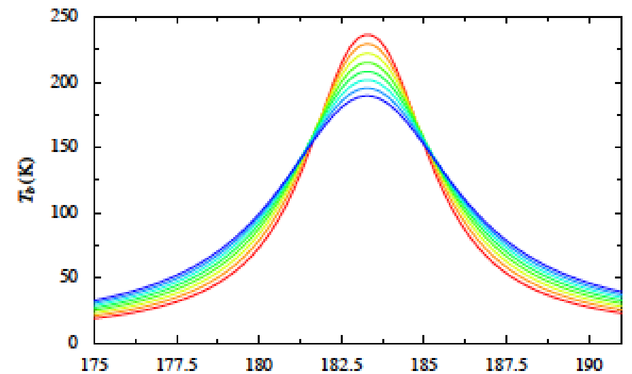

Pressure 400-750 mBar

Peculiarities @ mm

WVR correction

Band 6 (230 GHz)

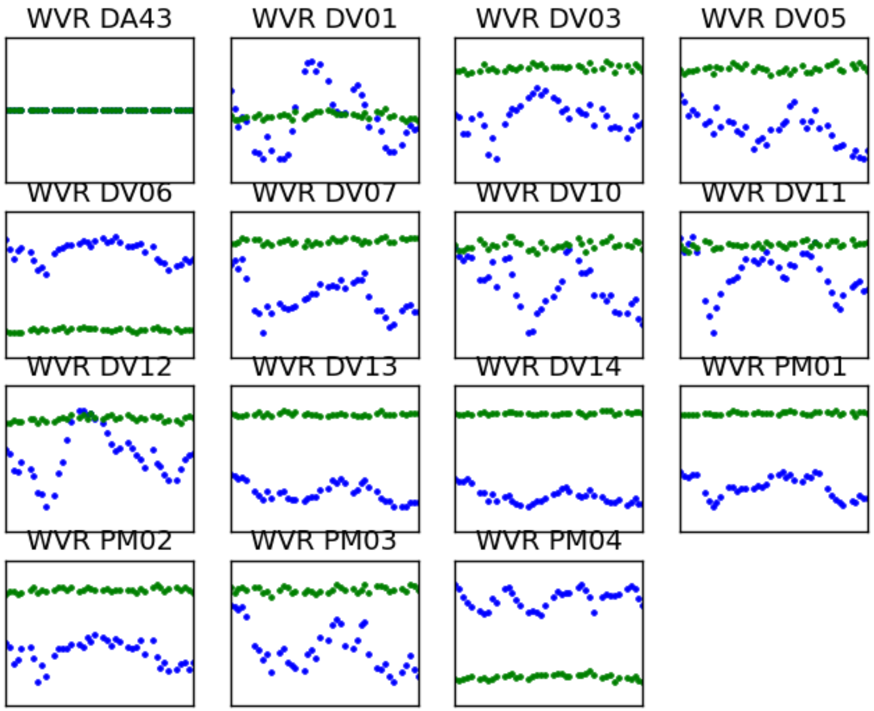

Raw phases & WVR corrected phases

Peculiarities @ mm

WVR correction

Band 6 (230 GHz)

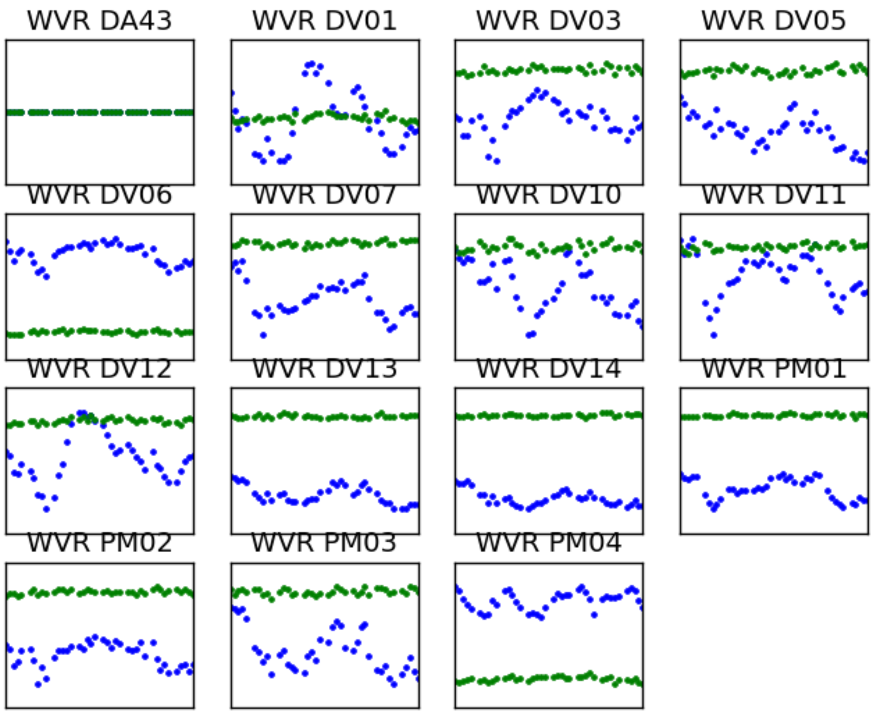

Band 7 (340 GHz)

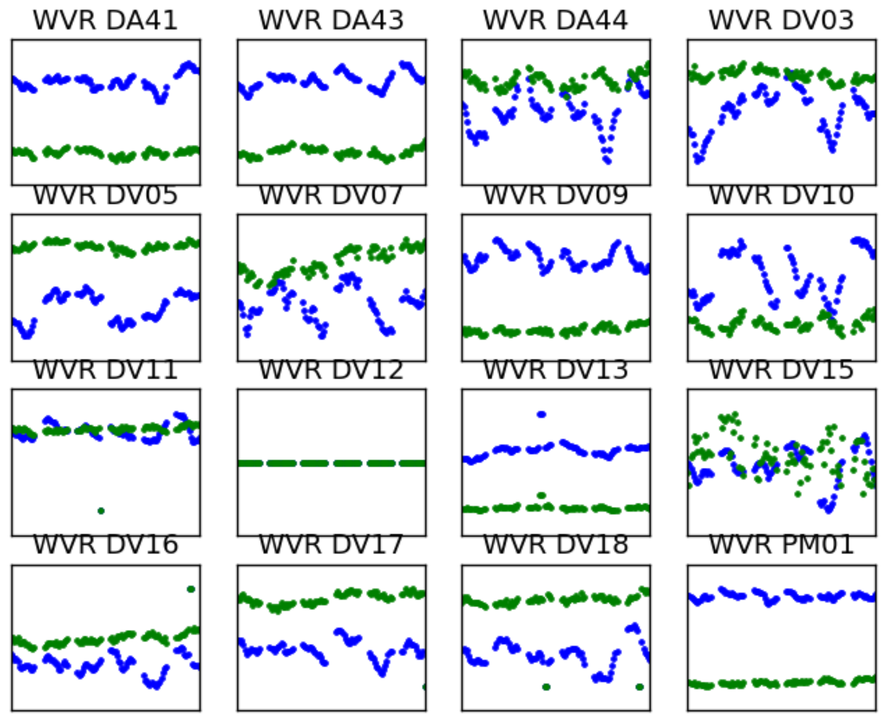

Raw phases & WVR corrected phases

Calibration in ALMA:

Tsys and wvr calibration are done “a priori” without observations of dedicated calibrators.

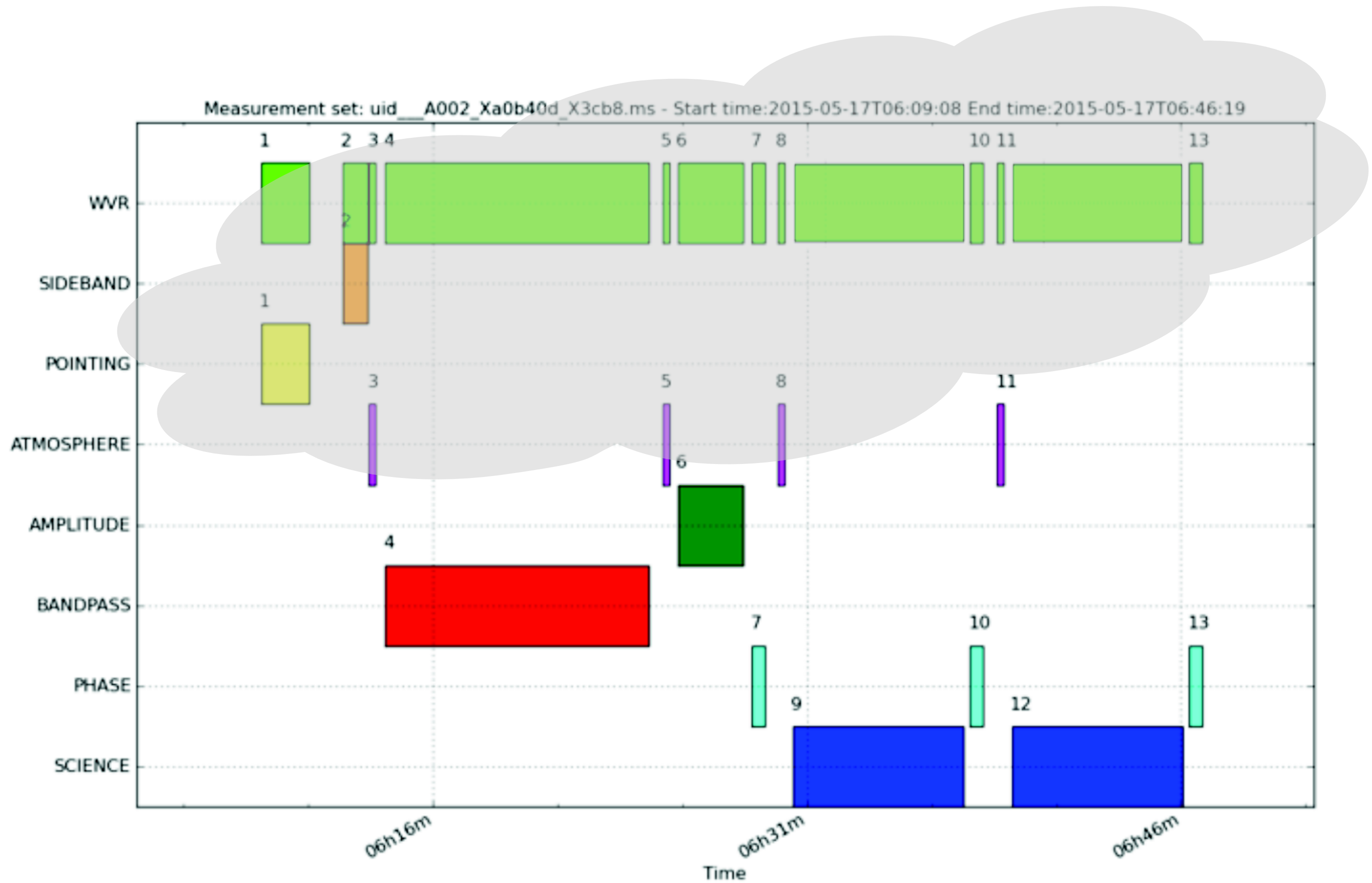

Mosaics

Why is mosaicking needed more @ ALMA frequencies?

Interferometer correlators

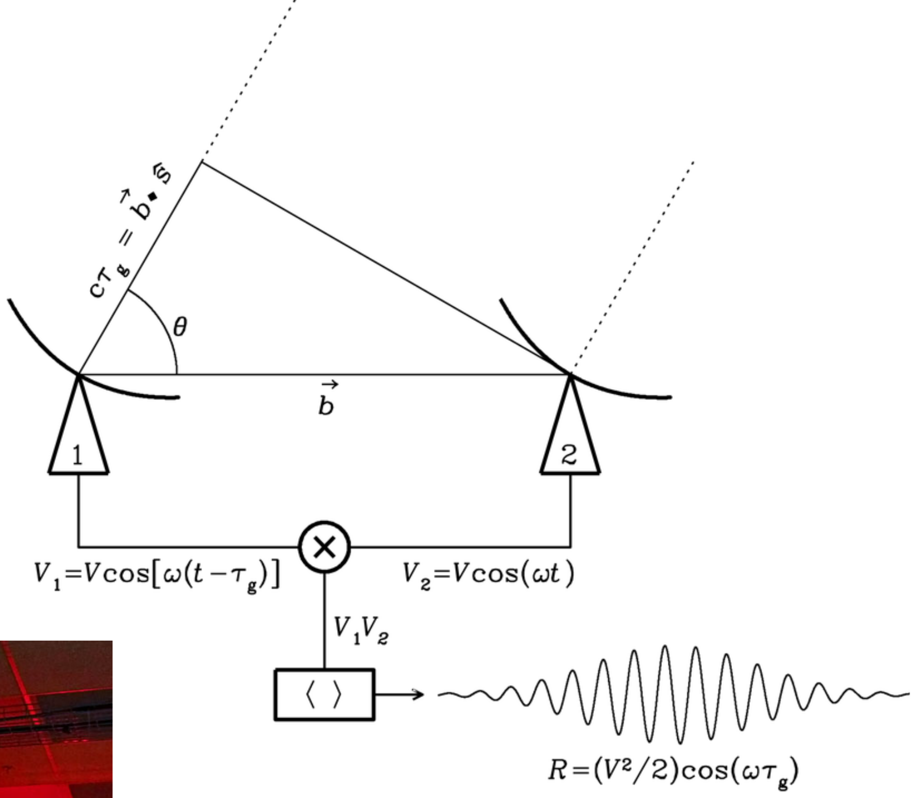

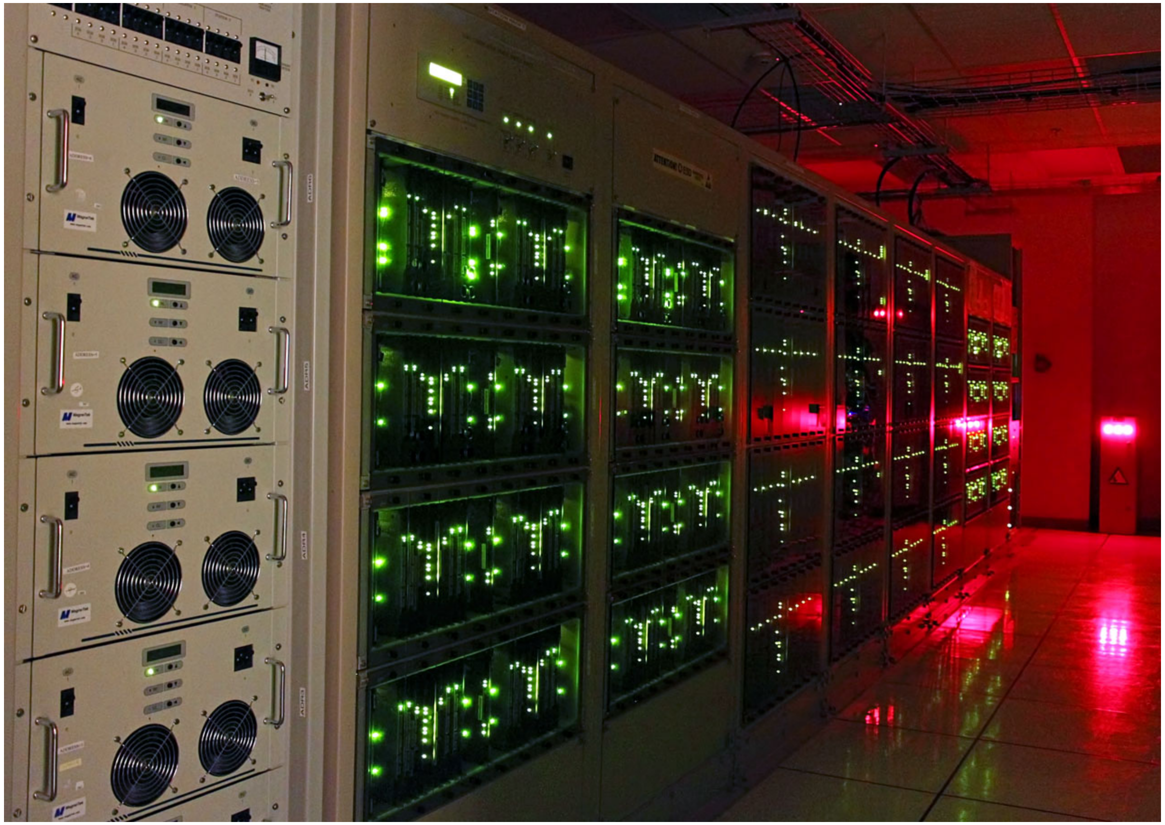

Output?

Mosaics

Why is mosaicking needed more @ ALMA frequencies?

If the region of interest is larger than the primary beam

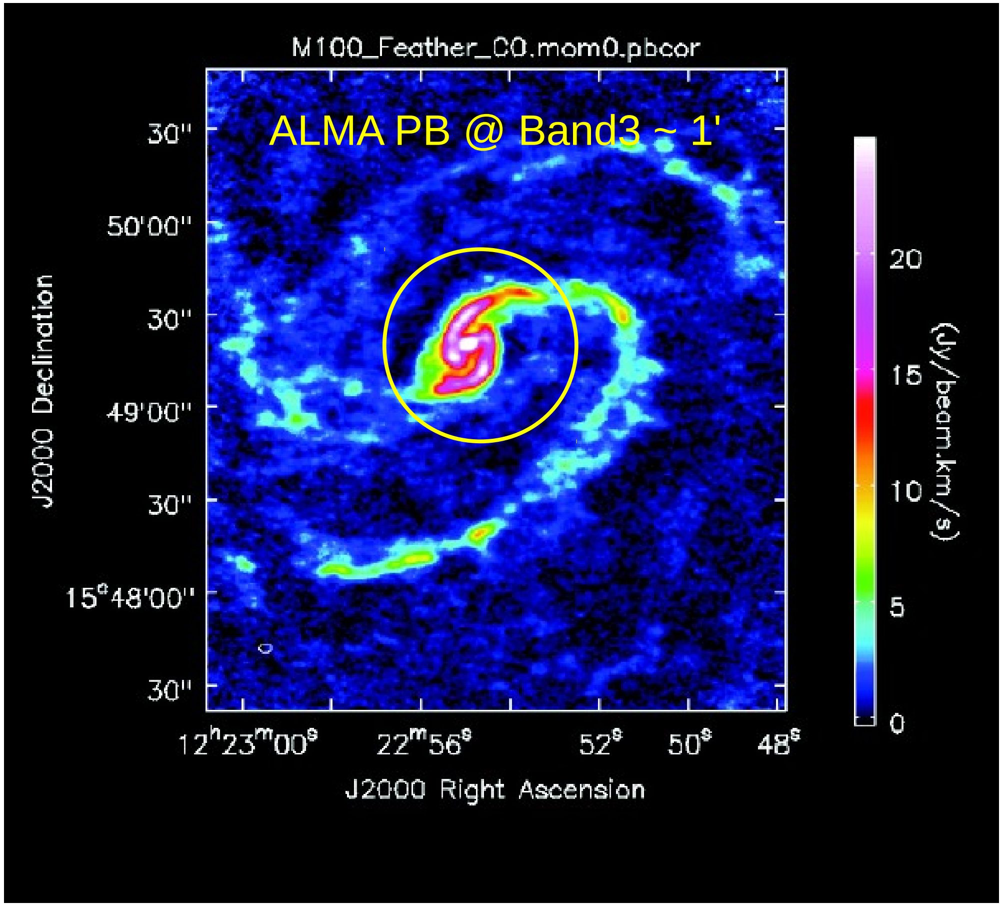

If the region of interest is larger than the primary beam

need to observe many overlapping pointings

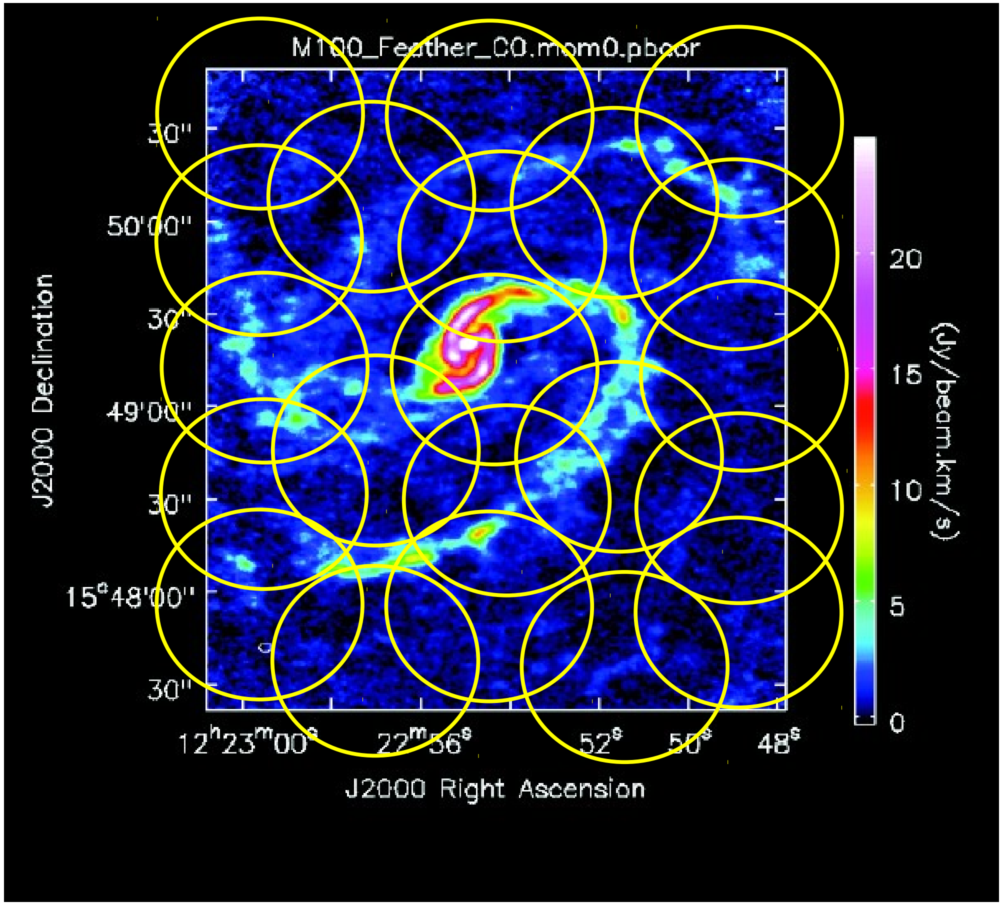

Interferometer correlators

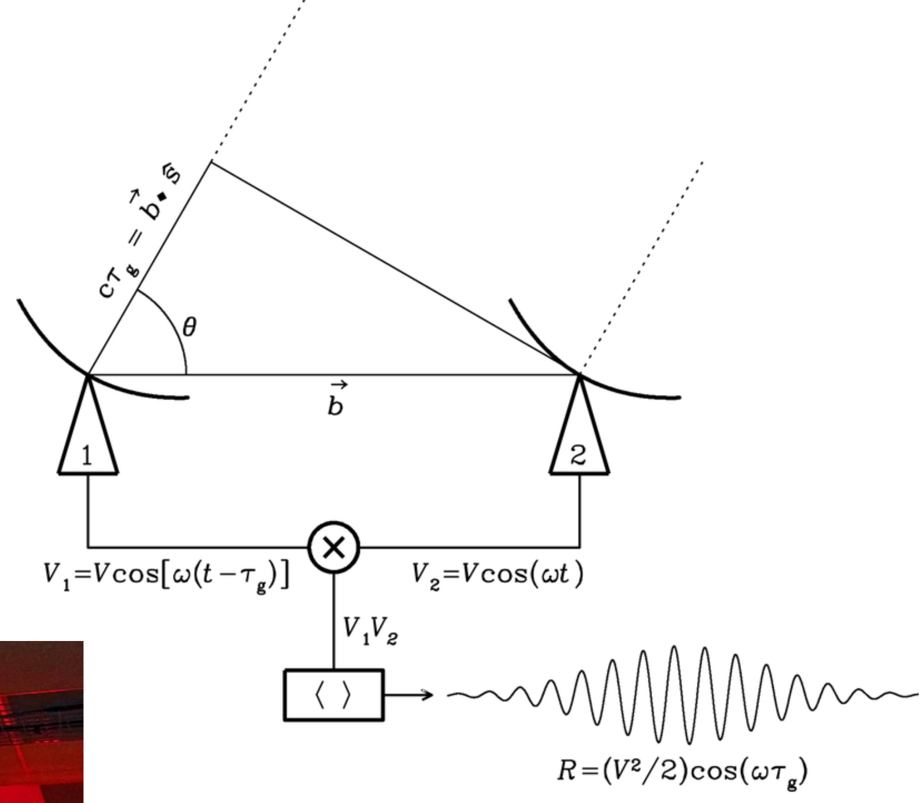

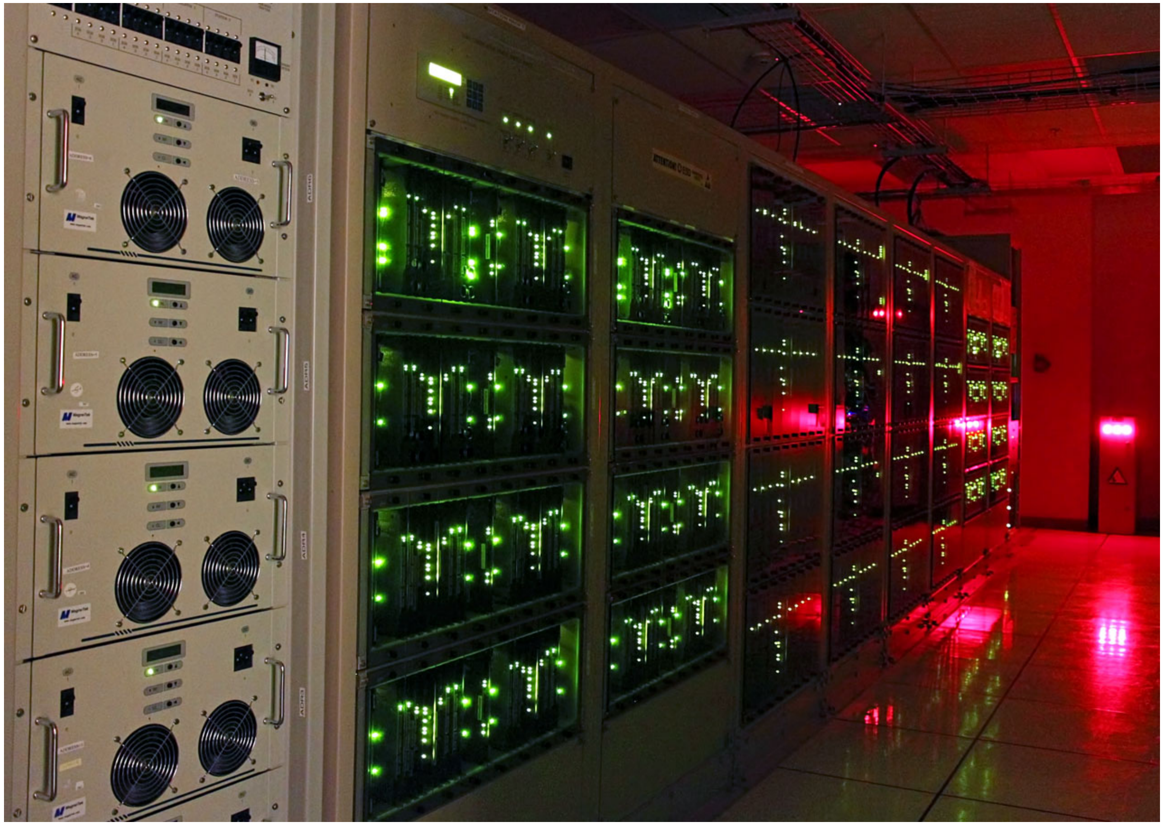

1 visibility

∀ ∀ **baseline**

∀ **time unit**

∀ **Frequency channel**

∀ **Polarization**

Calibration

In the interferometer the signals from two antennas are cross-correlated
each baseline measures one *visibility* (per int, per chan, per pol)

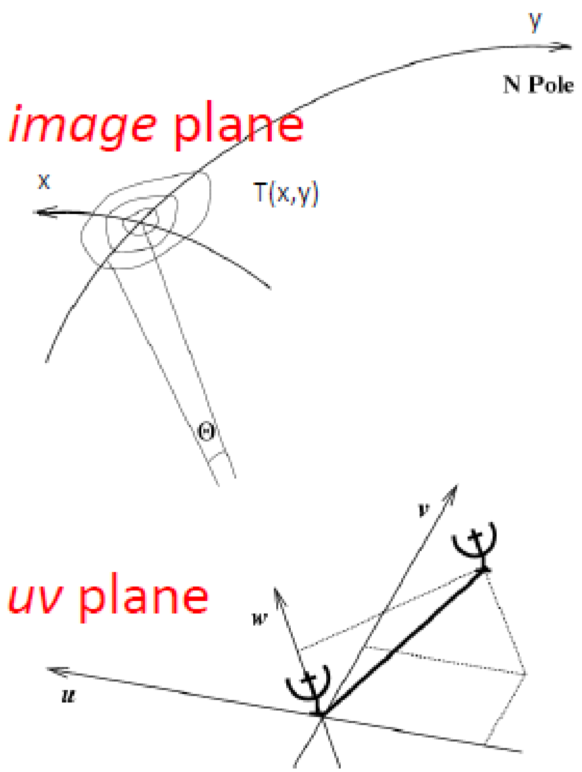

(van Cittert-Zernike theorem)

Fourier space/domain

$$V(u,v) = \int\int I(x,y)\, e^{2\pi i(ux+vy)} dx dy$$

$$I(x,y) = \int\int V(u,v) e^{-2\pi i(ux+vy)} du dv$$

Image space/domain

$I\ (x,y)$ = *source brightness*

$V(u,v) = FT\ I\ (x,y)$

If no calibration is applied....

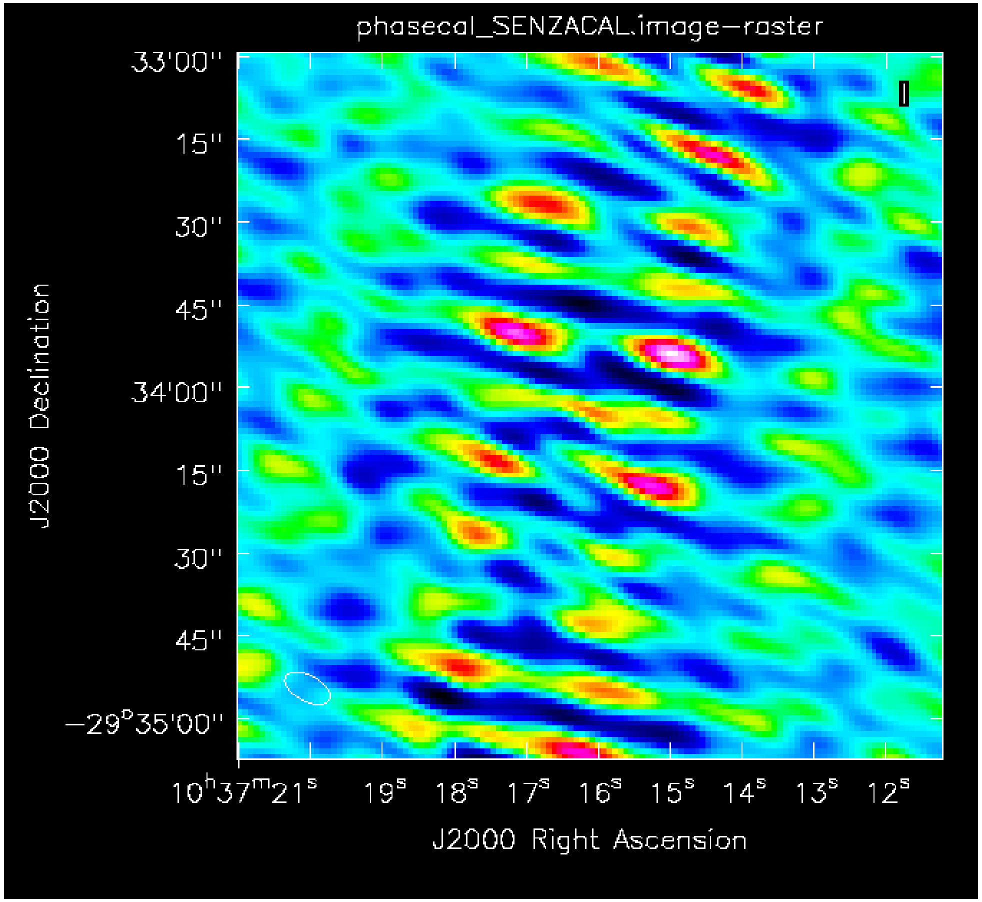

This would be the image of 1037-295 the calibrator of a dataset

deconvolving V^{ij}_{obs}

The actual source visibilities are corrupted while reaching the receiver by many factors

$$V^{ij}_{obs} = G^{ij} V^{ij}_{true}$$

$$\mathbf{G = K\ B\ J\ D\ E\ P\ T\ F}$$

F=ionosphere
T=troposphere
P=parallactic angle (alt-az mounting)
E=antenna voltage pattern
D=polarization leakages
J= electronic gains
B=bandpass response
K=geometric compensation

Antenna-based cross calibration

$$V^{ij}_{obs}(\nu,t) = G^{ij}(\nu,t) \quad V^{ij}_{true}(\nu,t)$$

The calibration is the process to determine the complex gains G^{ij}, with some assumptions

Most of the effects are antenna-based (pointing, focus, atmosphere, receiver noise, receiver bandpass)

$$V^{ij}_{obs} = G^{i} \; G^{*\,j} \; V^{ij}_{true}$$

Temporal dependence and frequency dependence are only lightly coupled so their variations can be determined independently or at least iteratively

$$G^{i}(\nu,t) = B^{i}(\nu) \, J^{i}(t)$$

We need to determine amplitude **a** and phase **θ** of the gains G, or **real** and **Imag** parts

$$A = \sqrt{(\Re^2 + \Im^2)}$$

$$\theta = \arctan\left(\frac{\Im}{\Re}\right)$$

$$A_{ij}^{obs} e^{i\,\phi_{ij}^{obs}} = A_{ij}^{true}\, a_i\, a_j\, e^{i\left(\phi_{ij}^{true} + \theta_i - \theta_j\right)}$$

N unknown

N(N-1) equations (being $V_{ij}=V_{ji}$)

Overdetermined problem

Closure Phase

Form total phase around 3 baselines

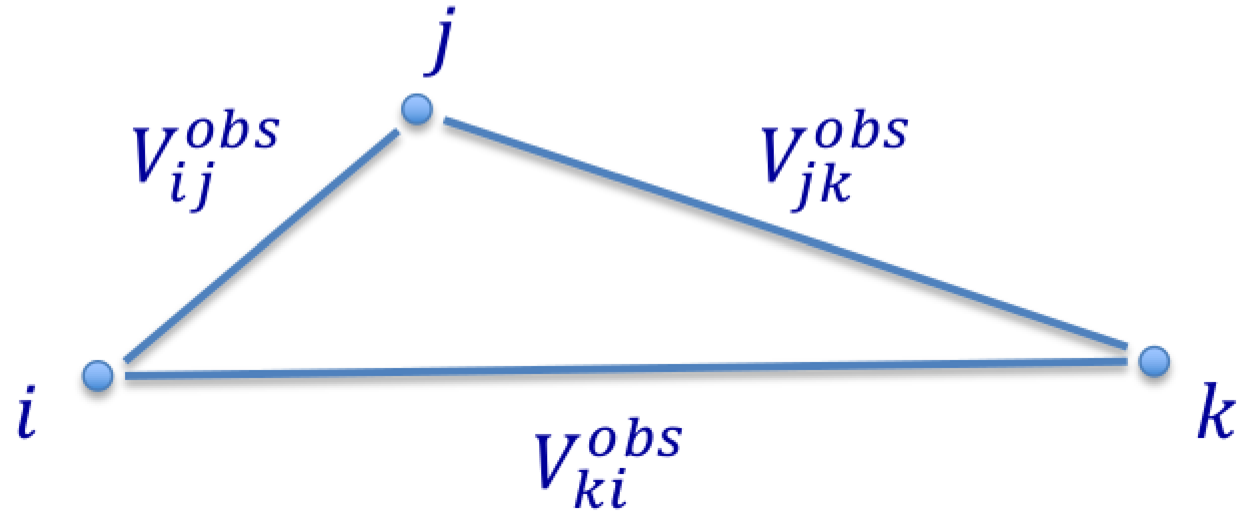

$$\phi_{ij}^{obs} + \phi_{jk}^{obs} + \phi_{ki}^{obs} = \phi_{ij}^{true} + \theta_i - \theta_j + \phi_{jk}^{true} + \theta_j - \theta_k + \phi_{ki}^{true} + \theta_k - \theta_i$$

=

$$= \phi_{ij}^{true} + \phi_{jk}^{true} + \phi_{ki}^{true}$$

Need to define a reference antenna, whose phase for both polarization is arbitrarily fixed to 0.
Typically choose an antenna at the center of the array.

Closure Amplitude

Form ratios of amplitudes products from 4 baselines

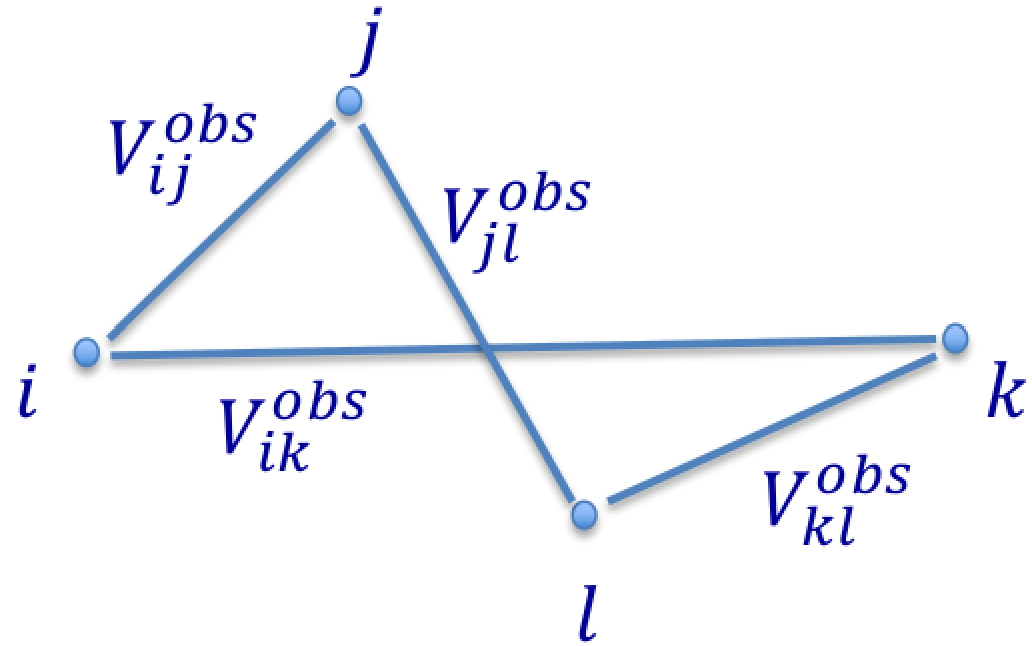

$$\frac{A_{ij}^{obs} A_{kl}^{obs}}{A_{ik}^{obs} A_{jl}^{obs}} = \frac{a_i a_j A_{ij}^{true} a_k a_l A_{kl}^{true}}{a_j a_k A_{ik}^{true} a_j a_l A_{jl}^{true}} = \frac{A_{ij}^{true} A_{kl}^{true}}{A_{ik}^{true} A_{jl}^{true}}$$

To solve the equations we observe sources for which we know the real visibilities: **calibrators**

$$V^{ij}_{obs} = G^{ij} \quad V^{ij}_{model}$$

$$A^{ij}_{obs} e^{i\theta^{ij}_{obs}} = A^{ij}_{model} a^i a^j e^{i(\theta^{ij}_{model} + \theta^i - \theta^j)}$$

We choose bright sources when possible, we know A^{ij}_{model}

We observe them at the phase center we know θ^{ij}_{model}

Bandpass calibration

$$G^i(\nu,t) = B^i(\nu)\,J^i(t)$$

- Calibrate for the response in frequency of each antenna ...basically, electronics
- Observations of a bright QSO (typically at the beginning of the observation)
- Amplitude constant within the band
- Observing time long enough to reach high S/N on each channel

Bandpass calibration

Observing at the **phase center** a source with known model

$$A_{mod}(\nu) = 1 \text{ and } \theta_{mod}(\nu) = 0$$

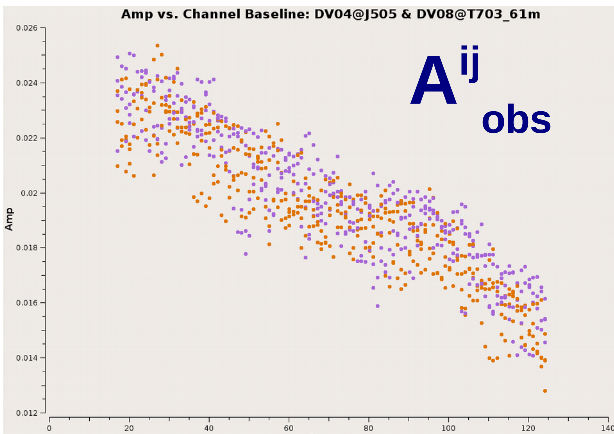

$$A^{ij}_{obs} = B^{i}\ B^{j}\ A^{ij}_{mod}$$

$$A^{ij}_{cal} = \frac{A^{ij}_{obs}}{B^{i}\ B^{j}}$$

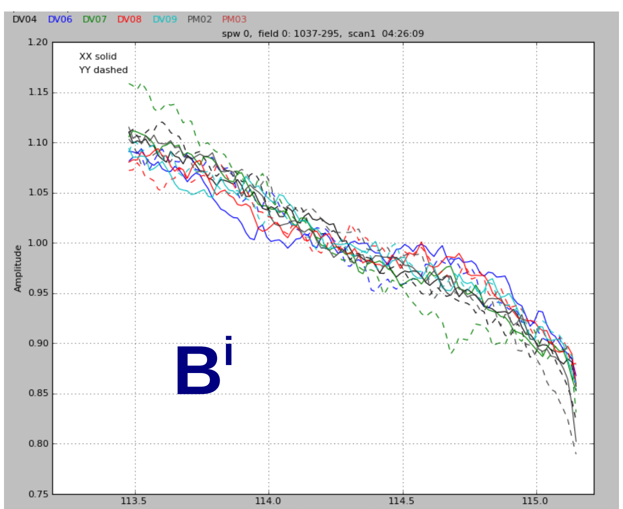

amplitude

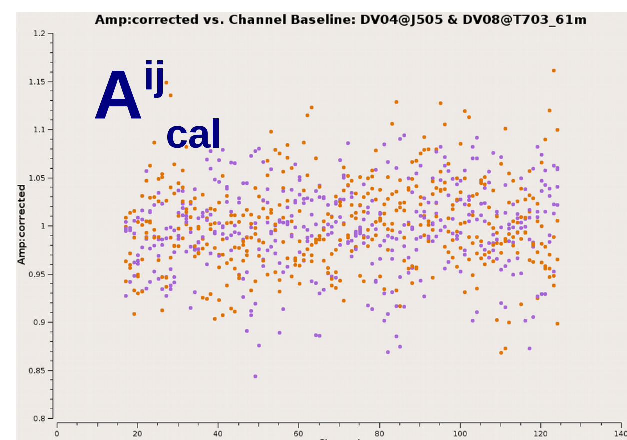

Bandpass calibration

Observing at the **phase center** a source with known model

$$A_{mod}(\nu) = 1 \text{ and } \theta_{mod}(\nu) = 0$$

θ^{ij}_{obs}

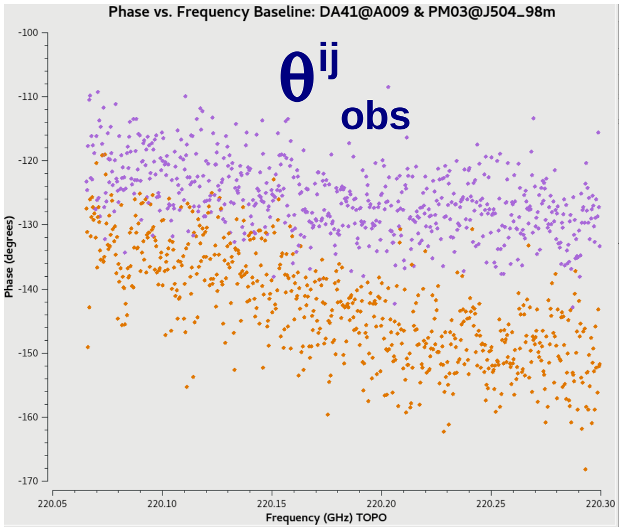

$$\theta^{ij}_{obs} = \theta^{i} + \theta^{j} + \theta^{ij}_{mod}$$

$$\theta^{ij}_{cal} = - \theta^{i} - \theta^{j} + \theta^{ij}_{obs}$$

θ^{i}

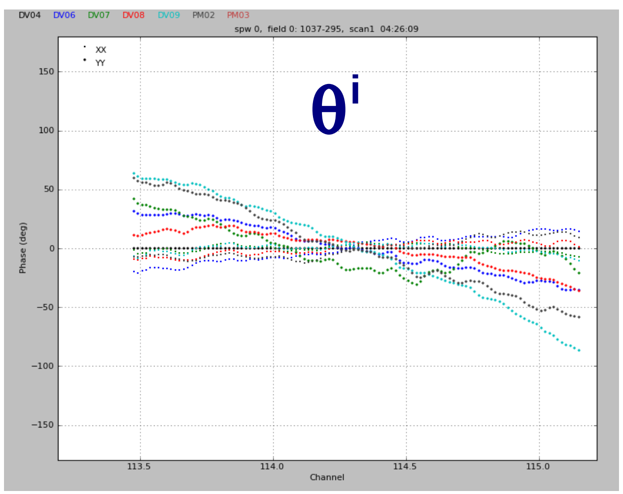

phase

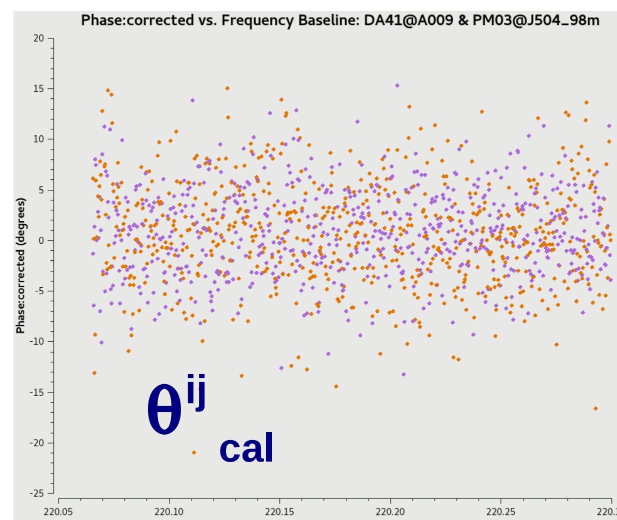

θ^{ij}_{cal}

Gain calibration

$$G^i(\nu,t) = B^i(\nu)\, J^i(t)$$

- Calibrate for the long time scale dependent response of each antenna
  ...basically, atmosphere
- Observations of a point like source (QSO)
- As close as possible to the target (< 4 deg)

Gain calibration

$$G^i(\nu,t) = B^i(\nu)\, J^i(t)$$

- Observed regularly before and after target scans

As for the bandpass
The calibrator is observed
at the **phase center**

$$\mathbf{A_{mod}(t) = 1 \quad and \quad \theta_{mod}(t) = 0}$$

We can determine **for each scan** on the calibrator the amplitude correction J^i_A and the phase correction J^i_θ

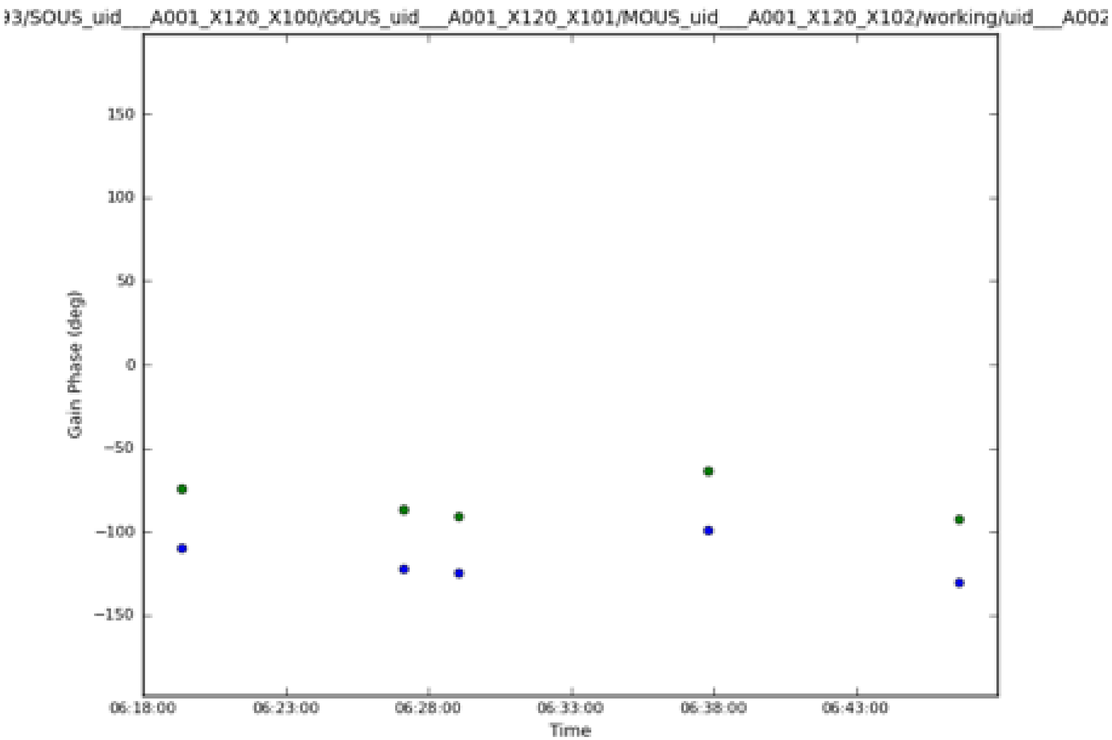

Gain calibration

$$G^i(\nu,t) = B^i(\nu)\, J^i(t)$$

- Observed regularly before and after target scans
- Coherence time
- Solutions J^i_A and J^i_θ applied to the target using a **linear interpolation**

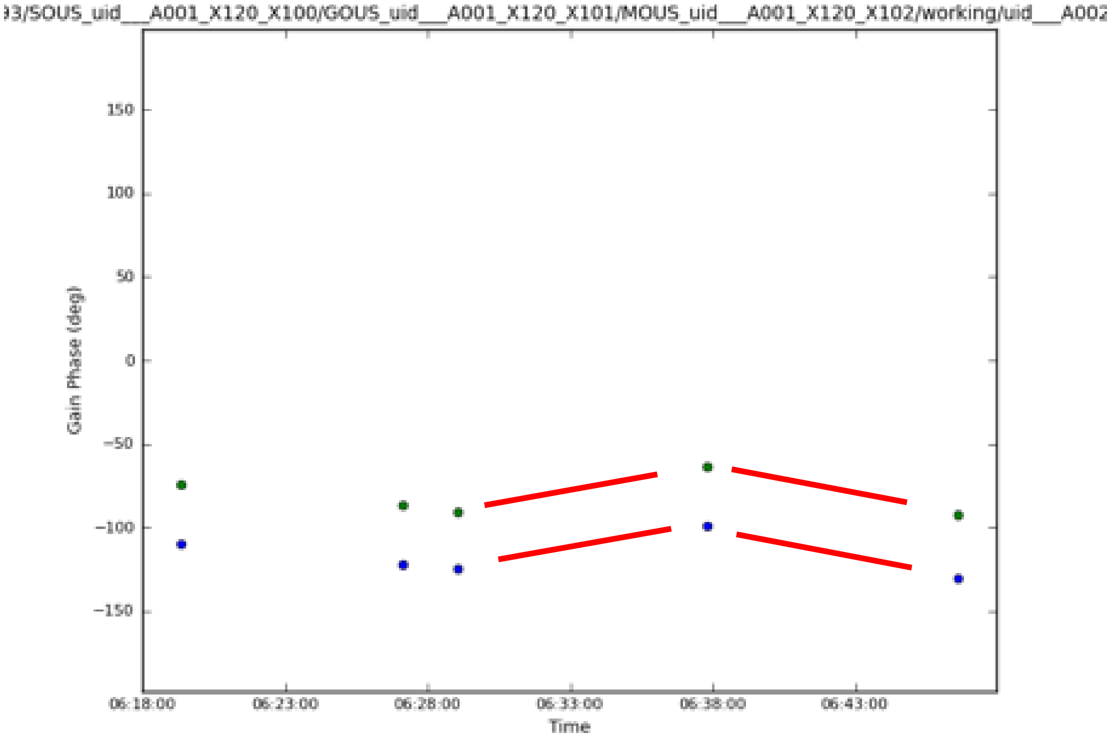

Amplitude calibration

- Define the Jy/K scale
  basically antenna efficiency

- Observations of a non variable object
  (typically at the beginning of the observation)

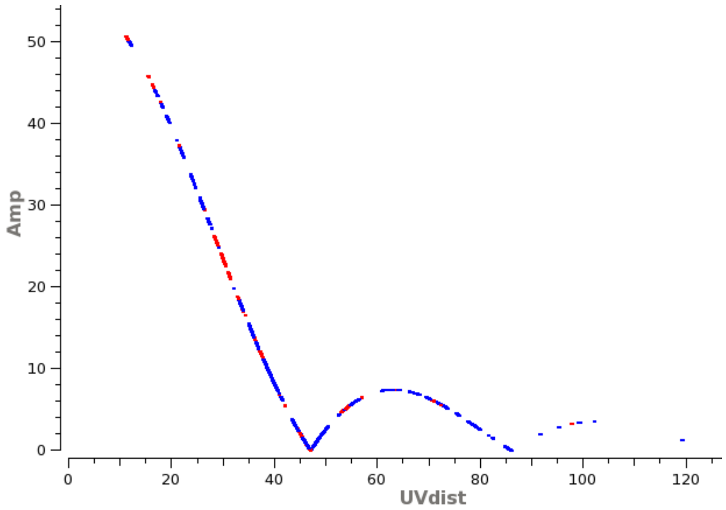

- No matter where in the sky

- The scale is calculated for the flux calibrator and transferred
  to bandpass and phase calibrator

After calibration

deconvolving V^{ij}_{cal}

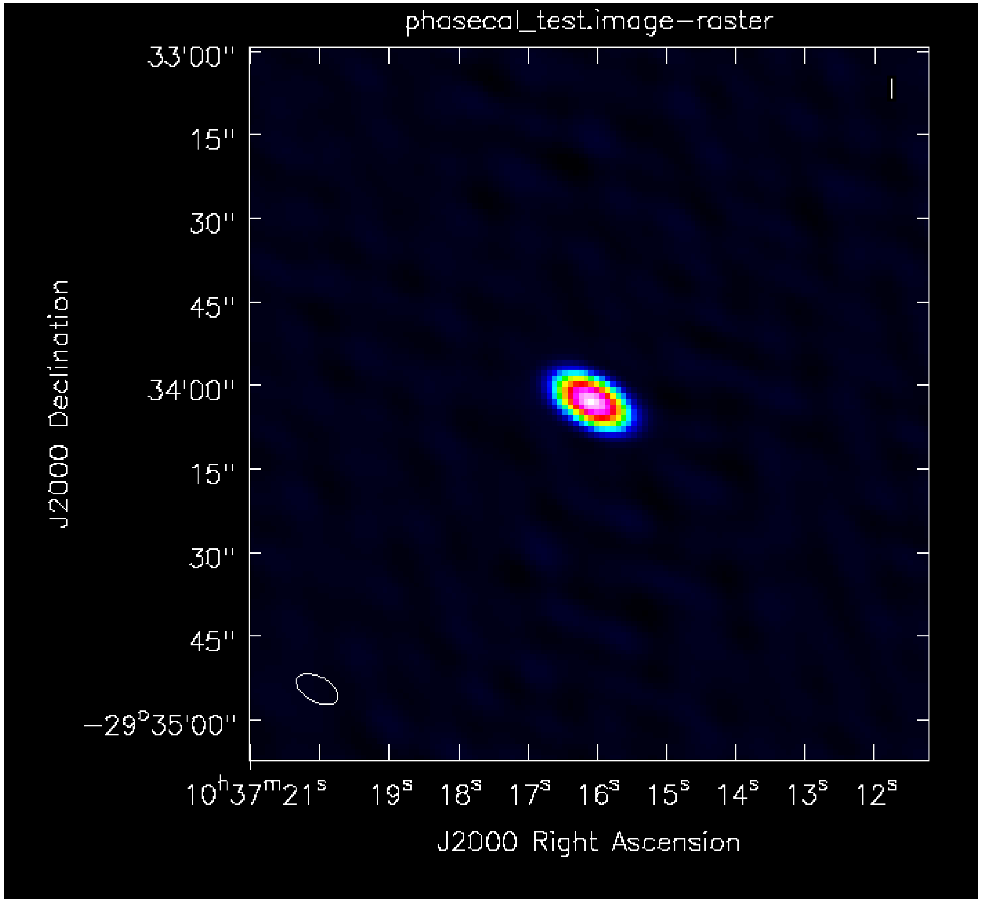

Imaging

Interferometry basics

In the next two weeks we are going to deal with

visibilities and **uv plane**

To get familiar with them you can play with

- a java applet online:

http://www.narrabri.atnf.csiro.au/astronomy/vri.html

- or a python script written by Ivan Marti-Vidal (nordic ARC node) APSYNSIM

https://launchpad.net/apsynsim

- Pynterferometer written by Adam Avison and Sam George

http://www.jb.man.ac.uk/pynterferometer/index.html

Interferometry basics

1 D

1. The pulse: $\delta\,(x - x_o)$

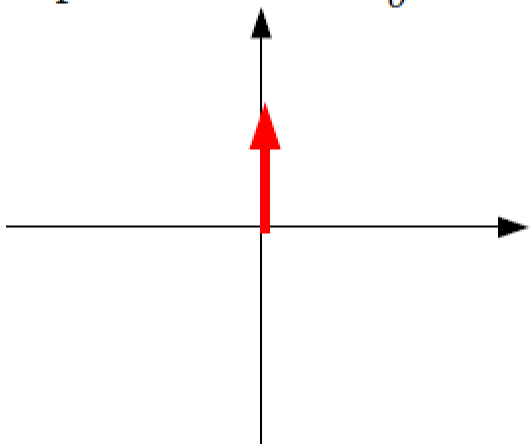

Dirac function

$\mathcal{FT}$?

Fourier Transform

Interferometry basics

1 D

1. The pulse: $\delta(x - x_o)$

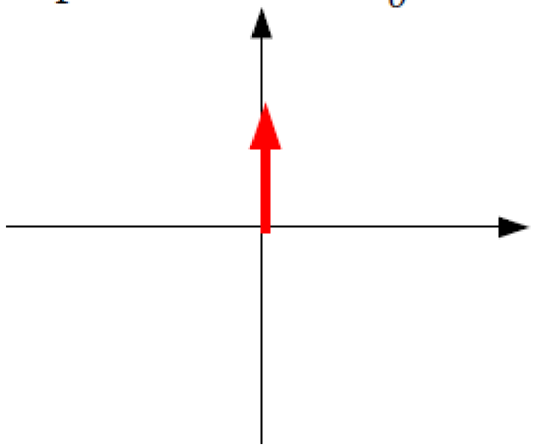

Dirac function

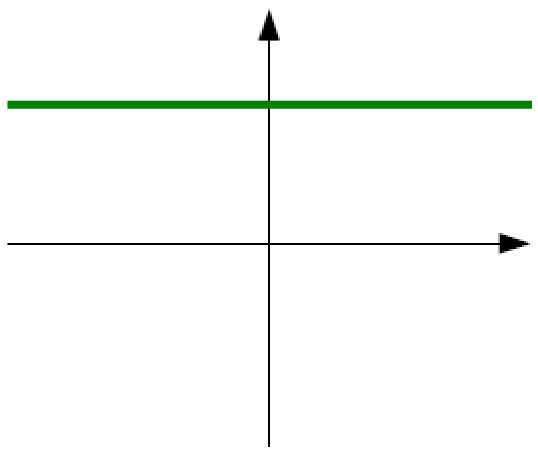

Fourier Transform

Interferometry basics

1 D

2 D

1. *The pulse:* $\delta(x - x_o)$

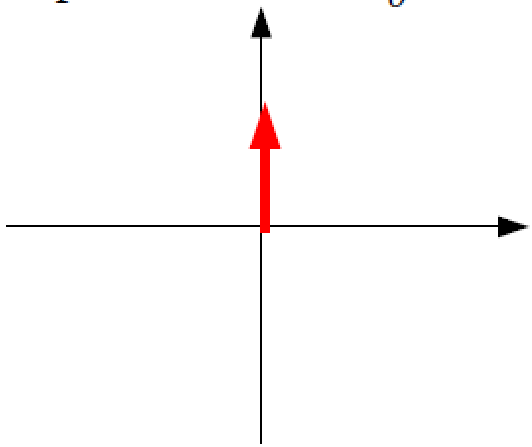

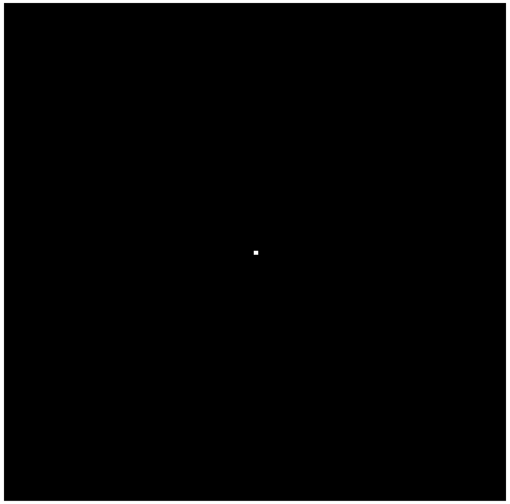

Point source in the sky

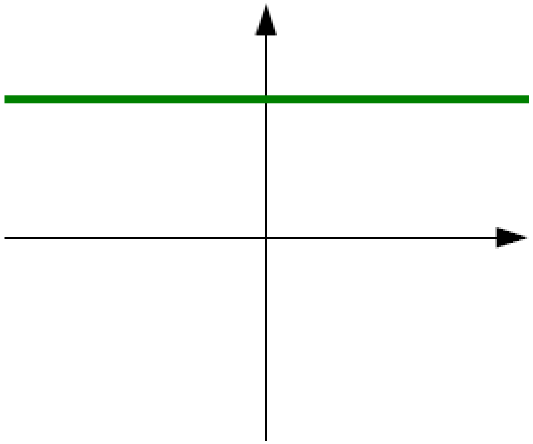

$\mathcal{FT}$?

Ideal uv plane

Interferometry basics

1 D **2 D**

1. *The pulse:* $\delta\,(x - x_o)$

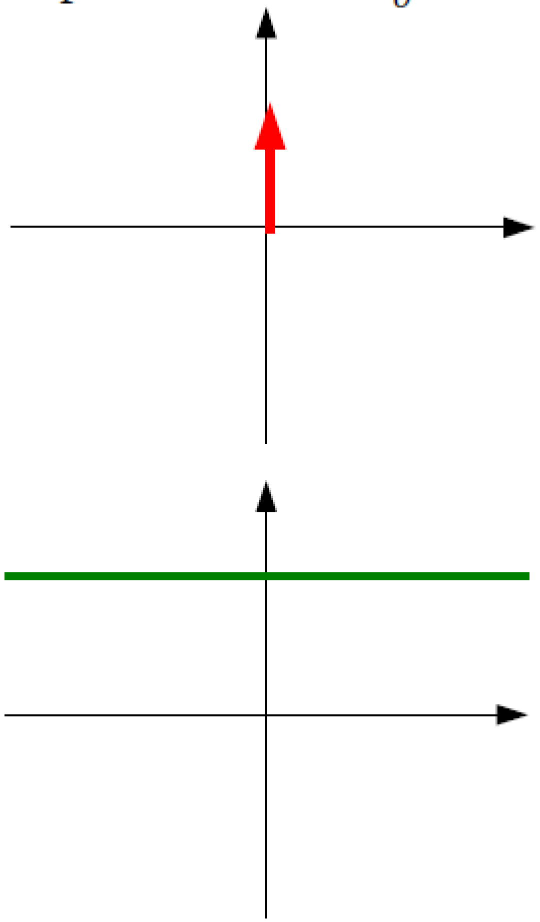

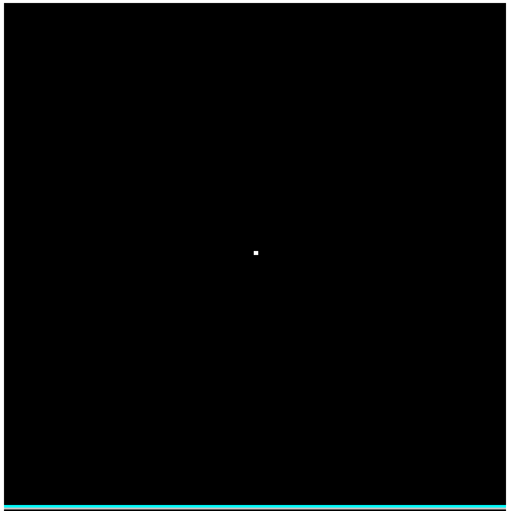

Point source in the sky

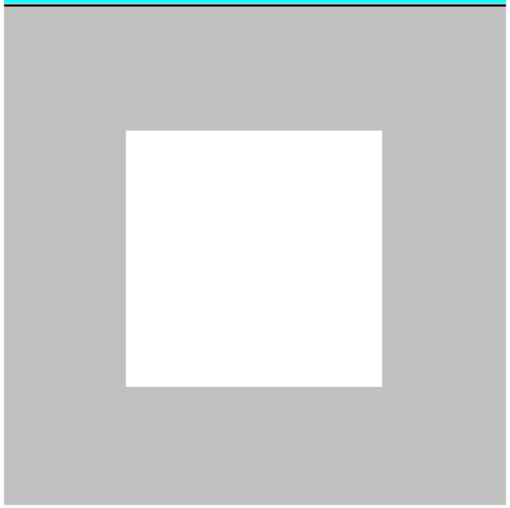

Ideal uv plane

Interferometry basics

Snapshot observation
with two antennas
1 baseline

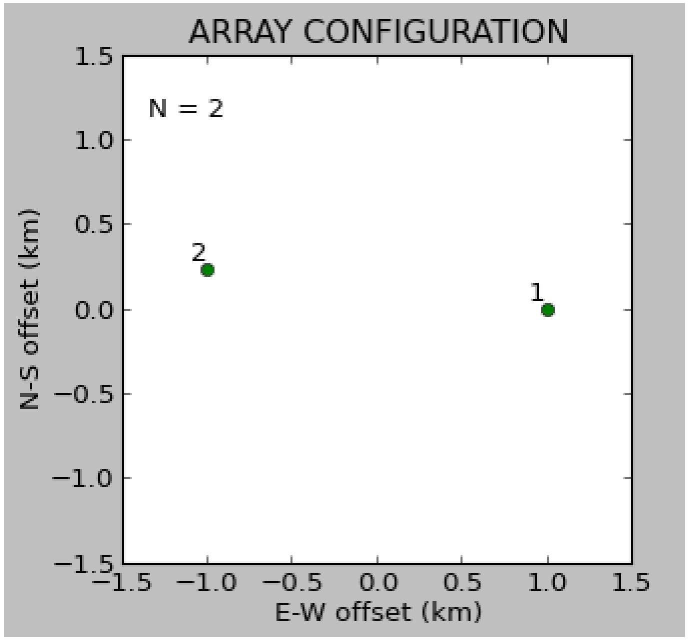

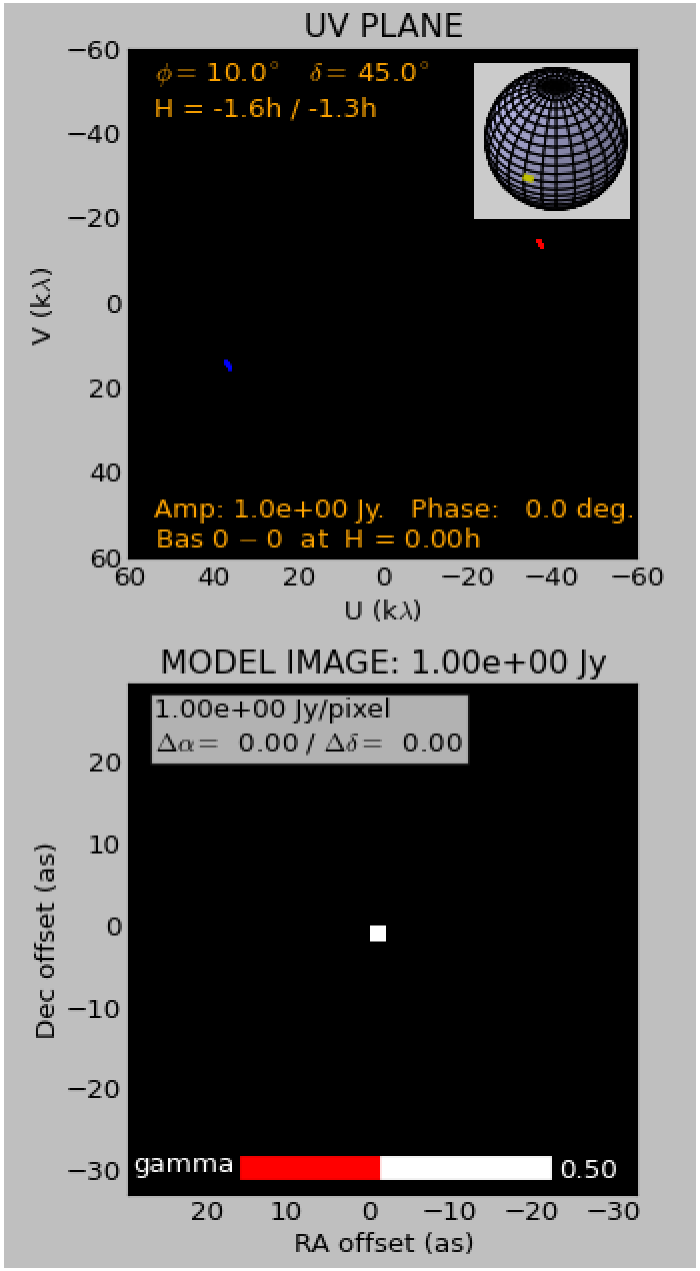

← uv-coverage

Resulting image

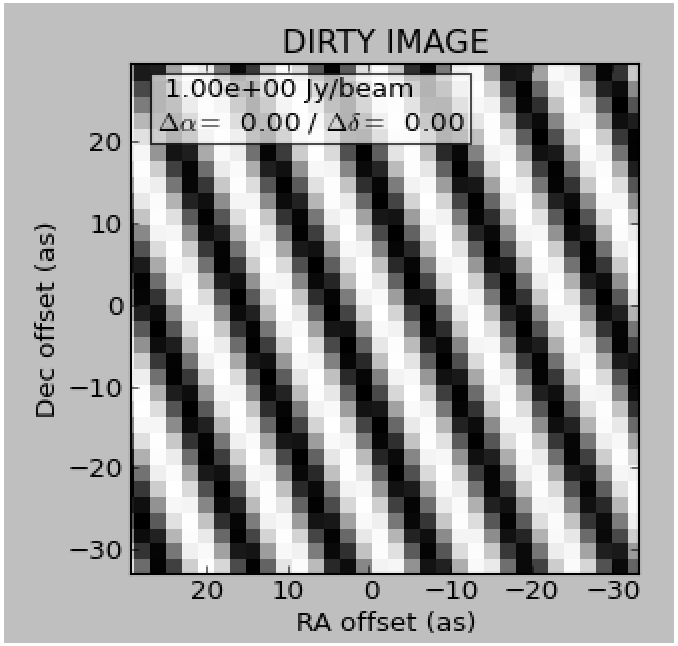

Interferometry basics

8 hrs observation
with two antennas
1 baseline (~2 km)

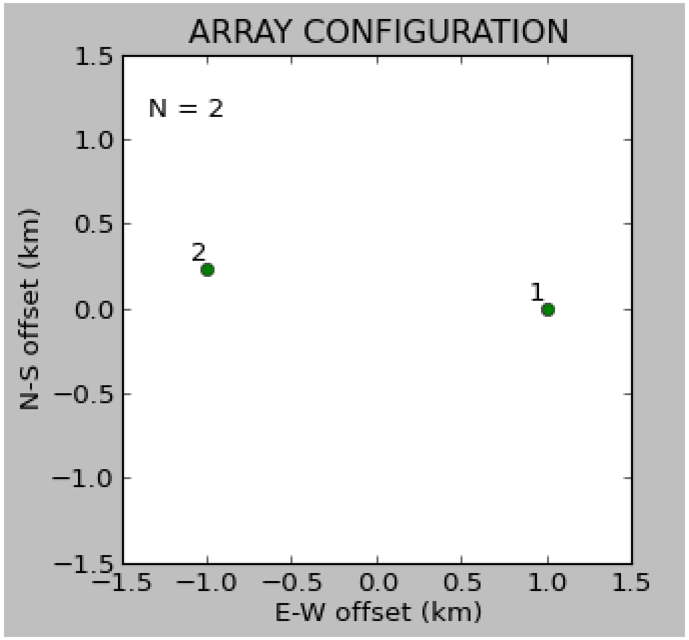

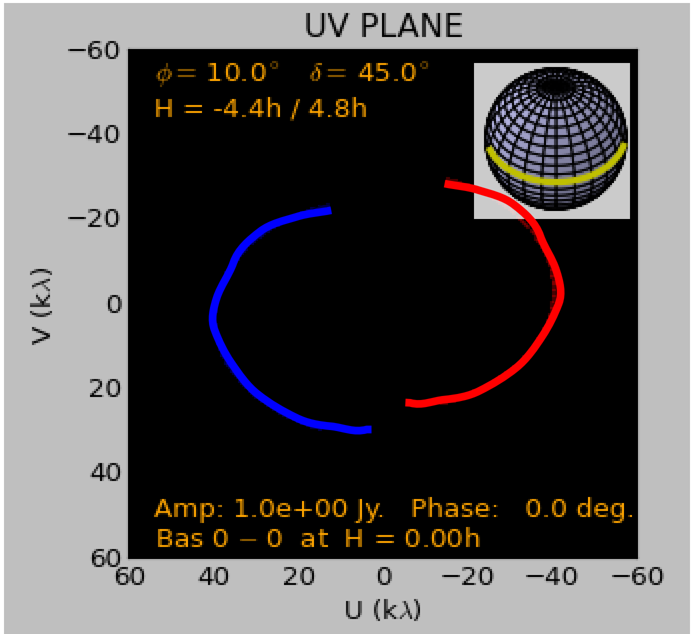

← uv-coverage

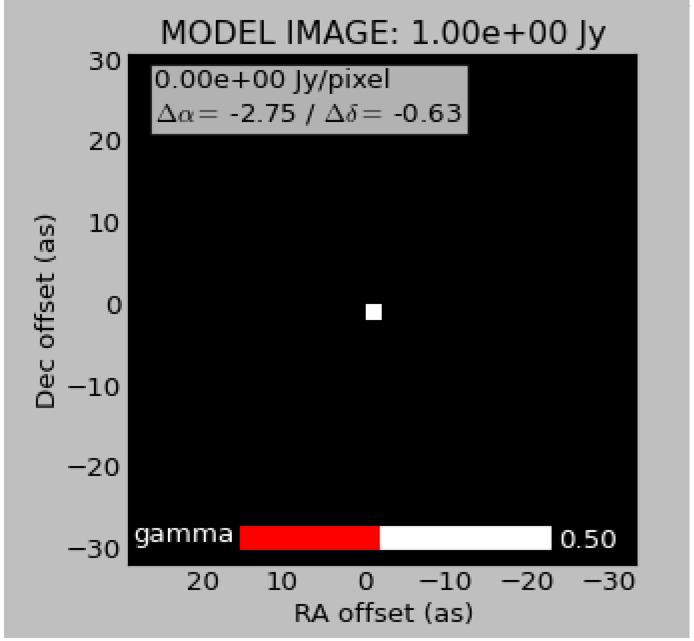

Resulting image

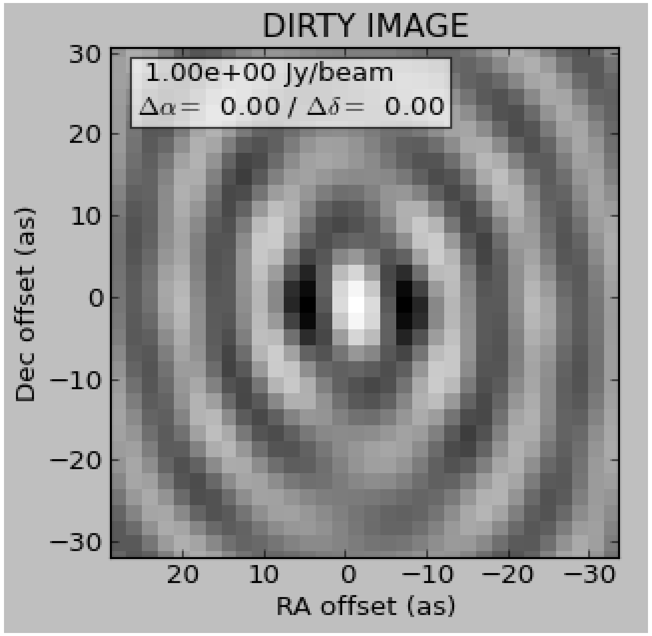

Interferometry basics

8 hrs observation
with two antennas
1 baseline (~800 m)

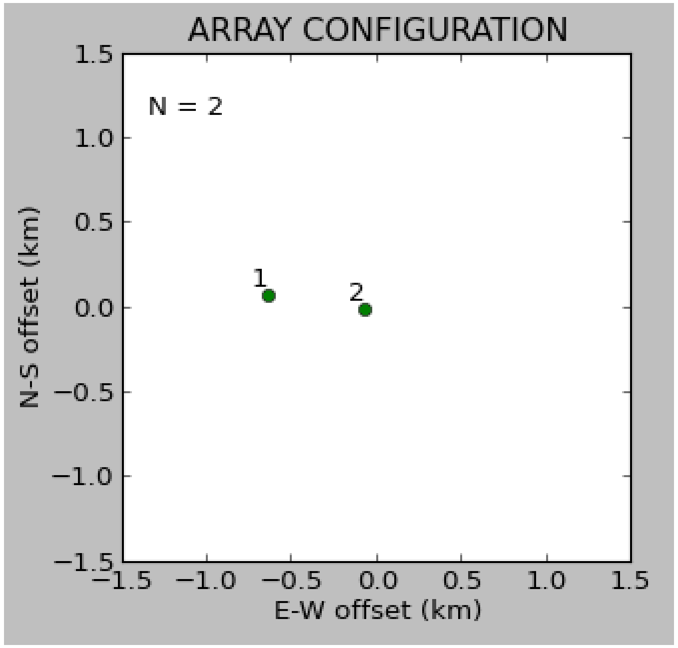

If antennas are closer?

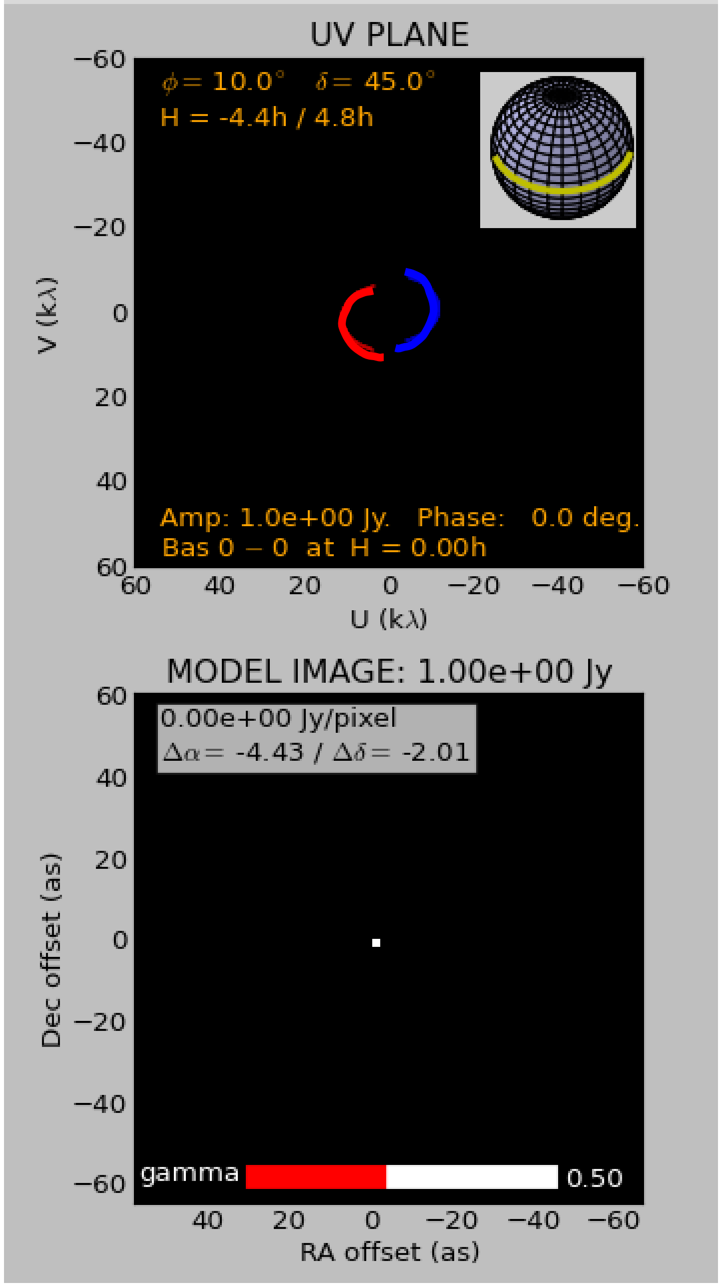

← **uv-coverage**

Resulting image

Interferometry basics

8 hrs observation
with two antennas
1 baseline (~800 m)

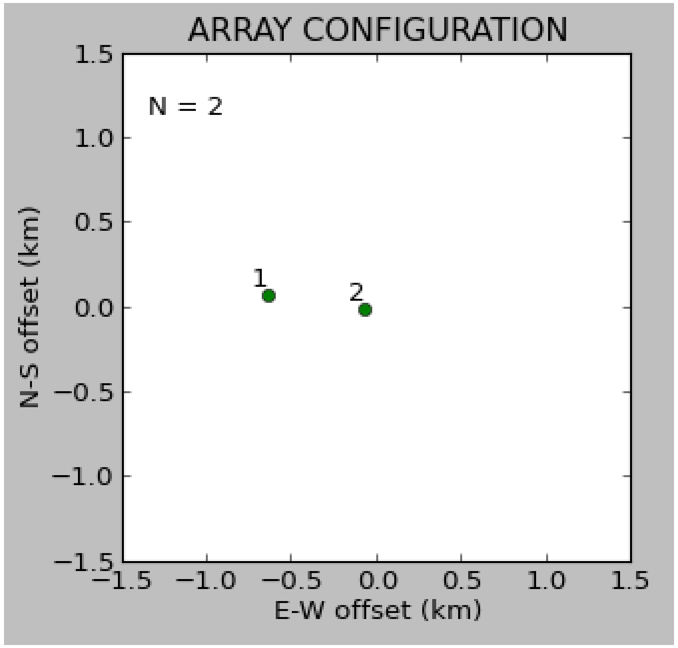

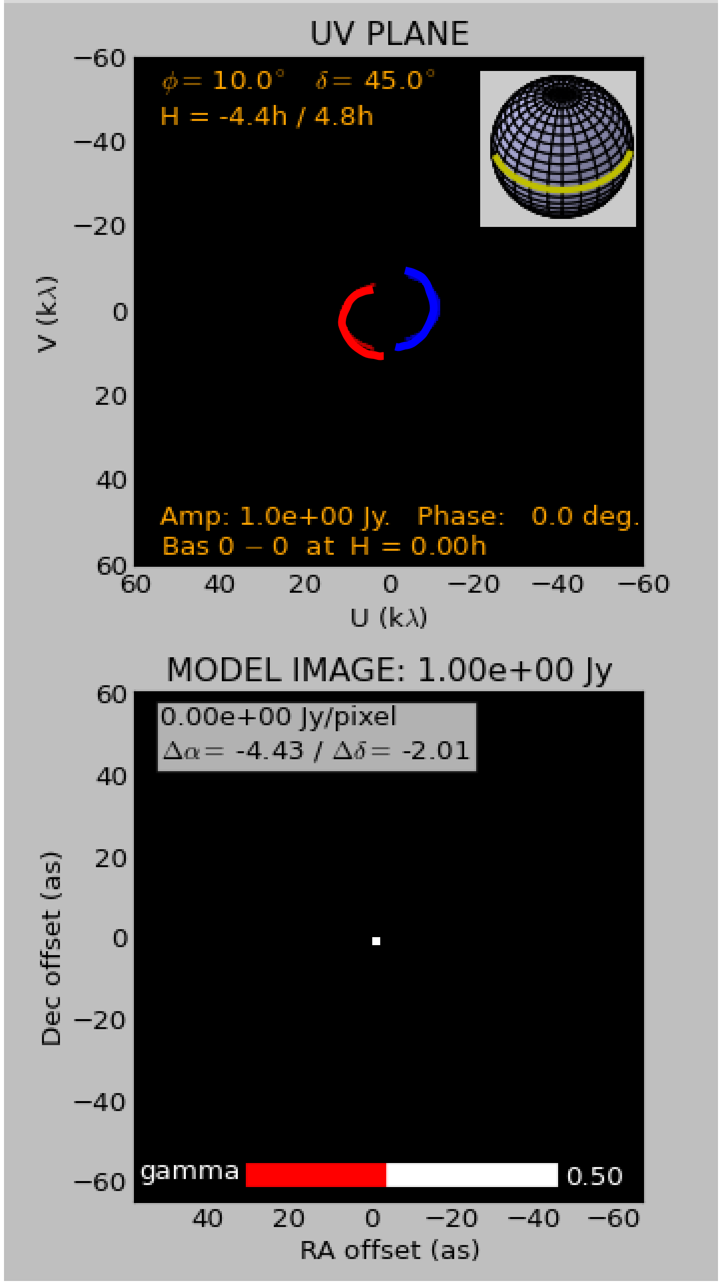

← uv-coverage

Resulting image

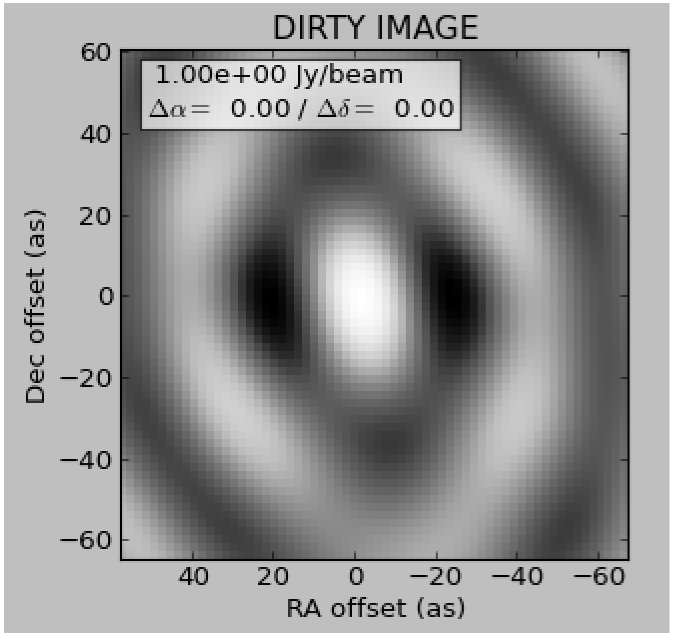

Interferometry basics

Snapshot observation with 36 antennas 1260 baselines

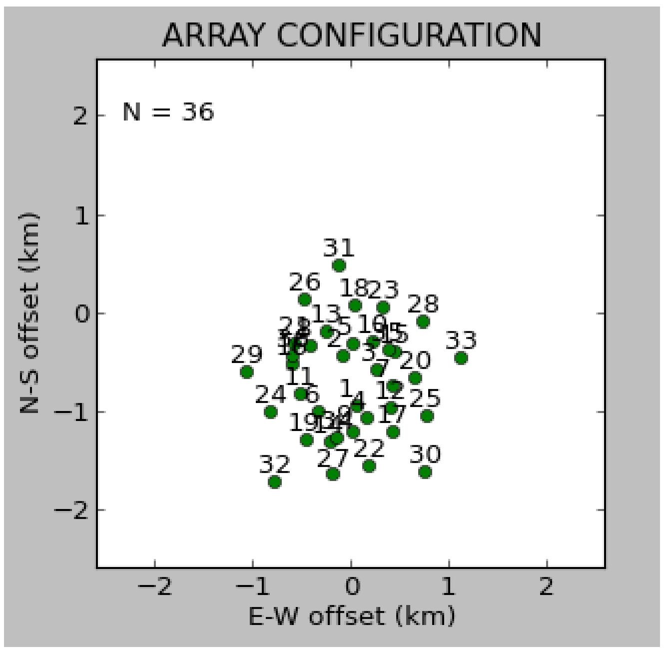

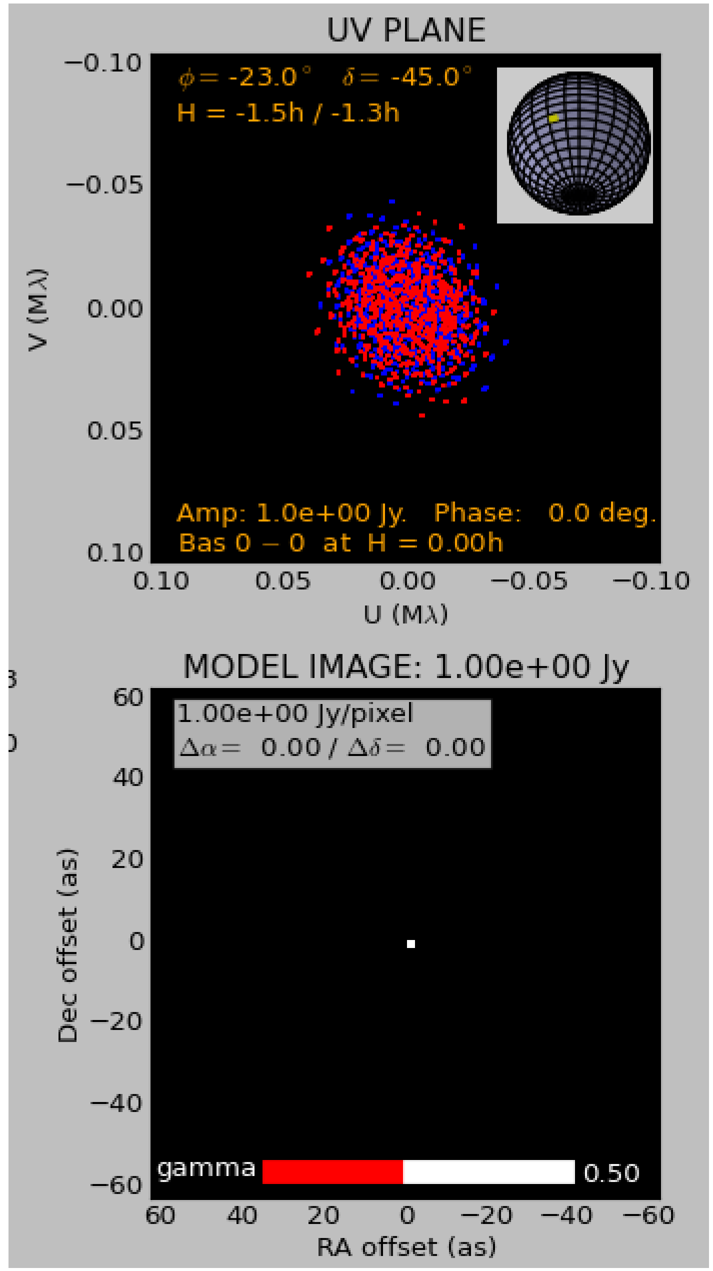

← uv-coverage

Resulting image

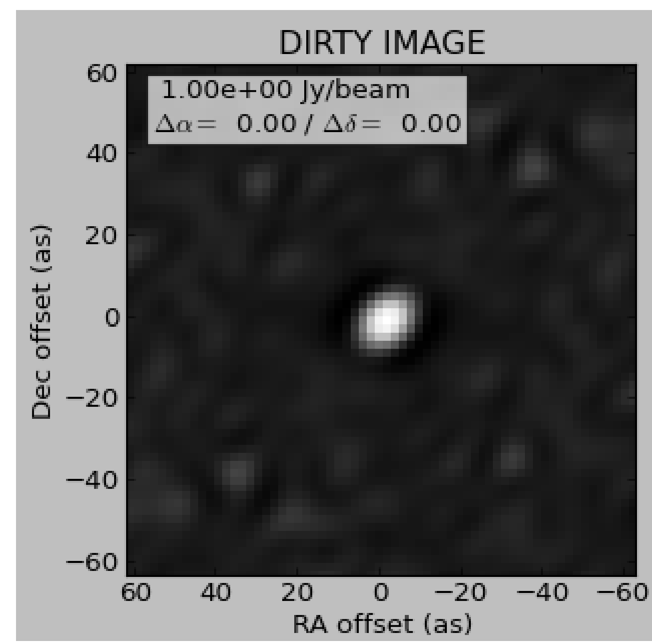

Aperture synthesis
Long observations make the Dirty beam better approximate a gaussian

Slides from IRAM school

Dirty Beam Shape and Number of Antenna:
2 Antenna

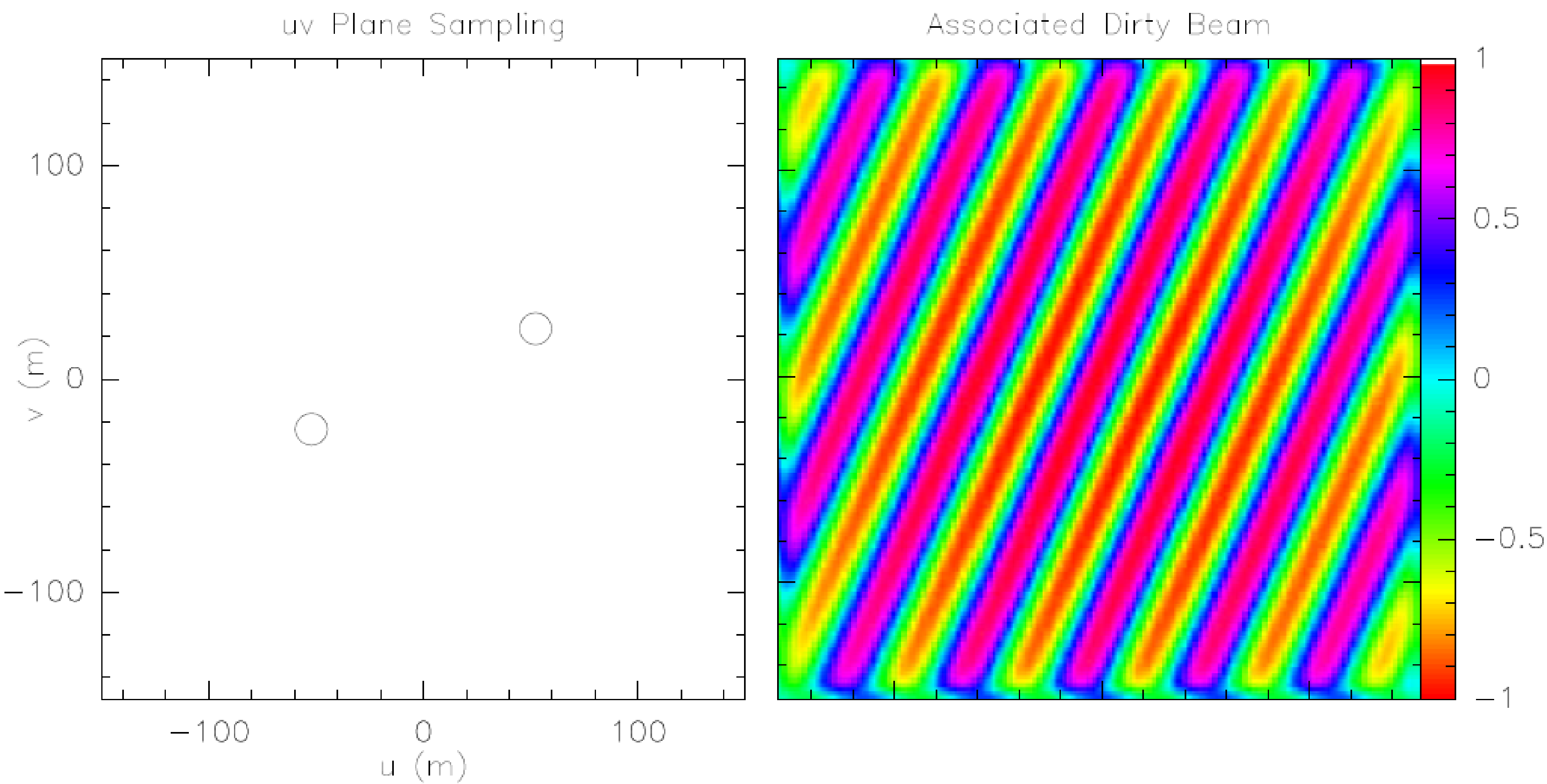

Dirty Beam Shape and Number of Antenna:
3 Antenna

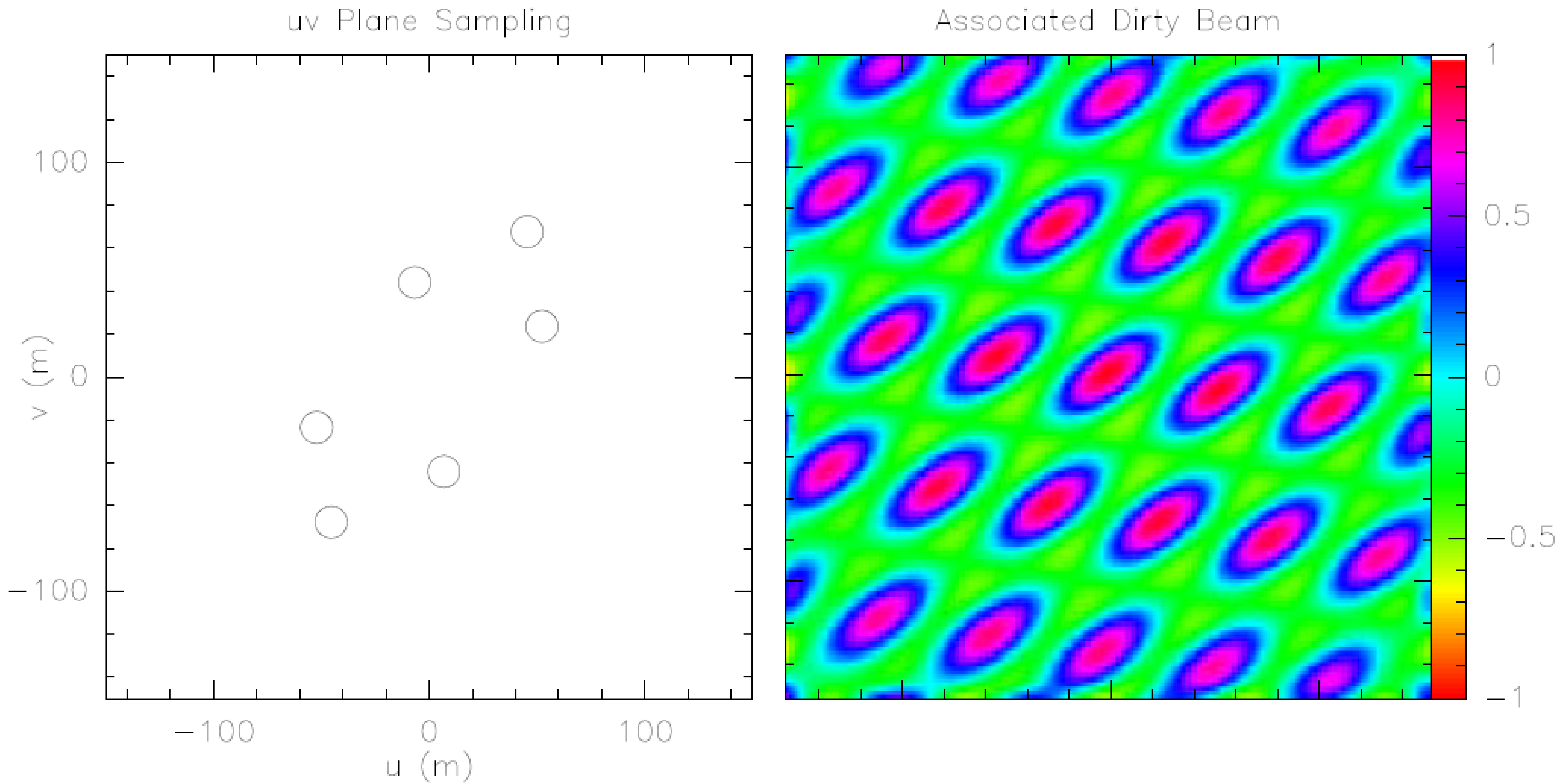

Dirty Beam Shape and Number of Antenna:
4 Antenna

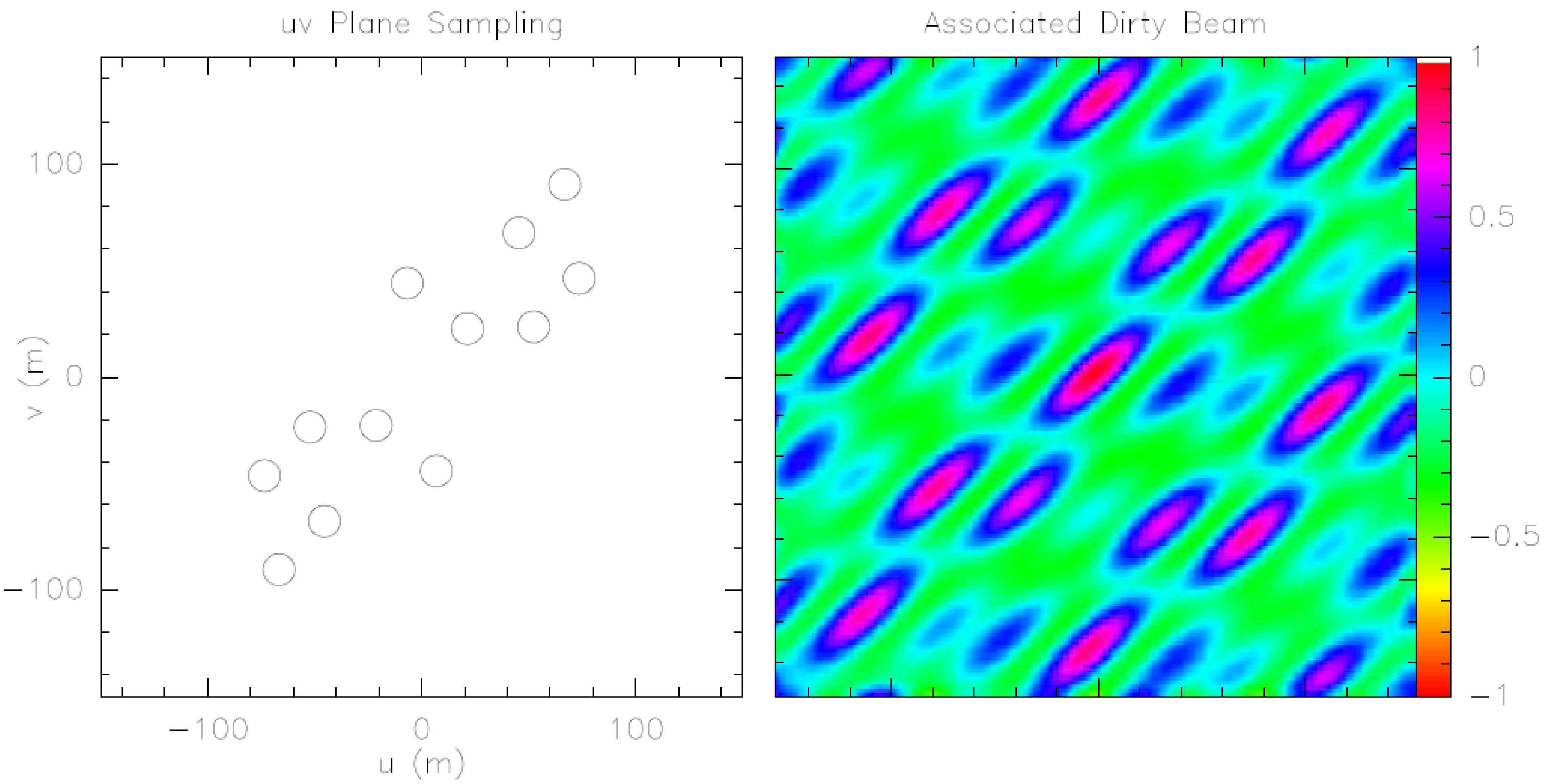

Dirty Beam Shape and Number of Antenna:
5 Antenna

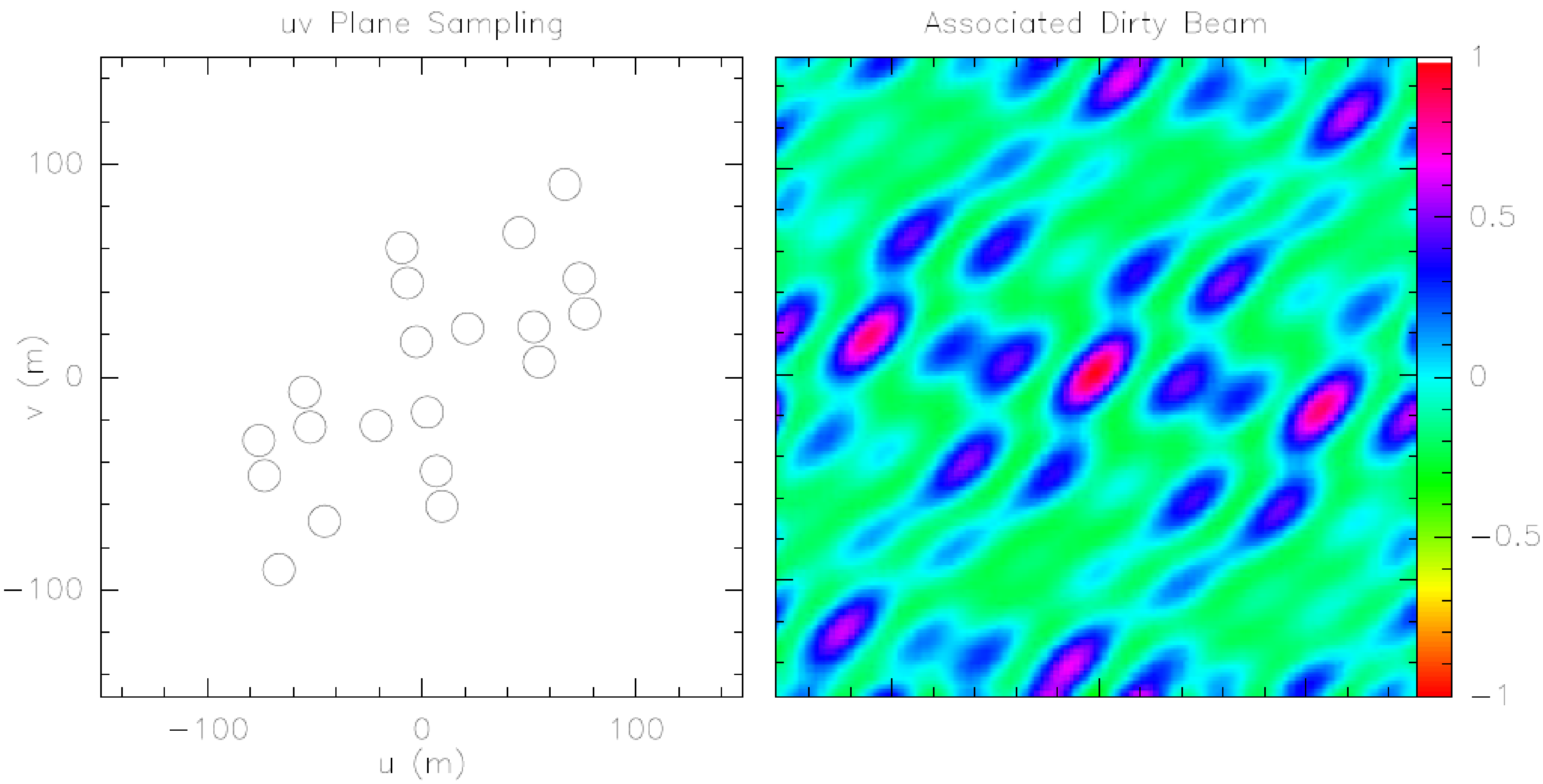

Dirty Beam Shape and Number of Antenna:
6 Antenna

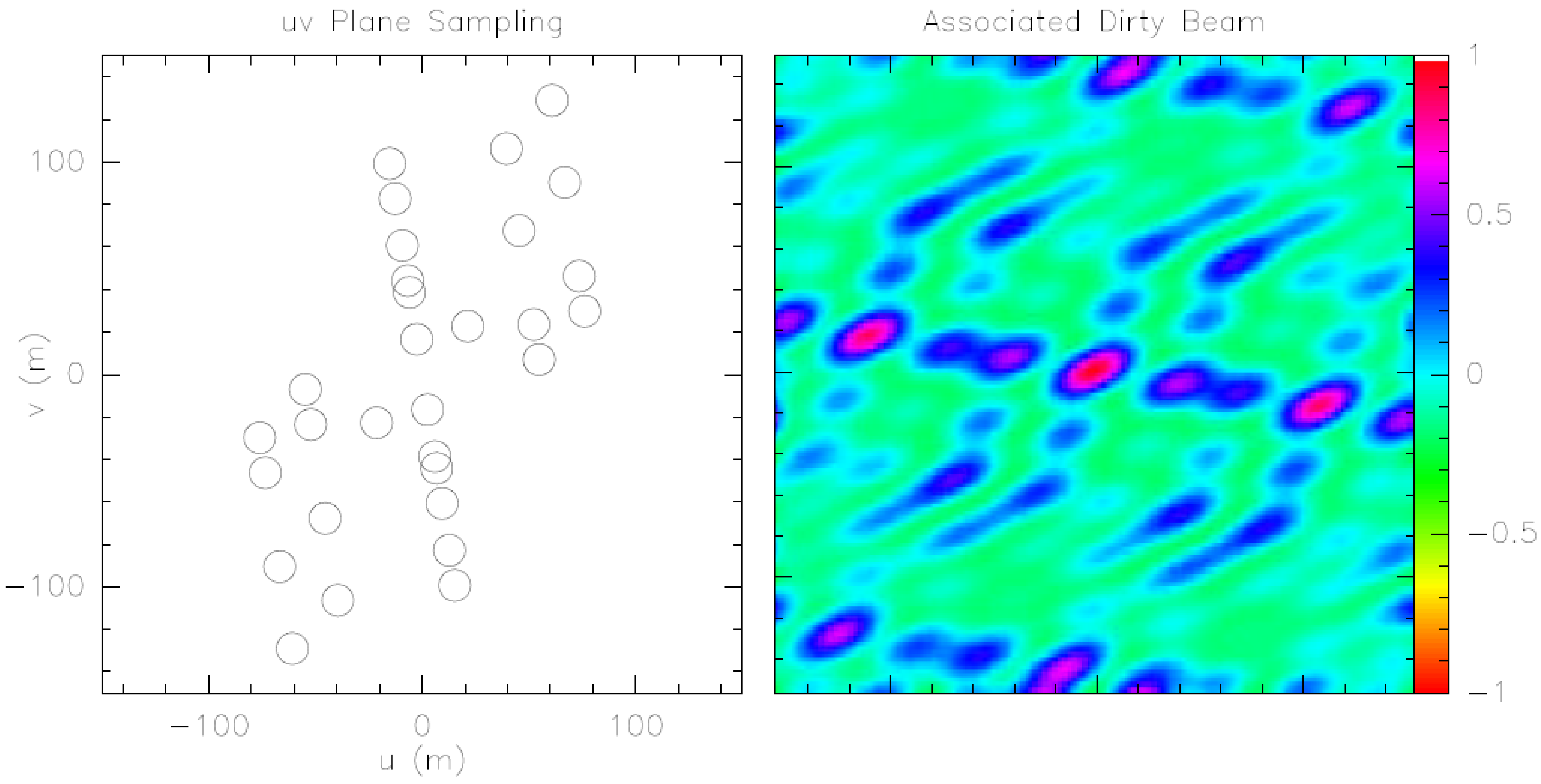

Dirty Beam Shape and Super Synthesis

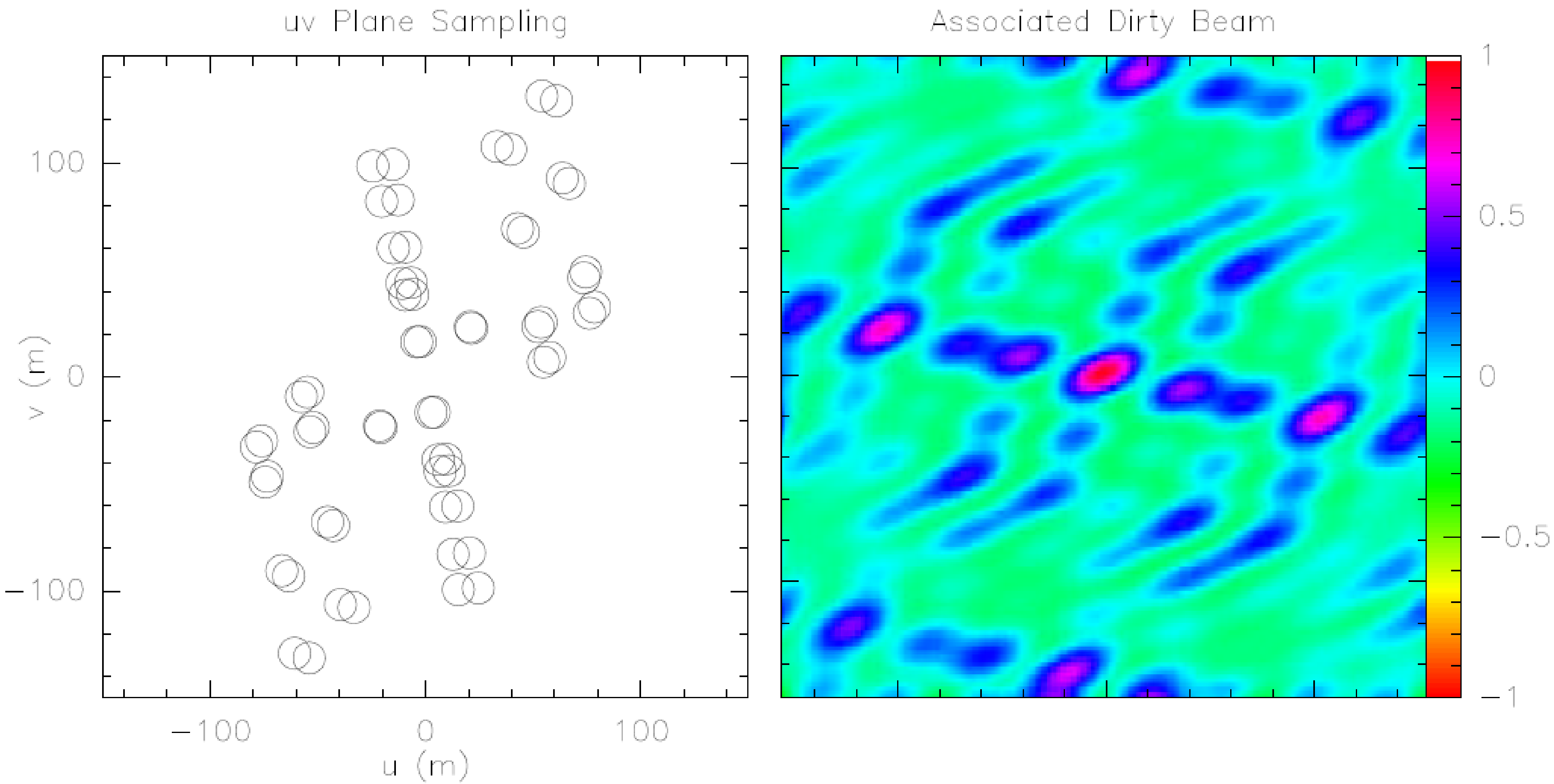

Dirty Beam Shape and Super Synthesis

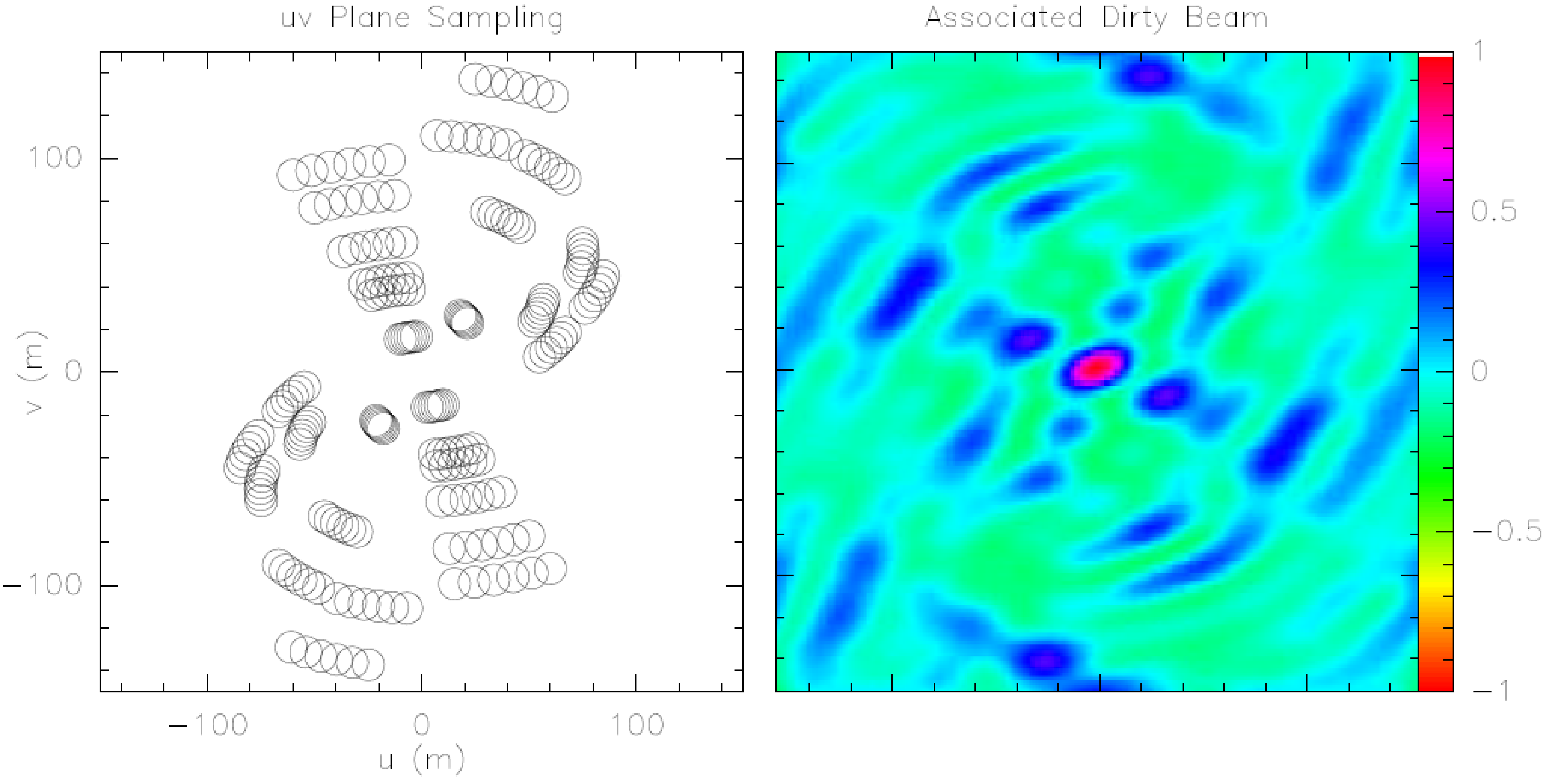

Dirty Beam Shape and Super Synthesis

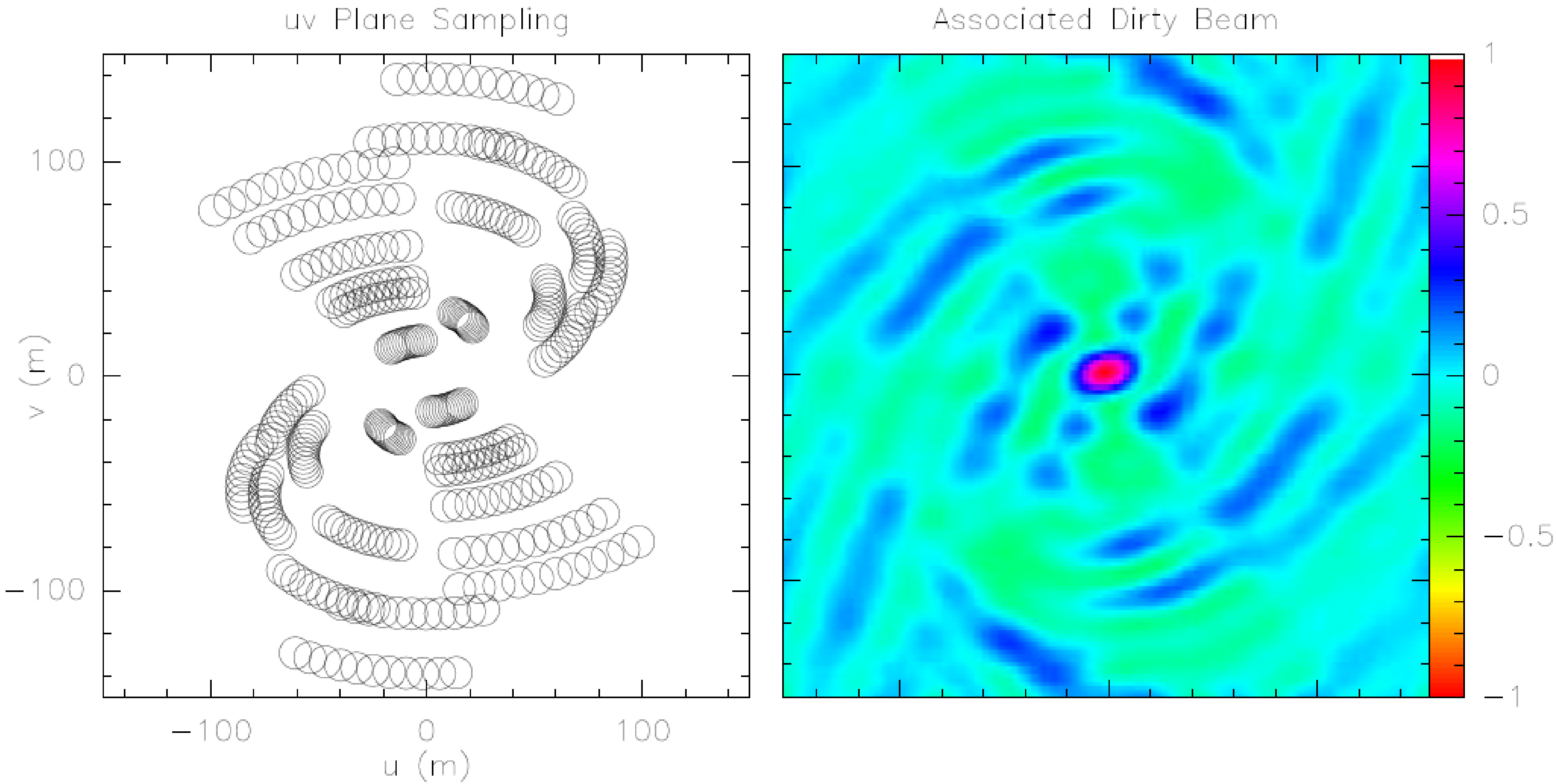

Dirty Beam Shape and Super Synthesis

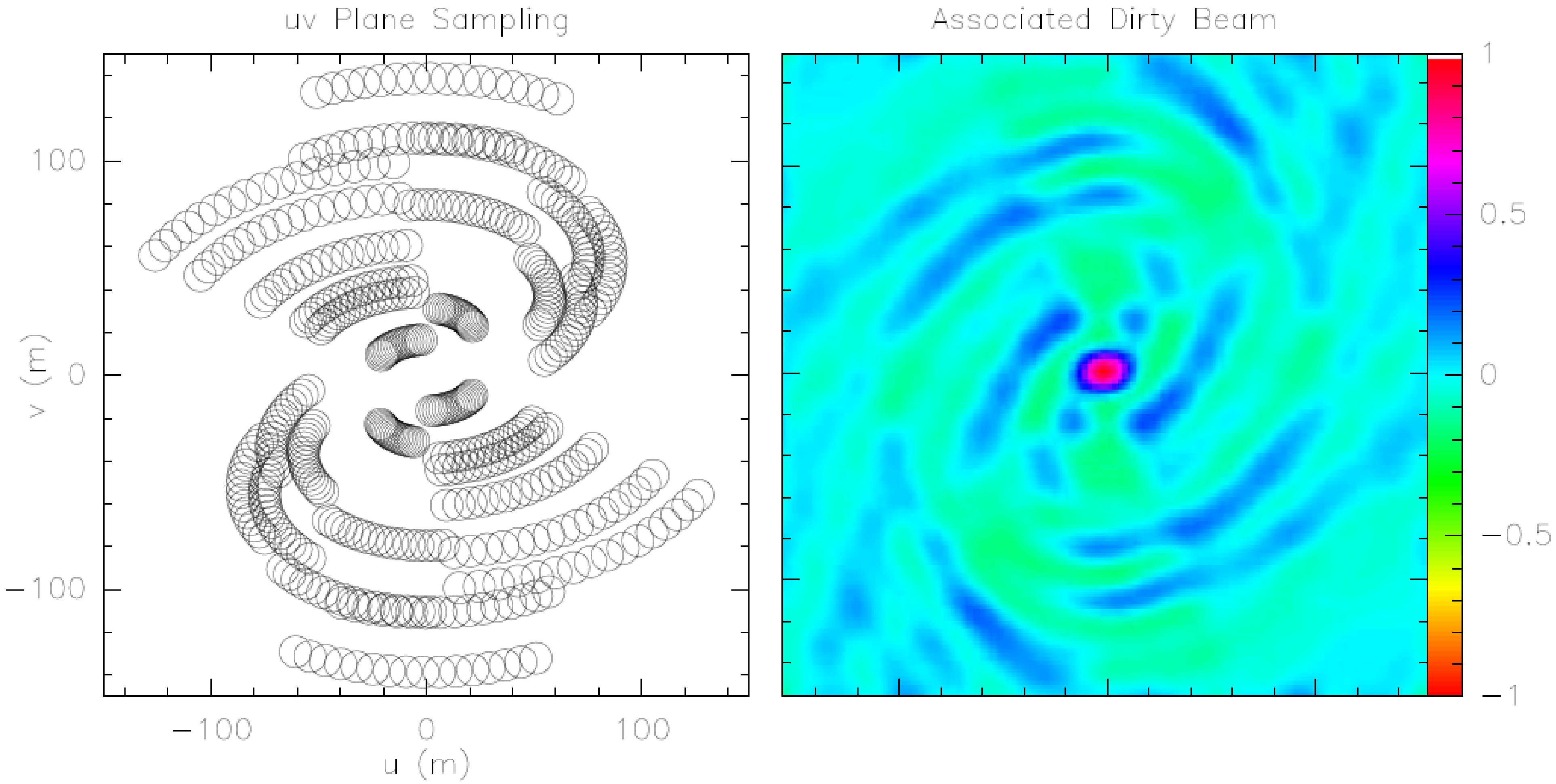

Dirty Beam Shape and Super Synthesis

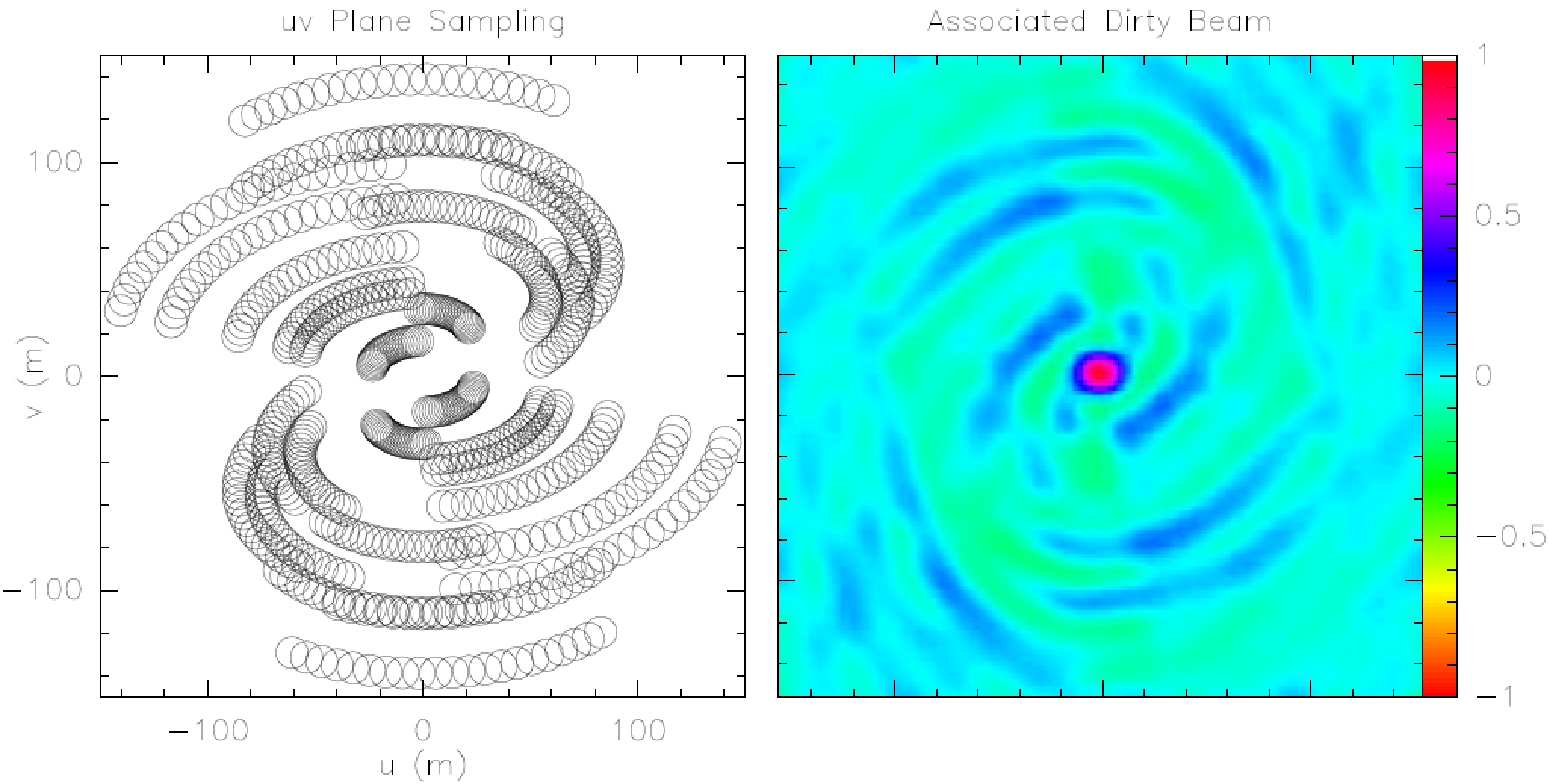

Dirty Beam Shape and Super Synthesis

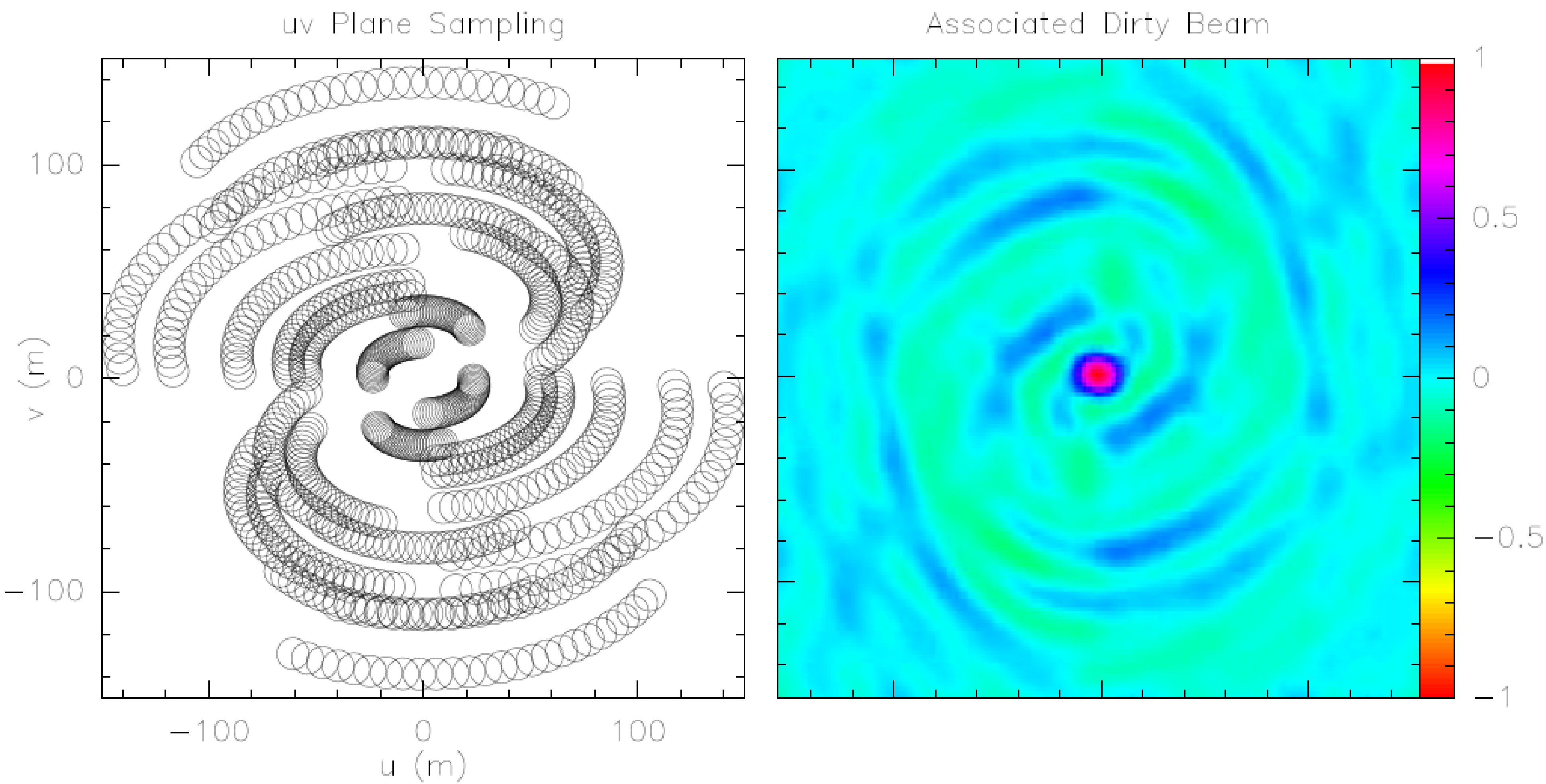

J. Pety lecture at 8th IRAM Millimeter Interferometry School

Dirty Beam Shape and Super Synthesis

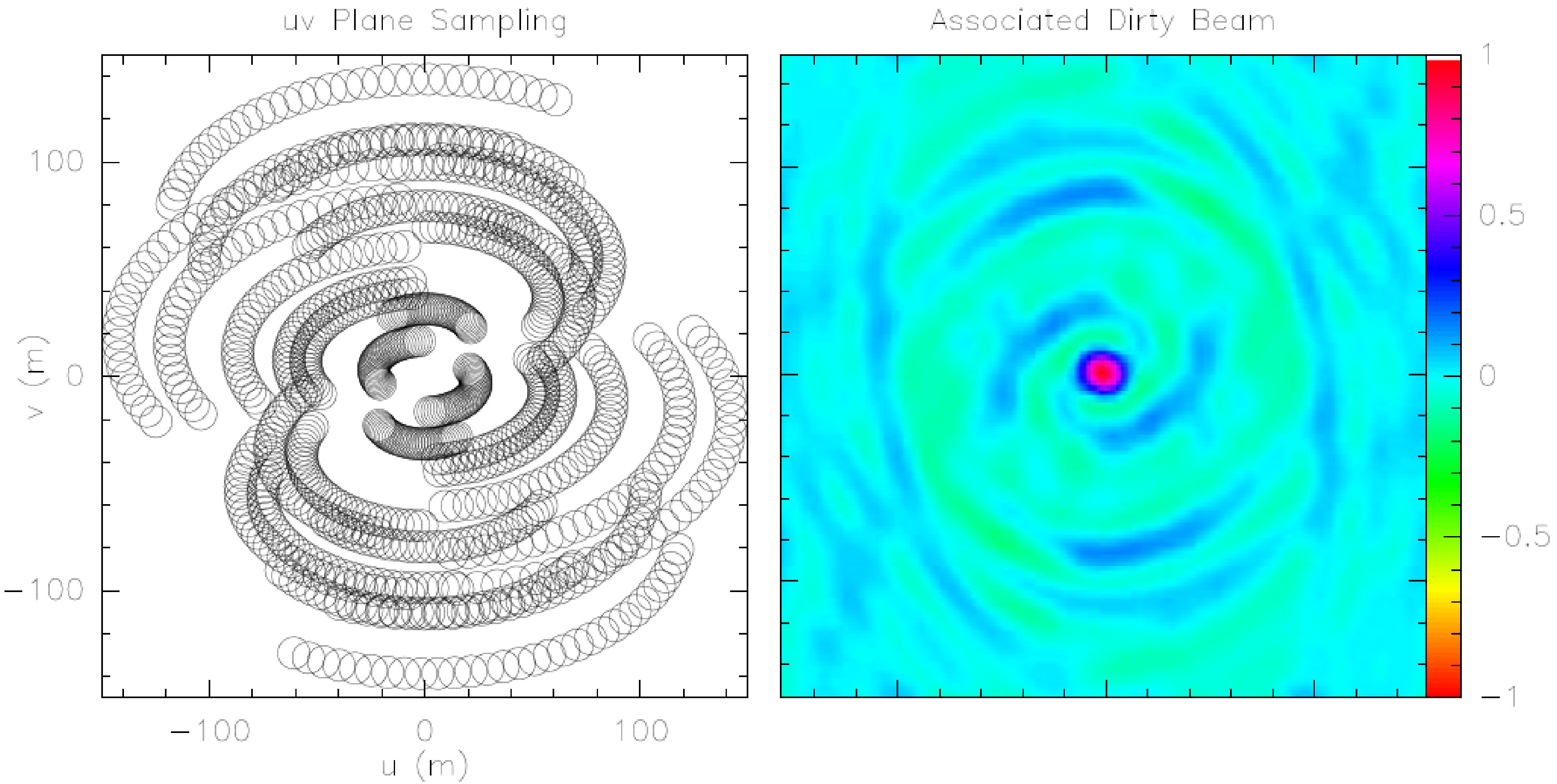

J. Pety lecture at 8th IRAM Millimeter Interferometry School

Dirty Beam Shape and Super Synthesis

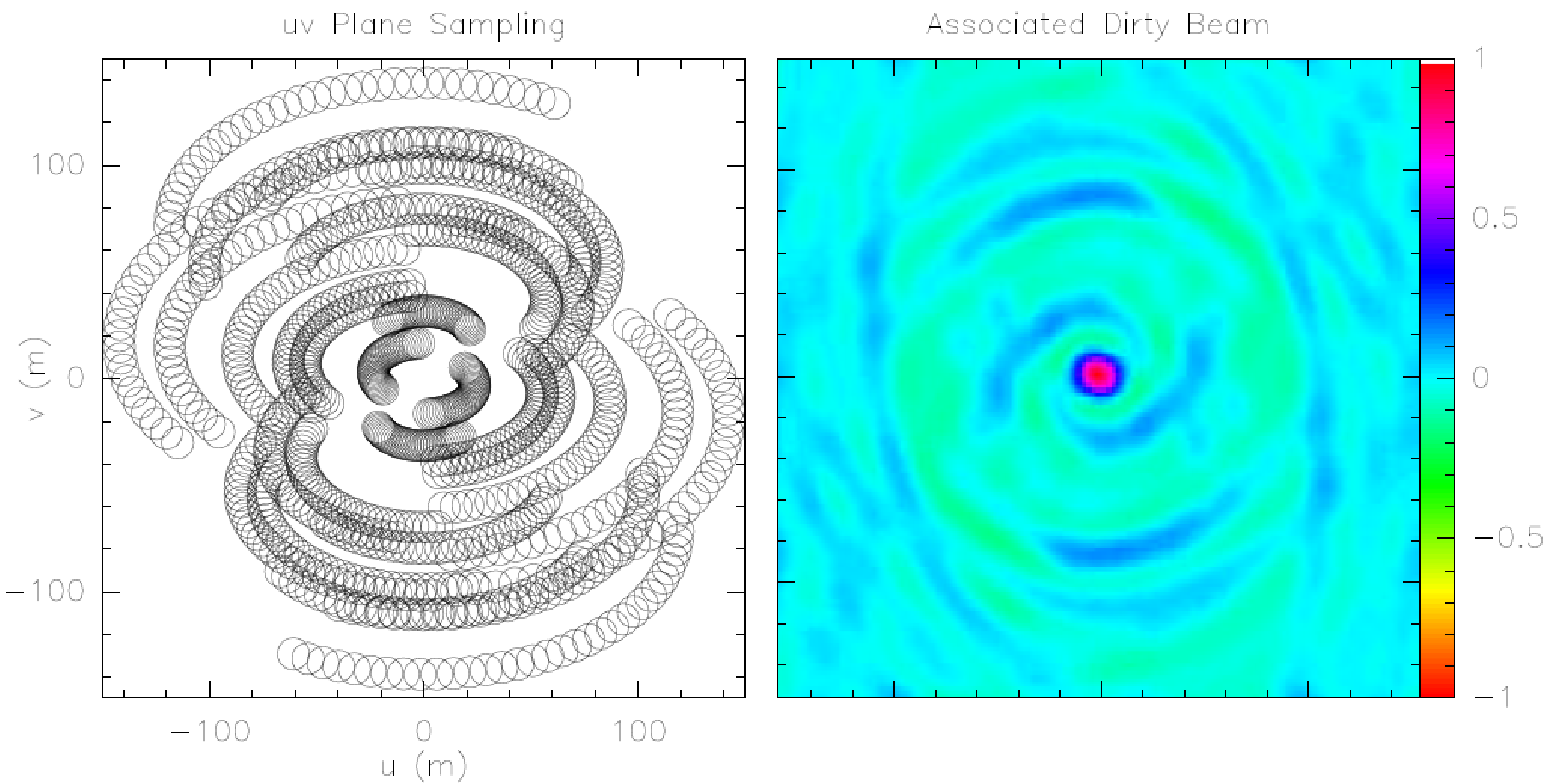

We need to get $I\,(x, y) = \int\int V(u,v)e^{-2\pi i(ux+vy)}dudv$

Consider a two point-like sources as target to observe

$I\,(x, y)$

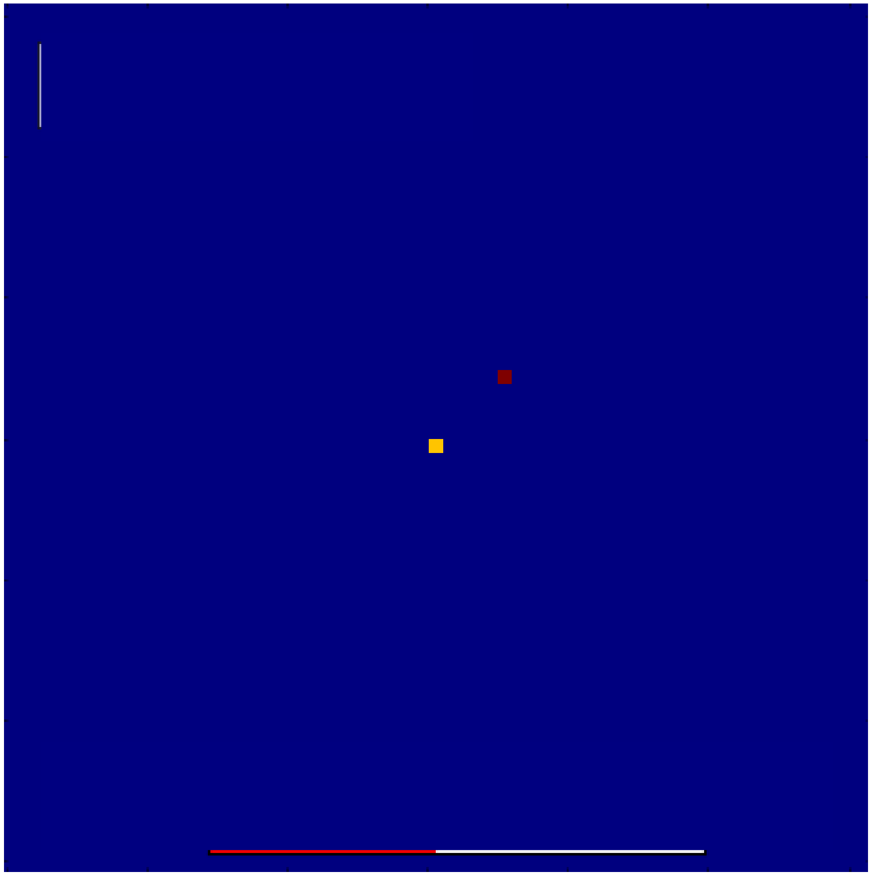

$V\,(u, v)$

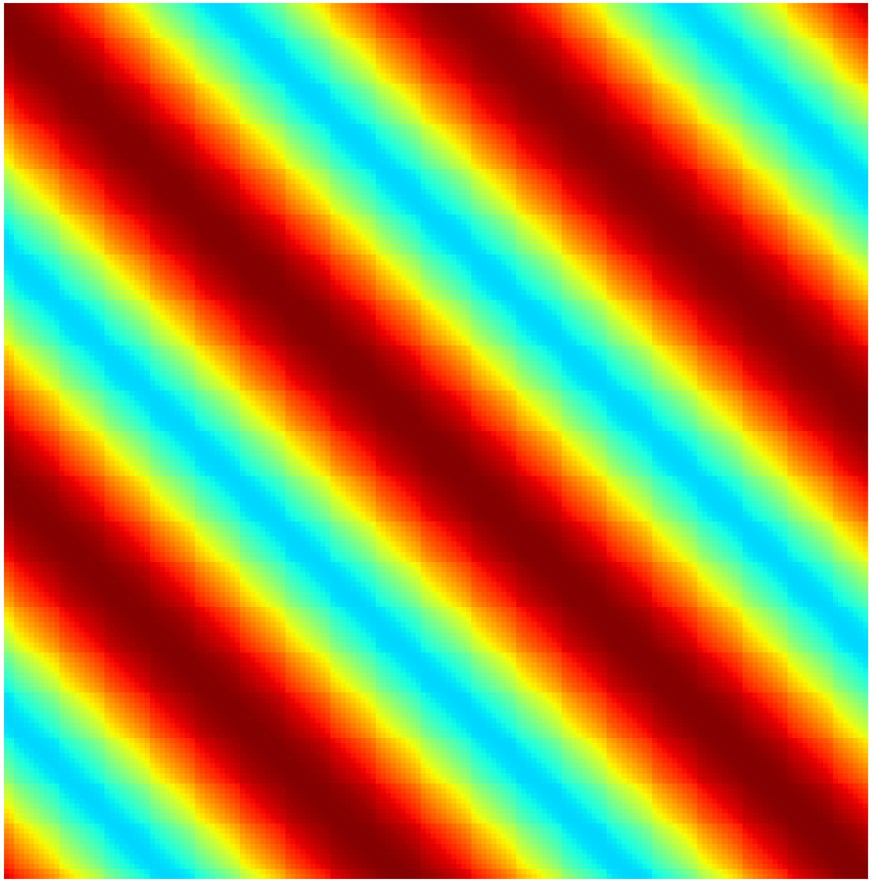

We need to get $I(x,y) = \int\int V(u,v) e^{-2\pi i(ux+vy)} du dv$

But

we actually sample the Fourier domain at discrete points

$$V_{cal}(u,v) = S(u,v) \cdot V_{true}(u,v)$$

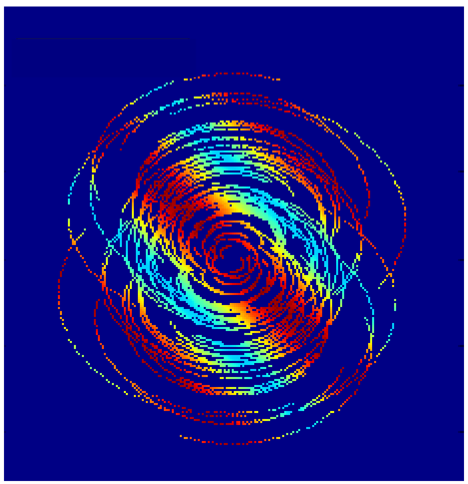

=

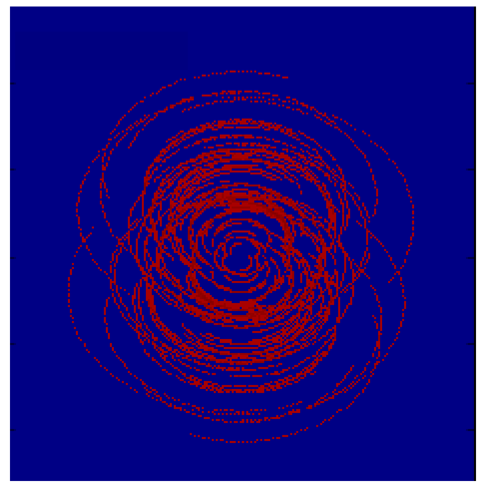

·

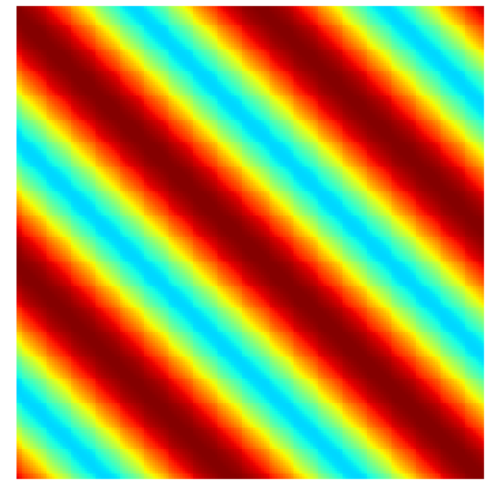

where S(u,v) is the sampling function
S= 1 at points where visibilities are measured
and S = 0 elsewhere

V_{true} is the 2 point-like sources ideal Fourier transform (example from APSYNSIM)

We need to get $I(x, y) = \int\int V(u,v)e^{-2\pi i(ux+vy)}dudv$

Applying the convolution theorem:

$$FT\,(V_{cal}) \;=\; FT\,(S) \;\otimes\; FT\,(V_{True})$$

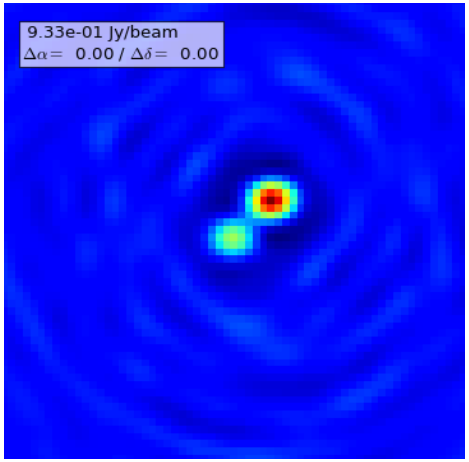

=

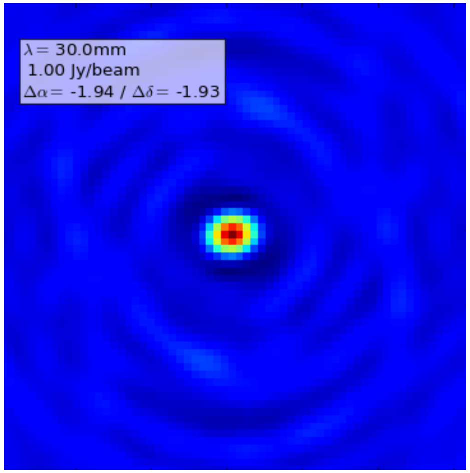

⊗

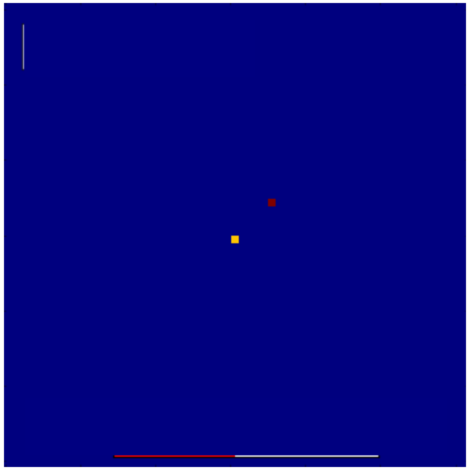

The Fourier transform FT of the sampled visibilities gives the true sky brightness convolved with the Fourier transform of the sampling function (called **dirty beam**).

$$I^D(x, y) = B_{dirty}(x, y) \otimes I(x, y)$$

To get a useful image from interferometric data we need to Fourier transform sampled visibilities, and **deconvolve for the dirty beam** → **clean**

We need to get $I(x, y) = \int\int V(u,v)e^{-2\pi i(ux+vy)}du dv$

$V_{cal}(u,v) \quad = \quad S(u,v) \quad \cdot \quad V_{true}(u,v)$

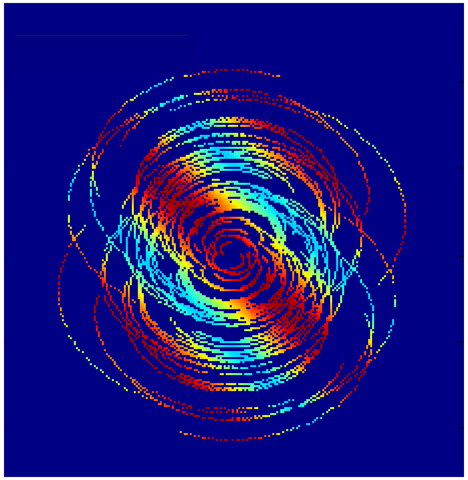

=

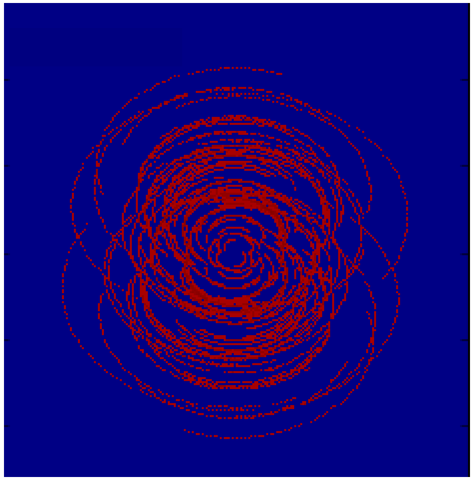

·

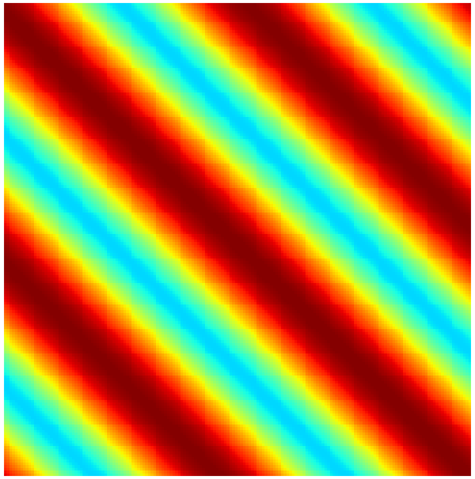

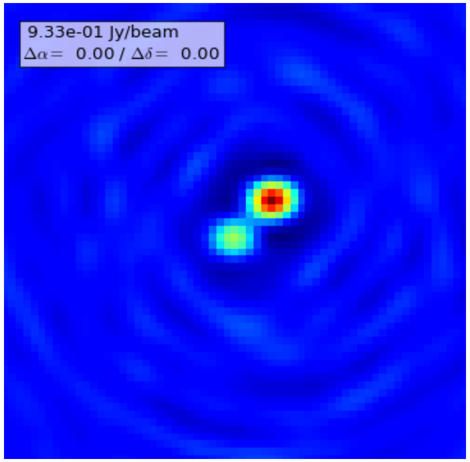

=

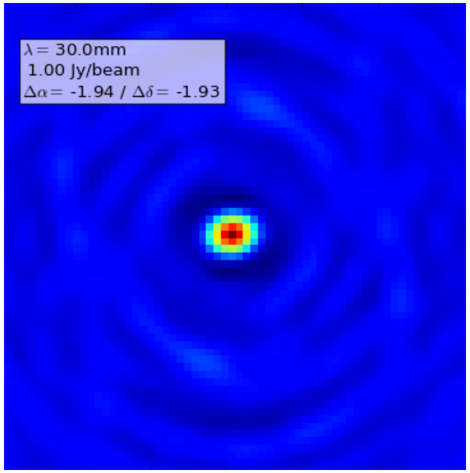

⊗

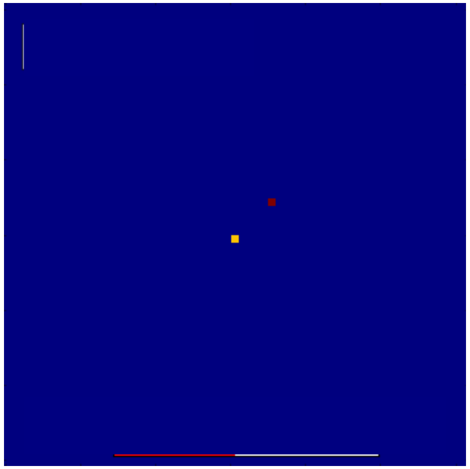

$FT(V_{cal}) \quad = \quad FT(S) \quad \otimes \quad FT(V_{True})$

Imperfect reconstruction of the sky

- **Incomplete sampling of uv plane → sidelobes**

$B_{dirty}(x, y)$

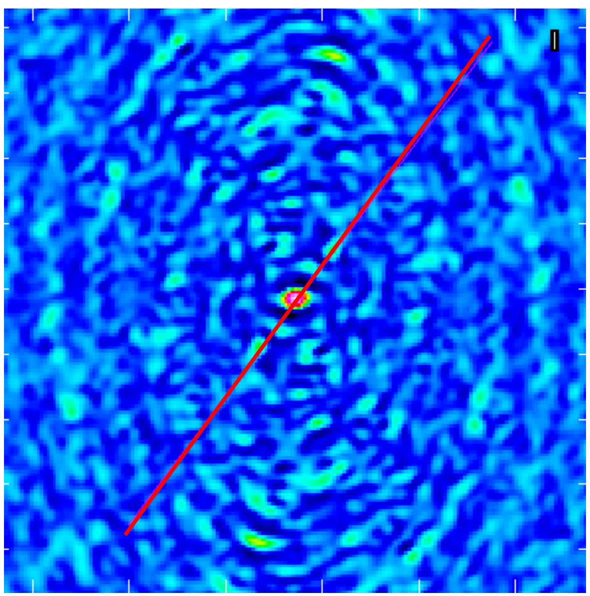

- Central maximum has width $1/(u_{max})$ in x and $1/(v_{max})$ in y
- Has ripples (sidelobes) due to gaps in uv coverage

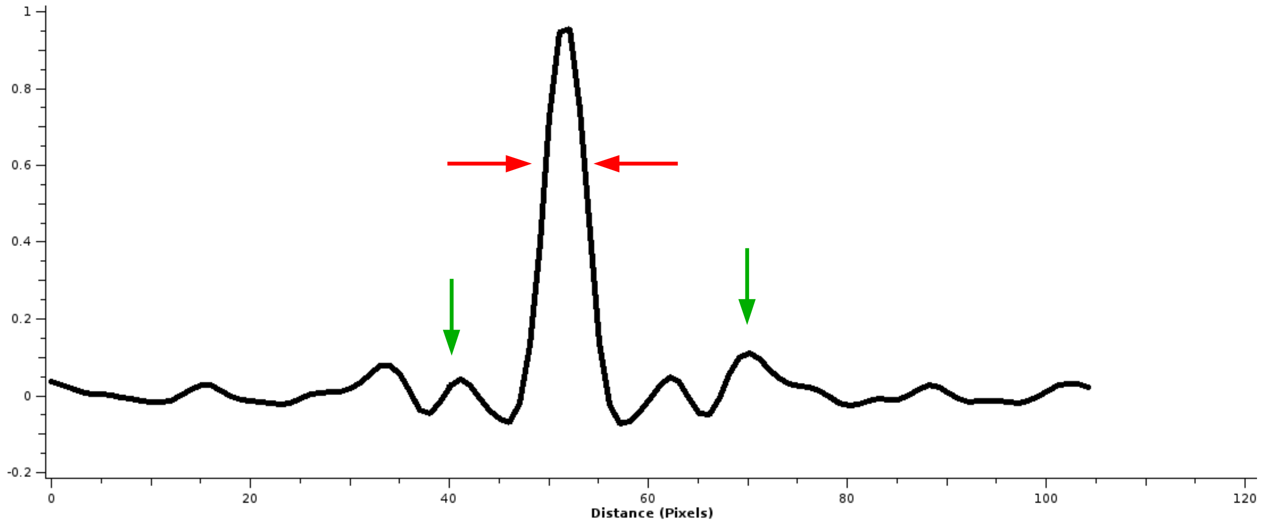

deconvolution → sidelobes removal

We need to get ***I (x, y)*** $= \int \int V(u,v) e^{-2\pi i(ux+vy)} du dv$

Need to choose:

Image pixel size (cellsize)

Make the cell size small enough for Nyquist sample of the longest baseline ($\Delta x < 1/2\ u_{max}$; $\Delta y < 1/2\ v_{max}$)

Usually 1/4 or 1/5 of the synthesized beam to easy deconvolution

Image size (imsize)

The natural resolution in the uv plane samples the primary beam

Larger if there are bright sources in the sidelobes of the primary beam (they would be aliased in the image)

Deconvolution - Classic CLEAN
Hogbom 1974, Clark 1980, **Cotton-Schwab 1984**

Basic assumption: each source is a collection of point sources

1) Initializes the residual map to the dirty map and the Clean component list to an empty value

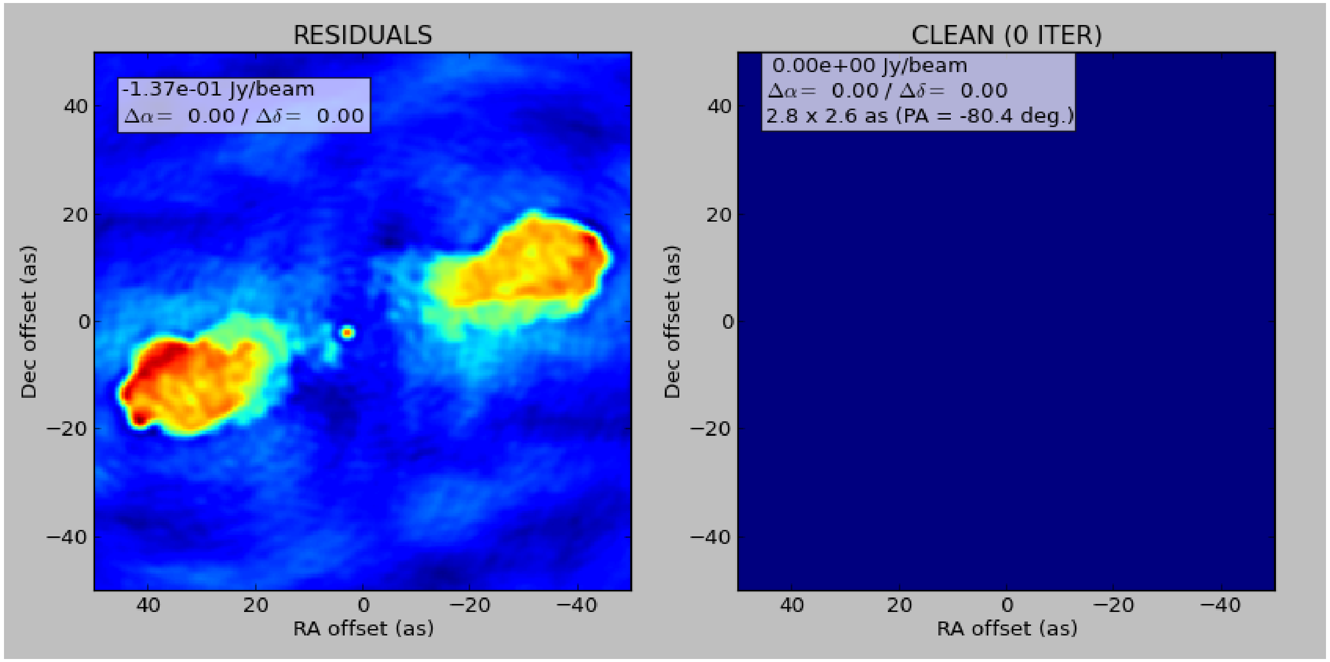

Deconvolution - Classic CLEAN

Hogbom 1974, Clark 1980, **Cotton-Schwab 1984**

Basic assumption: each source is a collection of point sources

2) Identifies the pixel with the peak of intensity (I_{max})in the residual map and adds to the clean component list a fraction of I_{max} = $\gamma\ I_{max}$

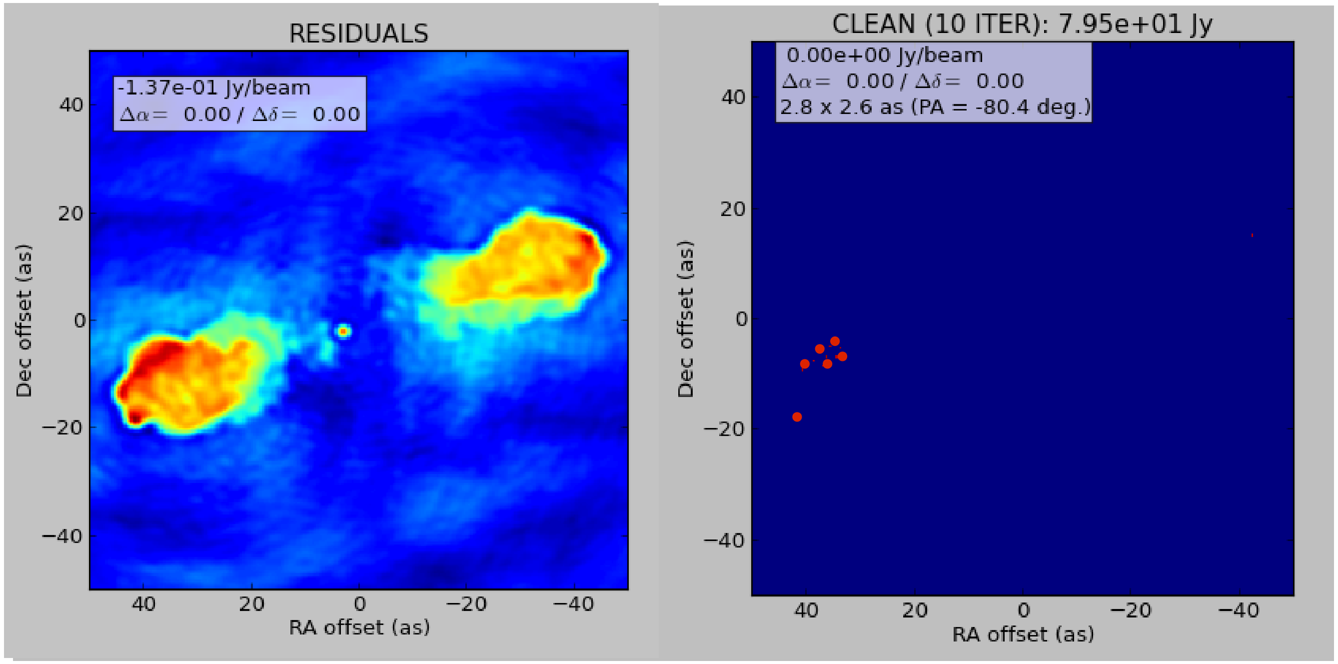

Loop gain

typically

$\gamma \sim 0.1 - 0.3$

Deconvolution - Classic CLEAN
Hogbom 1974, Clark 1980, **Cotton-Schwab 1984**

Basic assumption: each source is a collection of point sources

3) Subtracts over the whole map a dirty beam pattern, including the full sidelobes, centered on the position of the peaks saved in the clean component list, and normalized to the γI_{max} at the beam center.

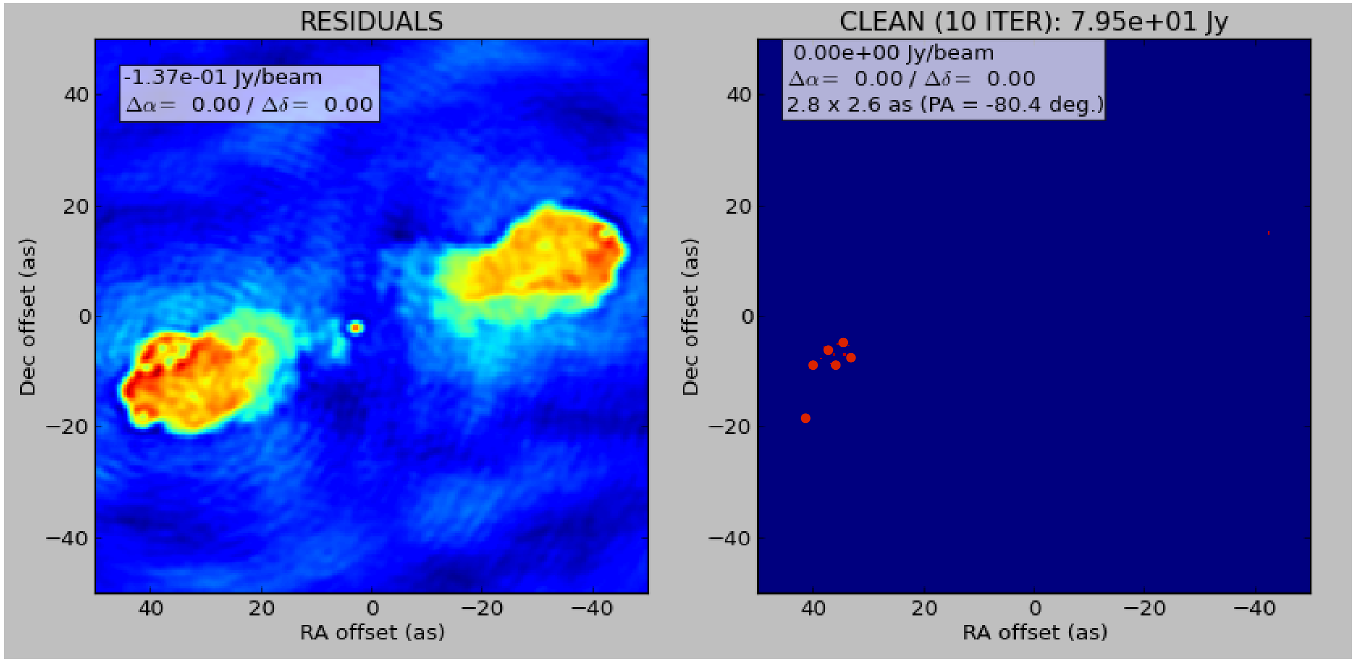

Deconvolution - Classic CLEAN
Hogbom 1974, Clark 1980, **Cotton-Schwab 1984**

Basic assumption: each source is a collection of point sources

4) Iterates until stopping creteria are reached

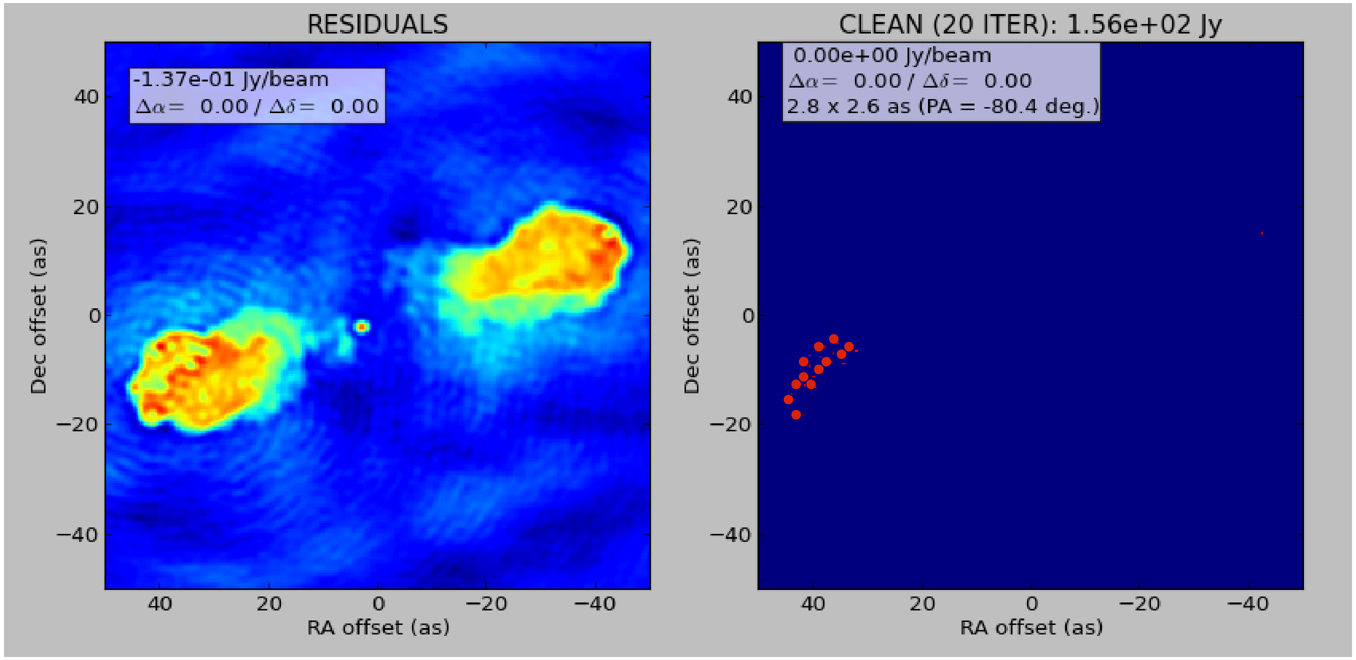

Stopping criteria

$|I_{max}|$ < multiple of the rms (when rms limited)

$|I_{max}|$ < fraction of the brightest source flux (when dynamic range limited)

Deconvolution - Classic CLEAN

Hogbom 1974, Clark 1980, **Cotton-Schwab 1984**

Basic assumption: each source is a collection of point sources

4) Iterates until stopping creteria are reached

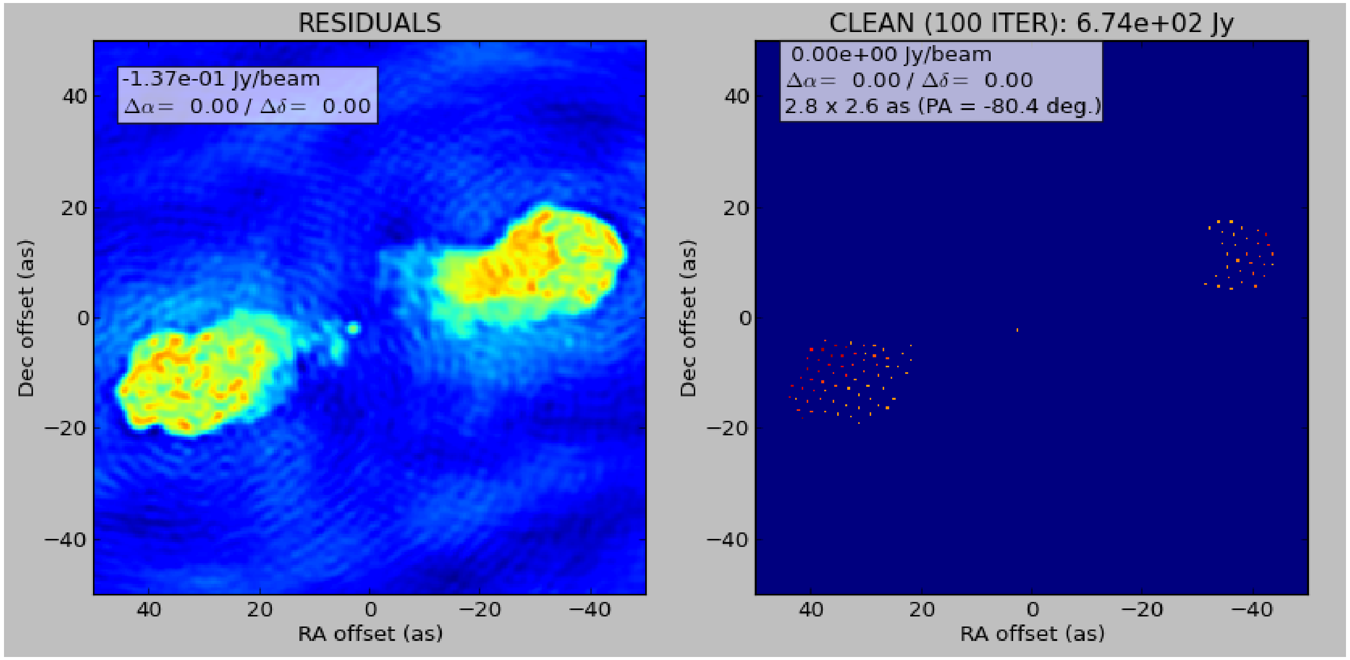

Stopping criteria

$|I_{max}|$ < multiple of the rms (when rms limited)

$|I_{max}|$ < fraction of the brightest source flux (when dynamic range limited)

Deconvolution - Classic CLEAN

Hogbom 1974, Clark 1980, Cotton-Schwab 1984

Basic assumption: each source is a collection of point sources

4) Iterates until stopping creteria are reached

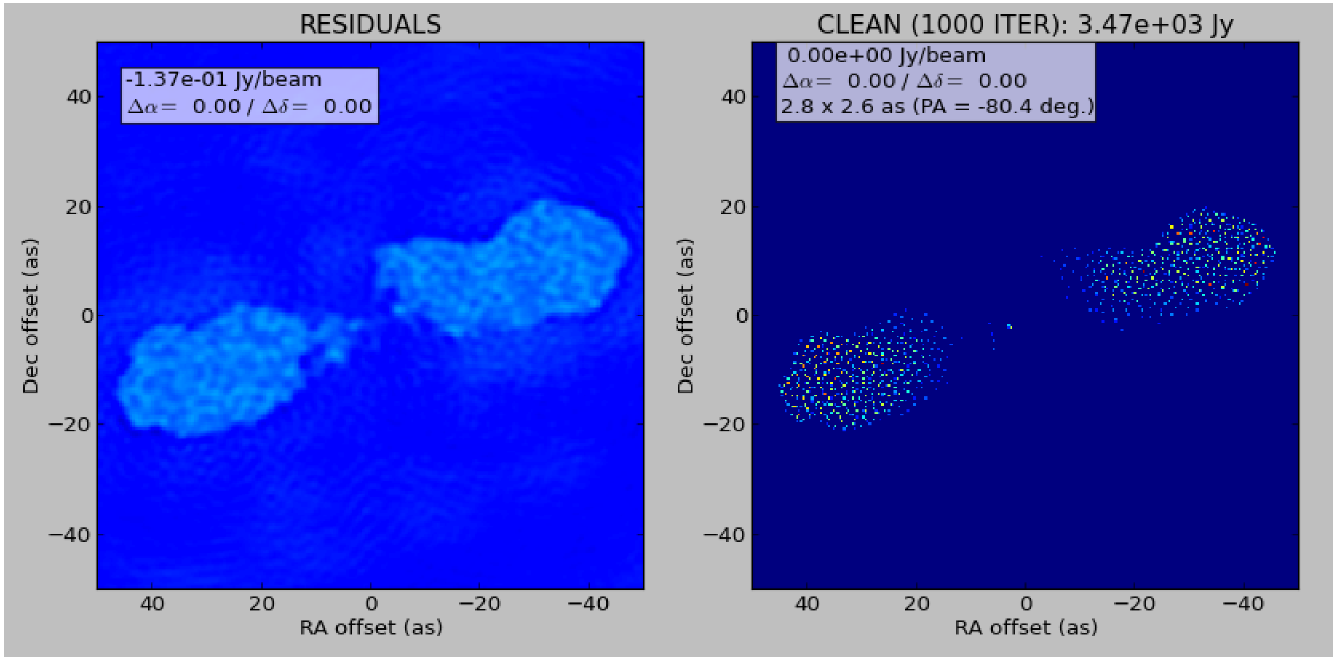

Stopping criteria

$|I_{max}|$ < multiple of the rms (when rms limited)

$|I_{max}|$ < fraction of the brightest source flux (when dynamic range limited)

Deconvolution - Classic CLEAN
Hogbom 1974, Clark 1980, **Cotton-Schwab 1984**

Basic assumption: each source is a collection of point sources

4) Iterates until stopping creteria are reached

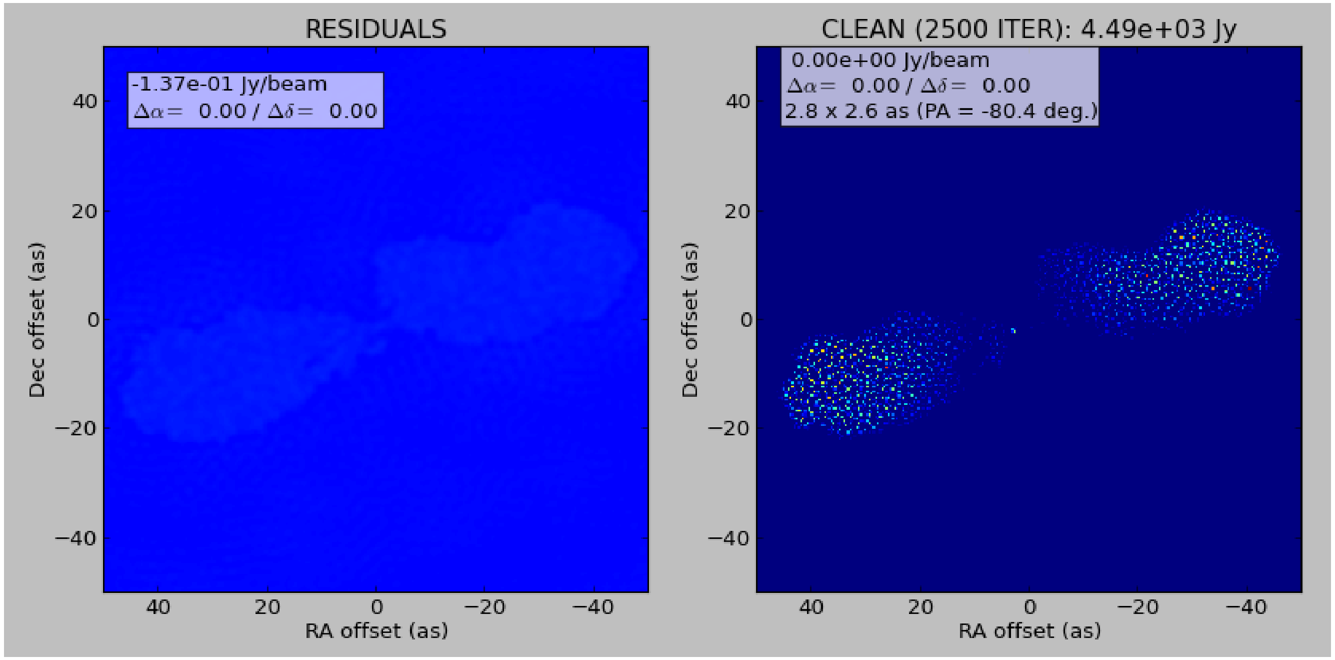

Stopping criteria

$|I_{max}|$ < multiple of the rms (when rms limited)

$|I_{max}|$ < fraction of the brightest source flux (when dynamic range limited)

Deconvolution - Classic CLEAN
Hogbom 1974, Clark 1980, **Cotton-Schwab 1984**

Basic assumption: each source is a collection of point sources

5) Multipies the clean components by **the clean beam**
an elliptical gaussian fitting the central region of the dirty beam
→ **restoring**

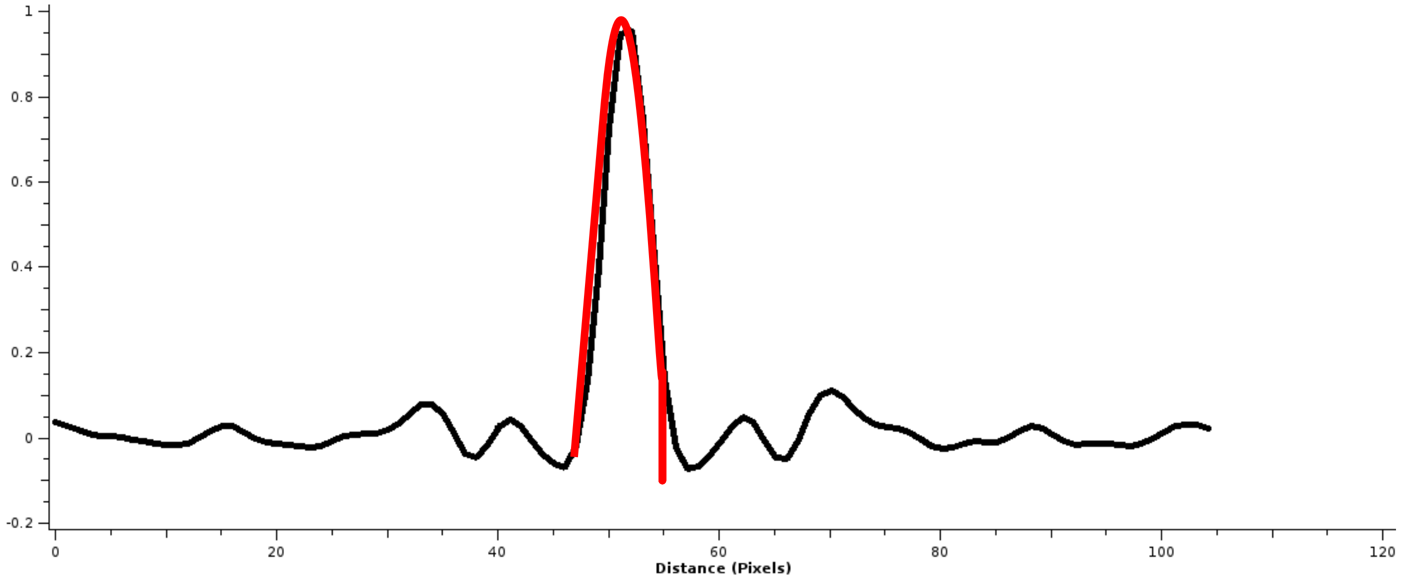

Deconvolution - Classic CLEAN
Hogbom 1974, Clark 1980, **Cotton-Schwab 1984**

Basic assumption: each source is a collection of point sources

5) Multiplies the clean components by the clean beam (**restore**) and add it back to the residual

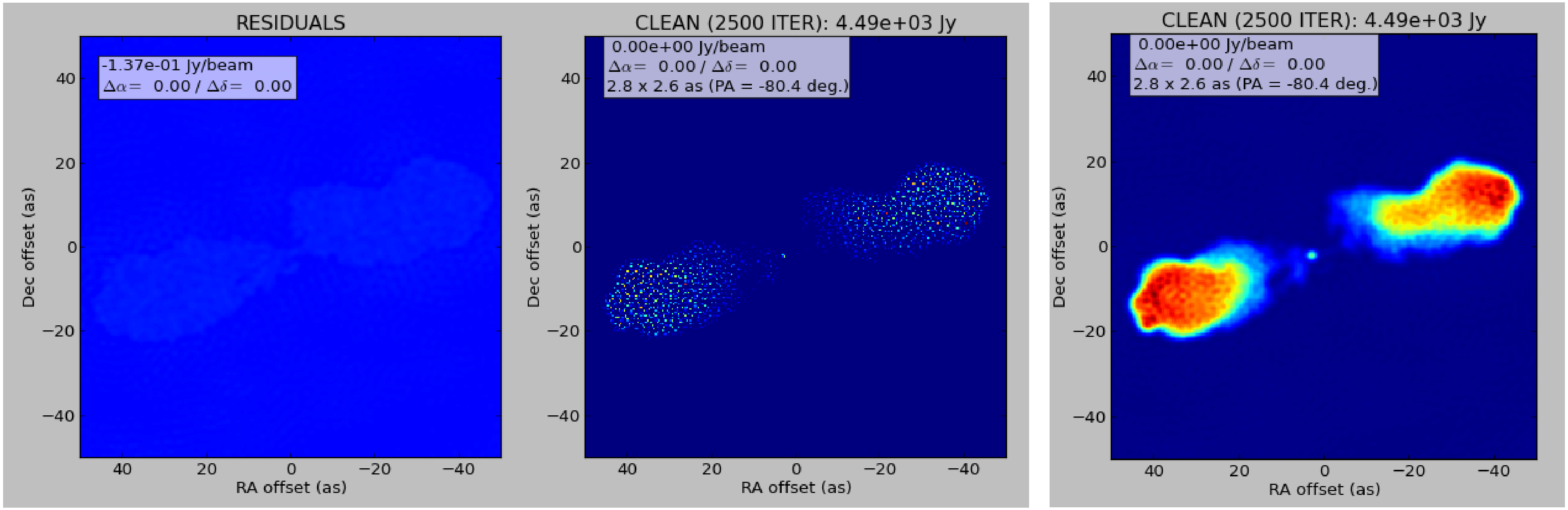

Resulting image pixel have units of Jy per clean beam

We need to get ***I (x, y)*** $= \int \int V(u,v) e^{-2\pi i(ux+vy)} du dv$

But

Interferometer elements are sensible to direction of arrival of the radiation

- **Primary beam effect** → ***I(x,y) = A(x,y) I′(x,y)***

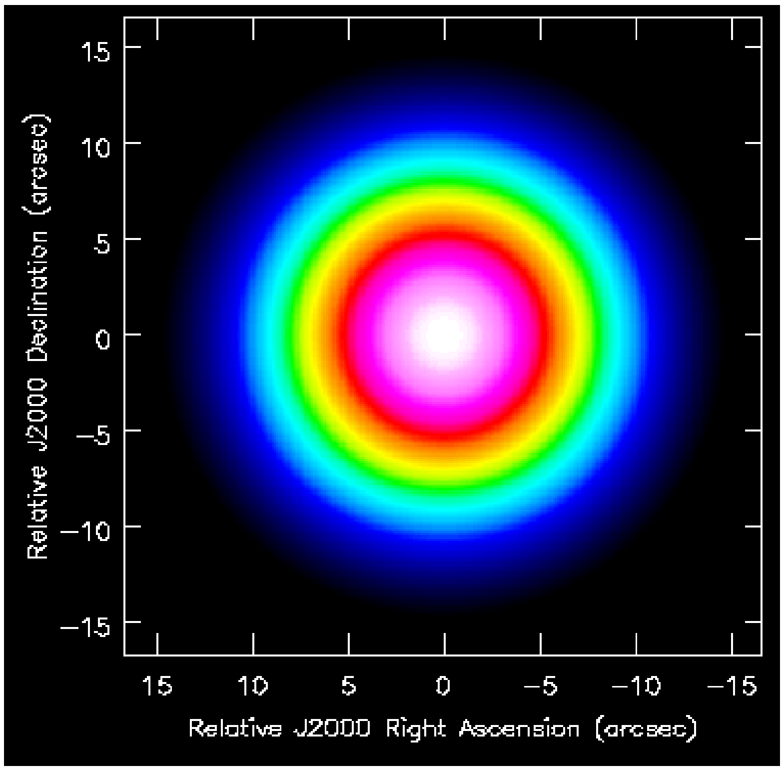

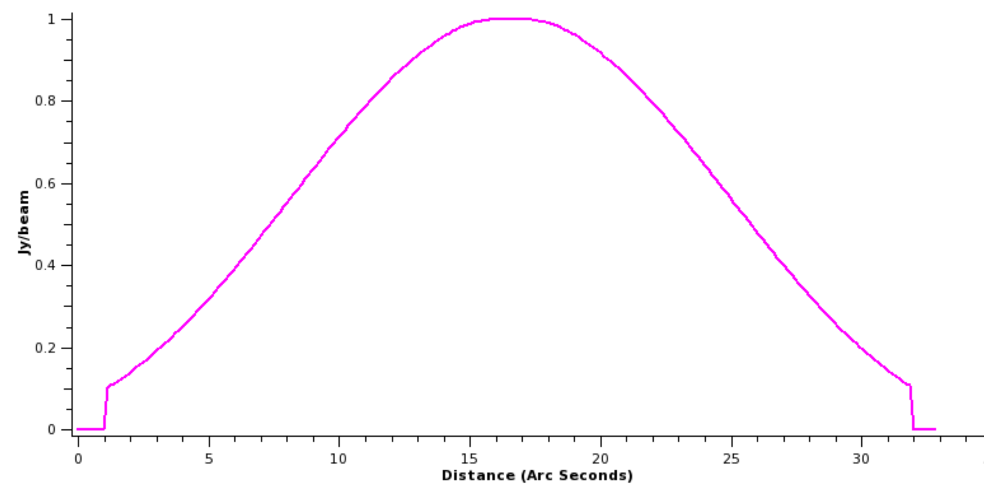

The response of the antennas in the array must be corrected for during imaging to get accurate intensities for source outside the core of the beam.

We need to get $I(x, y) = \int\int V(u,v)e^{-2\pi i(ux+vy)}dudv$

But

- **Primary beam effect** → $I(x,y) = A(x,y)\, I'(x,y)$

$I(x,y)$ | $I'(x,y)$

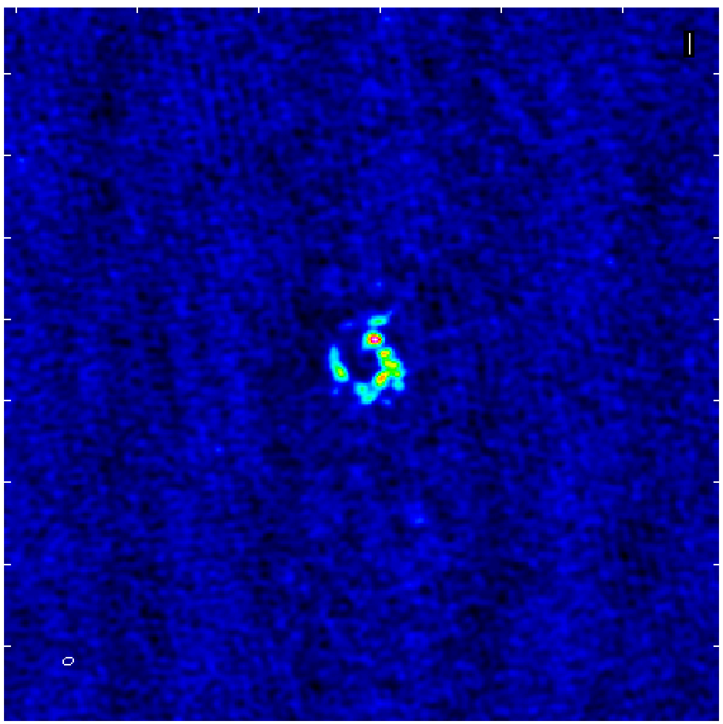

rms 8e-4

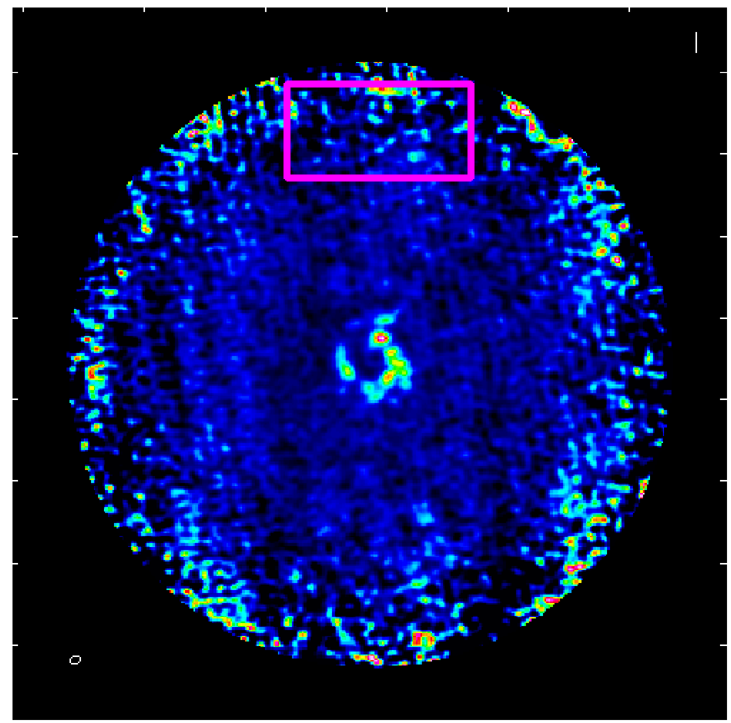

rms 3e-3

We need to get $I(x,y) = \int\int V(u,v)e^{-2\pi i(ux+vy)}dudv$

But

measured visibilities actually contain noise
and some uv ranges are sampled more than others

$$\sigma(u,v) \propto \frac{1}{\sqrt{T_{sys\,1}T_{sys\,2}}}$$

- **Gridded visibilities are** → $V(u,v) = W(u,v)\,V'(u,v)$

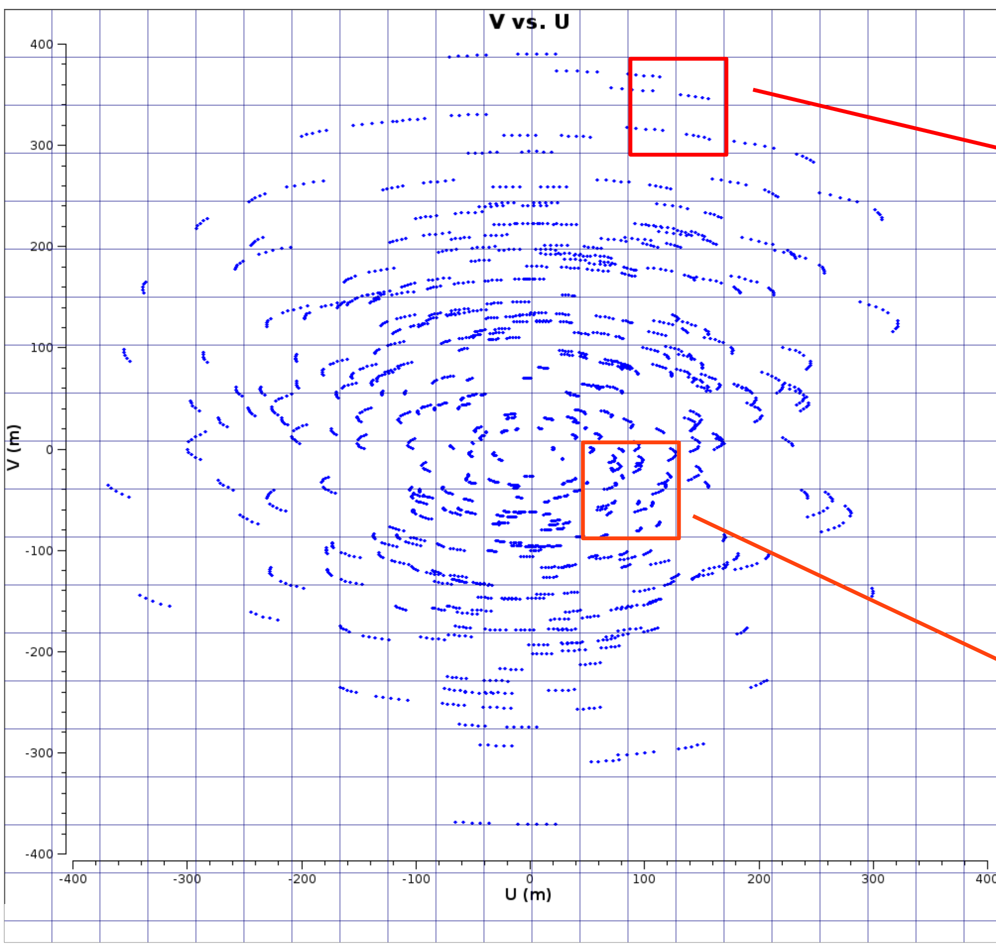

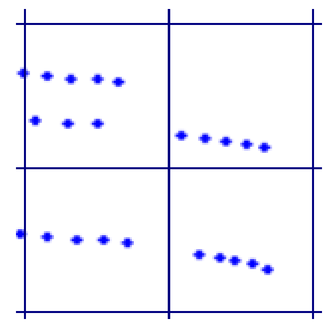

Tipically, short spacing
are sampled more than long

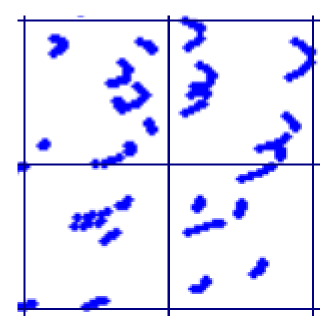

We need to get $I(x,y) = \int\int V(u,v)e^{-2\pi i(ux+vy)}dudv$

- **Natural weighting** $W(u,v) = 1/\sigma^2(u,v)$

σ is the noise variance of the visibilities

- **Uniform weighting** $W(u,v) = 1/\delta_s(u,v)$

δ_s is the density of (u,v) points in a symmetric region of the uv plane

Unfortunately, in reality, the weighting which produces the best resolution **(uniform)** will often utilize the data very irregularly resulting in poor sensitivity → compromises

- **Briggs weighting**

combines inverse density and noise weighting.
An adjustable parameter "robust " allows for continuous variation between natural (robust=+2) to uniform (robust=-2)

We need to get $I(x, y) = \int\int V(u,v) e^{-2\pi i(ux+vy)} du dv$

Weighting effects on the Dirty beam

Natural
0.29" x 0.23"
Best sensitivity

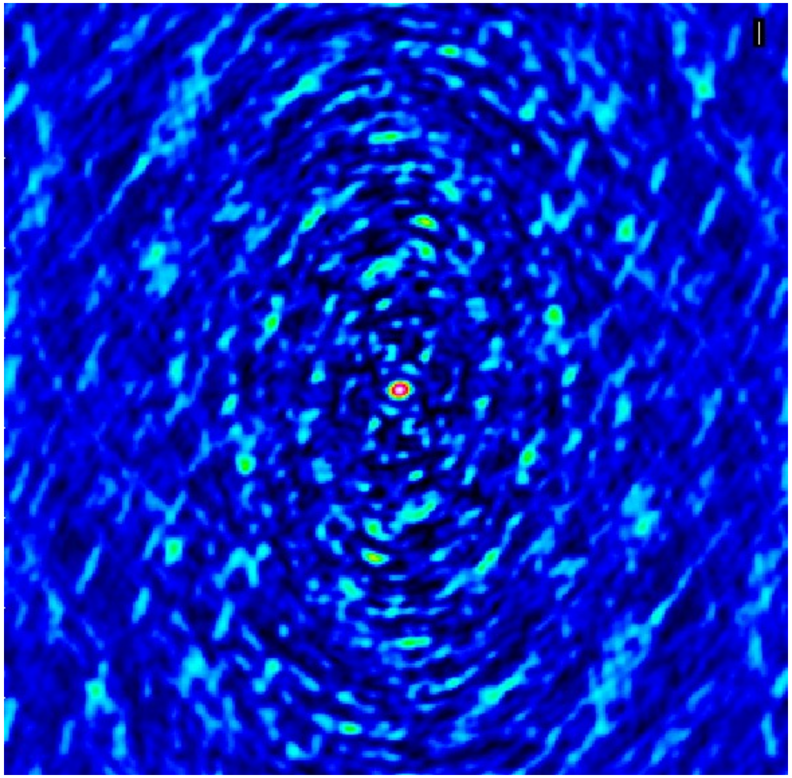

Uniform
0.24"x0.17"
Best angular resolution

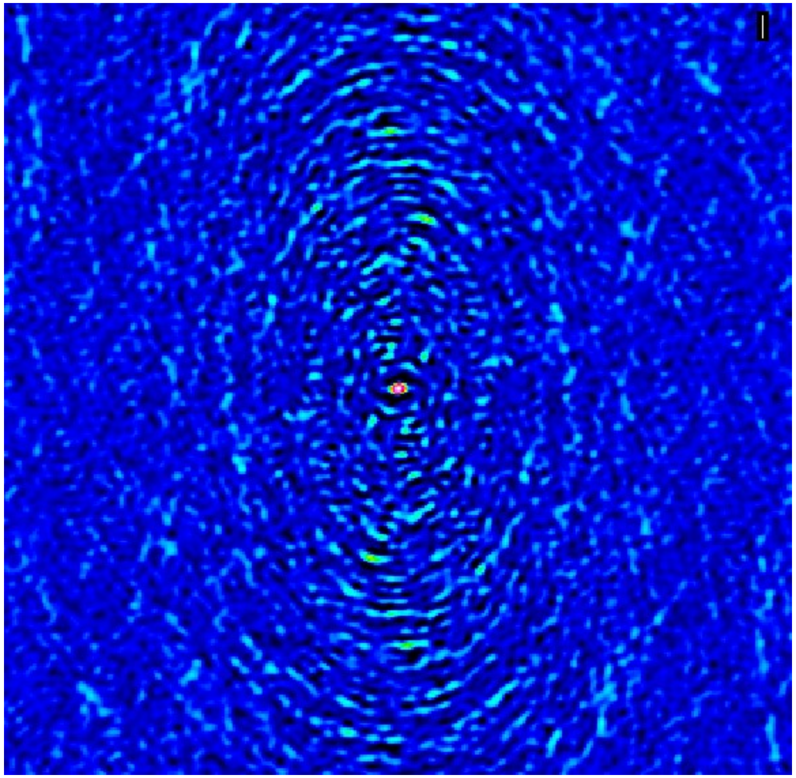

We need to get $I(x,y) = \int\int V(u,v) e^{-2\pi i(ux+vy)} du dv$

Weighting effects on the image

Natural
res = 0.29'' x 0.23''
rms = 0.8 mJy/beam

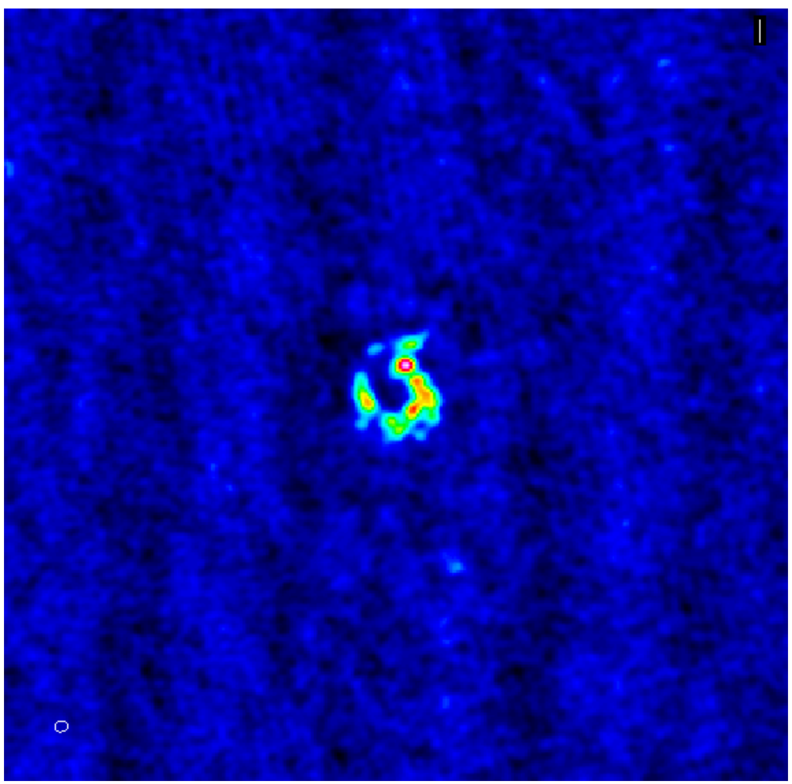

Uniform
res = 0.24''x0.17''
rms = 3 mJy/beam

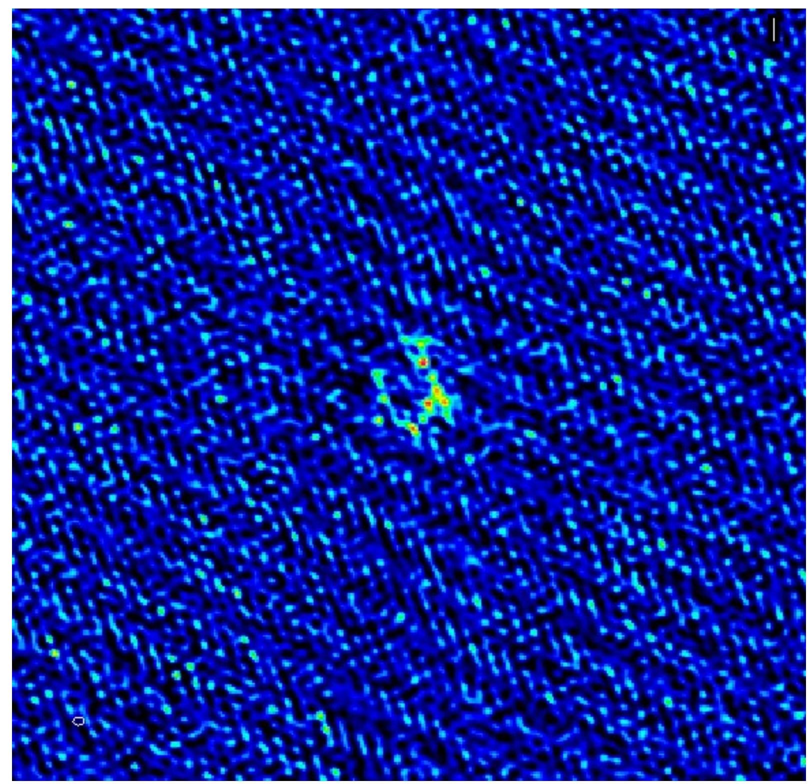

We need to get $I(x, y) = \int\int V(u,v)e^{-2\pi i(ux+vy)}dudv$

Weighting effects on the image

Natural
res = 0.29'' x 0.23''
rms = 0.8 mJy/beam

Uniform
res = 0.24''x0.17''
rms = 3 mJy/beam